

ANNUAL RESEARCH REVIEW WORKSHOP 2022-2023



V (a) Farm Machinery and Postharvest Technology Division
V (b) Workshop Machinery and Maintenance Division



BANGLADESH RICE RESEARCH INSTITUTE
GAZIPUR 1701

INDEX

CONTENT	PAGE
INDEX	01
INTRODUCTION	02
PERSONNEL	03
SUMMARY	04 - 07
USEFUL SCIENTIFIC INFORMATION	08
PROJECT 1: AGRICULTURAL MACHINERY DEVELOPMENT AND TESTING	08
Experiment 1.1	Design, development, and performance assessment of a BRRRI head feed combine harvester 08 -10
Experiment 1.2	Design and Development of a BRRRI Automatic Seed Sower Machine for raising mat-type seedling 10 - 12
Experiment 1.3	Assessment of BRRRI Whole Feed Combine Harvester (Model BRRRI WCH 2021) for Mechanized Rice Harvesting 12 - 16
Experiment 1.4	Performance test of the BRRRI developed mini whole feed combine harvester 16 - 24
Experiment 1.5	Validation and up-scaling of rice transplanting and harvesting technology in the selected sites of Bangladesh 24 - 41
Experiment 1.6	Modification of power transmission system of BRRRI hydro-tiller 41 - 44
Experiment 1.7	Design and Development of a manually operated Briquetting Machine. 44 - 49
PROJECT 2: MILLING AND PROCESSING TECHNOLOGY	49
Experiment 2..1	Test, evaluation and modification of rubber roll de-husker and friction type polisher 49 - 51
PROJECT 3: RENEWABLE ENERGY TECHNOLOGY	52
Experiment 3.1	Design and development of a small-scale recirculating type dryer 52 - 59
Experiment 3.2	Study on solar energy utilization for small agricultural machinery 59 - 71
PROJECT 4: PRECISION AGRICULTURE	69
Experiment 4.1:	Evaluating the Effects of Climate Change on Thermal Bioclimatic Indices in Bangladesh Using Climate Projections from Bias-Corrected CMIP6 Models 69 - 71
Experiment 4.2:	Compound Precipitation and Temperature Extremes in the coastal region of Ganges Delta: A 50-Year Analysis (1971-2021) 72 - 75
PROJECT 5: INDUSTRIAL AND FARM LEVEL EXTENSION OF AGRICULTURAL MACHINERY	76
Experiment 5.1	Training on operation, repair and maintenance of BRRRI farm machinery 76 - 78
REPAIR-MAINTENANCE AND SUPPORT SERVICE WORK	79
Appendix- 1	Support Services for different division of BRRRI rendered by FMPHT Divisional Research Workshop during 2022-2023 79
Appendix- 2	Cost and times of repair and maintenance work of different vehicles/transport and farm machinery of BRRRI from July 2019 to June 2020 79 - 81

INTRODUCTION

There are two research divisions under “**Farm Mechanization and Postharvest Technology Programme Area**” and have been conducting research on the following projects.

Project Title	No. of Experiment
Project 1: Agricultural Machinery Development and Testing	07
Project 2: Milling and Processing Technology	01
Project 3: Renewable Energy	02
Project 5: Precision Agriculture	02
Project 6: Industrial and Farm Level Extension of Agricultural Machinery	01
Total	13

PERSONNEL

Programme Performing Unit 1: Farm Machinery and Postharvest Technology Division

Name and Designation	Abbreviation	Working months
Md. Durrul Huda, <i>PhD</i> <i>Chief Scientific Officer and Head</i>	MDH	12
AKM Saiful Islam, <i>PhD</i> <i>Chief Scientific Officer</i>	AKMSI	12
Md. Golam Kibria Bhuiyan, <i>PhD</i> <i>Principal Scientific Officer</i>	MGKB	12
Md. Anwar Hossen, <i>PhD</i> <i>Principal Scientific Officer</i>	MAH	12
Bidhan Chandra Nath, <i>PhD</i> <i>Senior Scientific Officer</i>	BCN	04
Md. Kamruzzaman Milon, <i>PhD</i> <i>Senior Scientific officer</i>	MKM	12
Subrata Paul, <i>M Engg.</i> <i>Senior Scientific Officer</i>	SP	12
Md. Kamruzzaman Pintu*, <i>MS</i> <i>Senior Scientific officer</i>	MKP	11
Md. Monirul Islam, <i>MS</i> <i>Senior Scientific Officer</i>	MMI	12
Sharmin Islam, <i>MS</i> <i>Agriculture Engineer</i>	SI	12
Haimonti Paul, <i>MS</i> <i>Agriculture Engineer</i>	HP	12
Md. Mizanur Rahman, <i>MS</i> <i>Scientific Officer</i>	MMR	12
Md. Mahir Shahriyar, <i>MS</i> <i>Scientific Officer</i>	MMS	12
Arafat Ullah Khan, <i>MS</i> <i>Scientific Officer</i>	AUK	12
Md. Rasel Ahmed, <i>B Sc. Engineering (Mechanical)</i> <i>Foreman</i>		12
Md. Nurul Momin Mondal, <i>Dip-in-Engineering (Power)</i> <i>Research Assistant</i>		12
Md. Ahsan Habib, <i>Dip-in-Agriculture</i> <i>Scientific Assistant</i>		12

Programme Performing Unit 2: Workshop Machinery and Maintenance Division

Name and Designation	Abbreviation	Working months
Mohammad Afzal Hossain, <i>PhD</i> <i>Senior Scientific Officer</i>	MAfH	12
Hafizur Rahaman, <i>MS</i> <i>Scientific Officer</i>	HR	12
Md. Modud Ahmed, <i>MS</i> <i>Agriculture Engineer</i>	MMA	12

* On deputation for higher study

SUMMARY

The development of BRRRI head-feed combine harvester is a breakthrough to suit the fragmented land and soil of the country. The machine has been manufactured at Alim Industries Limited, Sylhet using locally available raw materials, thereby enhancing the capabilities of local manufacturers. The head-feed combine harvester is a machine which accomplishes major four functions (reaping, threshing, winnowing and bagging) of grain harvest in a single operation and keeps straw intact which can be used for beneficial purpose. More than an acre of land can be harvested per hour and crop loss is less than one percent. Paddy can be harvested easily by the machine in muddy and waterlogged field where plough (12-15cm) is available. Farmers and agricultural entrepreneurs can save their time, labor, and money by using this machine in harvesting paddy instead of conventional methods. There will be no problem in obtaining spare parts for the maintenance of the machine as it is manufactured locally. Farmers will get the machine at cheaper price if local assembly line is established and that will save foreign currency.

An attempt was taken to design and developed a power operated automatic rice seed sower machine to raise mat type seedling for mechanical transplanting. The design of the machine has completed and fabrication is under process according to design. This machine was fabricated at FMPHT divisional research workshop and Alam Engineering works, Wari, Dhaka as well. About more than 75% of fabrication work (tray conveyer, bed soil hopper, top soil hopper, power transmission system and different type of levers for controlling seed rate) has completed using locally available materials. Performance test will be done after the fabrication of the machine.

The BRRRI whole-feed combine harvester, model BRRRI WCH 2021, was developed under the SFMRA project. It underwent assessments during the Boro 2022 and Aman 2022 seasons in different locations in the Rangpur region of Bangladesh. To operate this harvester with a cutting width of 1.5 meters at maximum capacity, the field should be more than 1,500 square meters. The harvester was determined to have a theoretical total of 0.23 hectares per hour, but the actual field capacity is 0.11 hectares per hour. The harvester's field efficiency was 62.5% in the Boro season and 57.9% in the Aman season. Additionally, it was noted that in the Boro season, the harvester consumed 2.77 liters of fuel per hectare, while in the Aman season, this figure was 2.31 liters per hectare. The optimal total grain losses (1.64%) were observed at a moisture content of 23.2% and a forward speed of 3.5 kilometers per hour. The average losses, including various losses during harvesting, were 0.56% in the Boro season and 0.48% in the Aman season. Compared to manual harvesting, the BRRRI whole-feed combine harvester reduced paddy losses by 5.81%. The evaluation showed that the harvester operated effectively, and using it during peak periods could reduce the need for manual labor. This technology is expected to provide sustainable mechanization for rice harvesting to advanced farmers, promoting the adoption of improved practices in Bangladesh. The performance of the BRRRI combine harvester was rated as good and very satisfactory, indicating its suitability for use in both small and large fields.

The FMPHT Division of BRRRI has developed a prototype of whole feed mini combine harvester at divisional workshop. which was aimed to develop a machine that was simple and cost-effective to produce but boasted a high capacity inexpensively, had a high capacity and required minor repair and maintenance. The third whole-feed combine harvester prototype was developed in the FMPHT departmental workshop while considering the challenges encountered with the earlier models. The most difficult phase in operating the machine arises during grain harvesting, where improper handling could lead to significant crop losses, consequently impacting farmers' income. Preliminary tests were conducted in the BARI research field to assess its preference in capacity, travel speed, fuel consumption, grain and straw output. The whole-feed combine harvester demonstrated a harvesting capacity ranging from 0.252 to 0.262 ha/h, with a fuel consumption of 3.00 to 3.50 l/h. The field efficiency for the developed combine is about 71%. The average grain and straw output were recorded at 1013.88 and 922.06 kg/h, respectively. The machine exhibited a crop throughput of 1935.94 kg/h. The estimated pre-harvest loss for the selected field was 27.19 kg/ha at 14% moisture content. The total grain loss for the developed combine harvester was 1.27%. Further comprehensive performance tests are imperative to obtain more detailed insights into the capabilities of the BRRRI-developed whole-feed combine harvester.

A total of 08 systematic trials were conducted in farmers field during Boro 2022-23 and Aman 2023 seasons (report of Boro 2022-23. Treatments of the study were T_1 = One weeding by developed power operated weeder (PoW) succeeded by (sb) one hand-weeding (HaW); T_2 =

Herbicide application (Pyrazosulfuron ethyl@125g/ha), T₃ = One weeding by manual weeder sb one HaW (Local practice), T₄ = No-weed, and T₅ = Unweeded (Control). The actual and theoretical field capacity of the multi-row power weeder were found 0.23 and 0.285 hah⁻¹ whereas average field efficiency was found 81.66%. The specific fuel consumption of the weeder was found 0.384 l/hp-h while fuel consumption per hectars were 2.40 and 1.18 liter in Habiganj and Sirajganj, respectively. Saving over traditional or manual weeding of the BRRRI manual weeder and BRRRI power weeder is 9.8 and 11.5 thousand tk/ha, respectively.

Another 12 trials were conducted to observe the field performance of the head feed and whole feed combine harvesters under different field length, crop density, cutting height and operator stillness entitle "Validation and grain loss assessment of the different model of paddy combine harvesters. Aman, 2022: Habiganj: FMWORLD Ruilong and Sirajganj: Yanmar AG600A. Field performance was measured under the field length of less than 30m, 30-40m, 41-50m, 51-60m, and above 60m. All the parameters of forward speed, effective field capacity, and field efficiency increased with the increased field length. The highest field efficiency of the head feed combine harvester was found 80.49% in Sirajganj-1 under the field length of 61-65 meters. Irrespectively, lower field efficiency was observed because of 37-38% in Habiganj. It might be concluded that the field length must be more than 40 m for getting 50% field efficiency of the machine. However, grain loss of the head feed combine harvester is less than 1% while it was about 1.81% for the whole feed combine harvester. In addition, power and hydraulic system transmission analysis of a whole feed combine harvester is conducted. Boro, 2022-23: Yanmar and Marksan. The mean value of field efficiency (FE), effective field capacity (AFC), forward speed (FS) and fuel consumption (FC) of Yanmar combine harvester were 53.00%, 0.28ha/hr, 3.41km/hr and, 28 l/ha and, respectively. The mean value of FE, AFC, FS and FC of Marksan were 50 %, 0.24 ha/hr, 3.33 km/hr and 33 l/ha, respectively. The Yanmar and Marksan model combine harvesters had break-even areas of 29 and 26 ha, cost savings of 77 and 73%, and labor savings of 68%, respectively.

A total of 08 validation trials were conducted during the reporting periods of which 04 were in Boro, 2022-23 and 04 were in Aman 2023 seasons. Boro, 2022-23 season. Treatments of the trials were - T1: Machine transplanting with 100% urea fertilizer, T2: Machine transplanting with 80% urea fertilizer, T3: Machine transplanting with 70% urea fertilizer, T4: Machine transplanting without fertilizer and T5: Farmers practice. The actual field capacity of the rice transplanter varied from was found 0.15 to 0.22 hah⁻¹ with fertilizer deep placement while it varied from 0.22 to 0.25 hah⁻¹ without fertilizer deep placement mechanism in Boro 2022-23 season, respectively. Field efficiency varied from 63 to 86% with fertilizer deep placement while it varied from 60 to 84% without fertilizer deep placement mechanism. Field capacity was found higher to some extent without fertilizer deep placement mechanism during transplanting due to extra fertilizer re-filling time and slow operation. It is observed in the liner regression curve (R² = 0.90) that the field performance of the rice transplanter cum mixed fertilizer applicator varied relatively in line with field length in an average of 04 locations (02 locations in Sirajganj and 02 locations in Habiganj) where 90% variable explained the prediction of field efficiency varied with the field length. In all location, treatment-1 gave significantly higher yield followed by treatment-2. Transplanting cost under 05 different treatments were 2371.4, 2218, 1927, 1635 and 20961 tk/ha. BCR of rice production under the mentioned 05 treatments were found 1.94, 1.85, 1.84, 1.78 and 1.42 during Boro, 2022-23 season.

The existing BRRRI Hydro-tiller was tested at BRRRI West byde to find out the causes of frequent tearing of hydro-tiller chain. Its capacity was found 0.023 ha/h. The reason associated with the fault of hydro-tiller chain tearing was identified i.e. thickness of the chain is not sufficient to bear the load, strength of the bearing of the rotary box is not sufficient to bear the load. To overcome the problem, thickness of the sprocket was increased to 11 mm. ASME #60 chain was used instead of ASME #50 chain. Width of the ASME #60 chain is 23 mm. In addition, two bearing was set in combine to the rotary box shaft instead of single bearing to increase the strength of the Hydro-tiller in smooth operation at full load condition. Size of each bearing was 62 mm x 16 mm. The complete design of the modified hydro-tiller was done with the help of Solid works tool. After that, the modified hydro-tiller was tested at BRRRI west byde, Gazipur. After modification, the capacity of the hydro-tiller was increased to 0.039 ha/h. Average fuel consumption of the modified hydro-tiller was 2.01 l/h. The number of chain and belt tearing of the

hydro-tiller has been decreased drastically to below 8 per year after the modification. No event of engine stopping due to overloading arose during land cultivation.

The manual briquette machine offers a viable and accessible solution for producing biomass briquettes in areas with limited resources and electricity. While there are challenges associated with manual operation, the study's results demonstrate its potential for generating clean and efficient fuel sources. The manual briquette machine holds promise as a sustainable energy solution and a tool for community development.

BRRRI modified rubber roll husker and MNMP-15 polisher were used to evaluate the commercial value of rice milling parameters for BRRRI dhan104. For BRRRI dhan104, the modified rubber roll de-husker had a husking efficiency of around 90.97 %. In the MNMP-15 type polisher, milling recovery was 61.8%. The average head rice recovery based on input paddy was 52.67%, which is encouraging for quality rice processing. For better rice quality, steel engelberg huller can be replaced with one rubber roll de-husker and a polisher. Beside this, rubber roll de-husker separate husk and friction type polisher separate bran. Husk and bran collected separately were also suitable for briquette and edible oil production.

The BRRRI FMPHT division developed a solar-assisted paddy seed dryer with a central air distribution system. The study aimed to develop, manufacture, and test the prototype's performance. This report outlines the design, development, and fabrication of a solar-powered rice seed dryer specifically developed for the conditions of Bangladesh. The divisional workshop has already developed the machine. A black-painted solar collector was integrated into the dryer, designed to maximize the capture of solar heat and efficiently transfer it to the drying chamber. The dryer performed a preliminary test at BRRRI's FMPHT division to find mechanical problems in the unit. The ambient temperature varied between 27-34.8°C. The seed must dry for at least 10 hours if it has less than 15% moisture content. The machine was free of major flaws. The drying chamber capacity was 80-100kg of paddy seed. A complete performance test will be held at the FMPHT divisional research workshop throughout the upcoming season. Additional prototype development will be required to increase the machine's functions. This new dryer, which uses solar energy as its major heat source, intends to provide an efficient and environmentally friendly solution for paddy seed storage, thereby contributing to rice seed preservation and food security in the region.

The main focus of this study was to develop and fabricate a movable and portable solar panel carrier that enhances the accessibility and efficiency of solar energy utilization for small agricultural machinery and multipurpose use. The increasing demand for renewable energy has led to the development of portable solar panel systems that can be easily transported and deployed in different locations. The FMPHT division of BRRRI initiated the design, development, and fabrication of a prototype of a self-propelled mobile solar panel carrier, known as a portable solar-power bank (3 kW), for multipurpose use of solar energy. This carrier is an innovative solution for the efficient and safe transportation of solar panels. Using locally available materials, the movable/self-propelled solar panel carrier prototype was manufactured in the FMPHT divisional workshop. The carrier has 150-watt 20 solar panels, and a solar inverter (3-phase pure sine wave with MPPT and VFD) was incorporated into it to convert solar energy (DC) to alternative current (AC) where the input voltage and output power of the inverter were 300V (MPPT) and 3000VA, respectively. The carrier has 12-volt 130 Ah 04 batteries installed to provide power to the carrier and others. There is an MMPT battery charger (48 Volt, input=300 V (MPPT), Charging Current=10 Amps) for charging batteries. The solar energy produced by the panels in this solar panel carrier was used to power only 0.5, 1.0, and 2 horsepower motors. For the initial test, only the motors were run throughout the day. This 3-kW panel was initially able to run a 2-horsepower motor all day. The effectiveness of the developed system in using solar energy to operate small agricultural machinery will be evaluated in the coming season. Solar panel carriers designed for easy transportation of solar panels need to be further modified to harness solar energy properly.

This research evaluates the impacts of climate change on Thermal Bioclimatic Indicators (TBIs) in Bangladesh, a region vulnerable to climate change and heavily reliant on rice cultivation. Using a multi-model ensemble of 18 bias-corrected CMIP6 GCMs, the study projects variations in TBIs under three socio-economic pathways (SSPs) for near, mid, and far future periods. The findings indicate an anticipated increase in average annual temperature in Bangladesh, with variations depending on the SSP scenario. The study also predicts a potential decrease in the

diurnal temperature range and variations in temperature changes across different regions. The results suggest an increasing threat to rice cultivation due to rising temperatures and varying impacts across regions. The study calls for urgent climate change mitigation strategies and the integration of climate-resilient approaches in rice cultivation to safeguard food security and farming communities. The findings highlight the pressing need for policymakers and stakeholders to address the challenges posed by climate change to ensure the sustainability of rice production in Bangladesh.

This study investigated compound extremes in the coastal region of Bangladesh and West Bengal, India, from 1971 to 2021. Four types of compound extremes were analyzed: dry/cold, dry/hot, wet/cold, and wet/hot. The frequency and spatial extent of these extremes varied across seasons and regions. Pre-monsoon and monsoon seasons showed higher occurrences of dry/hot extremes, while post-monsoon and winter had more dry/cold extremes. Changes over time revealed an increase in hot extremes during pre-monsoon and a decrease in compound extremes during monsoon and post-monsoon (except in Sundarbans), as well as a decrease in most compound extremes during winter. The study also found significant relationships between compound extremes and large-scale atmospheric circulation modes. These findings emphasize the complex interactions between precipitation, temperature, circulation patterns, and compound extremes, highlighting the need for comprehensive adaptation strategies to address changing climate impacts. Further research is needed to deepen our understanding of these relationships and their long-term consequences.

Total 56 batch of two day long residential training programme was conducted under financial and technical support of SFMRA project of FMPHT division during the period of 2021-2022. Participants of the training programme were attended from all BRRI regional station adjacent area and from its jurisdiction districts. Total 1154 numbers of participants were trained among them 1085 were male and 69 were female. Participant were trained on operation, repair and maintenance of different agricultural machinery and technologies like; transplanter, combine harvester, diesel engine, power weeder, prilled urea applicator, self-propelled reaper, power tiller etc theoretically and practically in the threshing floor and in the main field. At the end of the training, a post-evaluation and trainee's reactions regarding the training were collected. Certificates, leaflets and a set of tools were distributed among the participants. Trainees opined that they are now more confident about the use of the agricultural machinery.

A total of 08 training programs and 14 demonstrations were conducted in the project locations on the proposed technologies under KGF funded project. Skilled manpower in machine operation were developed proving hands on training.

USEFUL SCIENTIFIC INFORMATION

PROJECT 1: AGRICULTURAL MACHINERY DEVELOPMENT AND TESTING

Experiment 1.1: Design, development, and performance assessment of a BRRI head feed combine harvester

Principal Investigator: AKM Saiful Islam

Co-Investigator: AUK, MKP

Objectives

- To design and develop of BRRI head feed combine harvester
- To evaluate the field performance of the developed head feed combine harvester
- To compare the performance with imported combine harvester

Materials and Methods

A prototype of a self-propelled combine harvester was fabricated at Alim Industries Ltd in Sylhet in collaboration with other local agricultural machinery manufacturers. The prototype was assembled using locally sourced raw materials, except for the crawler, gearbox, and engine. The rubber track/crawler and engine were imported with the assistance of a local agricultural machinery importer. Additionally, the gearbox was imported and utilized with certain modifications.

Design Consideration

The concept for the head-feed combine harvester was developed in response to the increasing demand from Bangladeshi farmers, aligning with the goals set in the mechanization roadmap and policy. The head-feed combine harvester comprises a basement, main body, engine unit, header, conveying hopper, threshing, and storage units. Besides enhancing operational conditions for the operator, the machine is designed to offer adequate visibility lighting when necessary. The design of the BRRI head-feed combine harvester was accomplished using AutoCAD engineering tools (software). The technical specification of BRRI Head Feed Combine Harvester shows in Table 1. The machine prototype was manufactured at Alim Industries Ltd in Sylhet, adhering to the design. Laboratory and field tests for the developed head-feed combine harvester were conducted in workshops and farmers' fields under load and unloading conditions.

The Design steps of proposed BRRI head feed combine harvester were as follows:

<p>First step</p> <p>➤ Walking Section</p> <ol style="list-style-type: none"> 1. Original Base Assembly 2. Walking Wheels Assembly 3. Double Brace Bar Assembly 4. Guide Wheel Assembly 5. Supporting Wheel Assembly 6. Thrust Wheel Assembly 7. Crawler Assembly 	<p>Second step</p> <p>➤ Main Power Section</p> <ol style="list-style-type: none"> 1. Main Gear Box Assembly 2. Engine Assembly
<p>Third step</p> <p>➤ Operating Section</p> <ol style="list-style-type: none"> 1. Panel Board Side Assembly 2. Ready water Box and Cover Assembly 3. Manipulation Turning Assembly 4. Main Gearshift Operating Assembly 5. Auxiliary Gearshift Operating Assembly 6. Working Clutch Operating Assembly 7. Walking Clutch and Tension Wheel Assembly 8. Reel Lifting up/down Operating Assembly 9. Parking Brake Assembly 10. Tension Pulley Assembly 	<p>Fourth step</p> <p>➤ Hydraulic Section</p> <ol style="list-style-type: none"> 1. No. 1 Slide Valve Hydraulic System Assembly 2. No. 2 Slide Valve Hydraulic System Assembly 3. HST Type Oil Supply System Assembly 4. Hydraulic Oil Tank Assembly 5. Hydraulic Transmission Input Assembly

<p>Fifth step</p> <p>➤ Cleaning Section</p> <ol style="list-style-type: none"> 1. Left and Right Rack Plate Assembly 2. Front Fan Assembly 3. Vibrating Screen Assembly 4. Screen Plates Assembly 5. Straw-Expelling Plate Assembly 6. Screen Body Assembly 7. Separating Plate Assembly 8. Vibration Screen Rear Axle Assembly 9. Cylinder Assembly 10. Suction Fan Gear Box (internal) Assembly 11. Suction Fan Gear Box (external) Assembly 12. Suction Fan Guide Assembly 	<p>Sixth step</p> <p>➤ Grain Conveying Section</p> <ol style="list-style-type: none"> 1. No. 1 Conveying Auger Assembly 2. No. 1 Horizontal Auger Assembly 3. No. 2 Conveying Auger Assembly 4. No. 2 Horizontal Auger Assembly 5. No. 1 Bottom Gearbox Assembly 6. No. 1 Lifting / Conveying Auger Assembly 7. No. 2 Lifting / Conveying Auger Assembly 8. No. 2 Bottom Gearbox Assembly
<p>Seventh step</p> <p>➤ Threshing Section</p> <ol style="list-style-type: none"> 1. Left and Right Rack Plate Assembly 2. Concave Screen Assembly 3. Separation Drum Assembly 4. Dusting Fan Assembly 5. Upper Frame Assembly 6. Rack Assembly 7. Rotary Axis Assembly 8. Tension Assembly 9. Roller Cover and Roller Cover Handle Assembly 10. Resale and Open Handle Assembly 11. Roller Shaft Assembly 12. Threshing drum Barrel and Threshing Drum Tooth Assembly 13. Feeding Chain Frame Assembly 14. Feeding Chain Assembly 15. Row of Grass Ear End Chine Assembly 16. Grass Guide Assembly 	<p>Eighth step</p> <p>➤ Large Grain Tank Section</p> <ol style="list-style-type: none"> 1. Big Grain Tank 2. Portfolio Cover Assembly 3. No. 3 Vertical Auger Assembly 4. Welded No. 3 Horizontal Auger Assembly 5. No. 3 Bottom of the gearbox combination Assembly 6. Gearbox Assembly 7. Transmission Input Assembly
<p>Ninth step</p> <p>➤ Header Section</p> <ol style="list-style-type: none"> 1. Harvest Gear Box and Harvest Shaft Box Assembly 2. Harvester Drive Case and pick-up Driving Shaft Assembly 3. Pick-up Speed Change Case and Pick-up Gear Case Assembly 4. Pick-up Drive Case Assembly 5. Right Crop-Root Conveying Case 1 and 2 Assembly 6. Left Crop-Root Conveying Case and Feed Case Assembly 7. Harvest Frame and divider Assembly 8. Pick-up Frame and Pick-up Chain Assembly 9. Side Cover and Pic-up Support Assembly 10. Dustproof Cover and Blade Reaping Assembly 11. Blade Reaping Crank 1(LH) and 2(LH) Assembly 12. Blade Reaping Crank 1(RH) and 2(RH) Assembly 13. Packer Left, Center, Right Assembly 14. Conveying Left, Center, Right Assembly 15. Conveying guide Bar and Crop-Root Frame LH/RH Assembly 16. Crop-Root Rail, Crop-Root Tension and Crop-Root Retainer Assembly 17. Crop-Head Frame 1 and 2 Assembly 18. Crop-Head Tension 1 and 2 Assembly 19. Feeding Frame and Crop- Root Feed Cover Assembly 20. Rail Base and Crop-Head Guide Plate Assembly 21. Depth Frame and Depth Chain Assembly <p>Depth Swing Case and Depth Motor Assembly</p>	

Field performance

The performance of BRRI developed head-feed combine harvester was assessed in the field during the Aman 2023 season (Plate 1). The evaluation occurred at the BADC farm, farmers' fields in Sylhet district, and the West Byed research plot at the Bangladesh Agricultural Research Institute. Notable attendees included the Honorable Secretary of MoA, Director General of Research Institutes, Director (Research), Director (Admin & Common Service), Project Director, Divisional scientists, teachers from Bangladesh Agricultural University, local agricultural machinery manufacturers, operators of imported combine harvesters, and farmers. Every one present during the field test expressed satisfaction with the effectiveness of the head-feed combined harvester.

Further development and detailed studies are planned for the upcoming Boro and Aman seasons in 2024 and 2025.



Plate 1. Field performance of the developed BRRi head feed combine harvester.

Table 1. The specification of the BRRi head Feed Combined Harvester.

Particulars	Unit
Model	BRRi HCH2023
Dimension, (L×W×H) mm	4250×2030×2580
Cutting width, mm	1450
Engine power, hp	77
Rubber track (Crawler)	400×90×51
Grain tank, kg	500
Total weight, kg	2900
Ground clearance, mm	270
Harvesting capacity, hah ⁻¹	0.5-0.6
Fuel consumption, lh ⁻¹	10~11

Conclusion

This research has shown that it's possible to develop a combine harvester that addresses the harvesting challenges farmers face in Bangladesh. Every effort was made to reduce production costs significantly, making the combine harvester easily accessible to small-scale farmers in the country. It is more efficient for harvesting rice from scattered farmlands in Bangladesh and has an advantage over imported combine harvesters. The head-feed combine harvester developed in this study is more efficient and provides a distinct advantage over imported alternatives. With support from favorable policies and financial backing from the government, the BRRi-developed combine harvester has the potential to meet domestic demand for agricultural machinery, reduce reliance on imports, and even explore opportunities for exportation.

Experiment 1.2: Design and Development of a BRRi Automatic Seed Sower Machine for raising mat-type seedling

Principal Investigator: AKMSI

Co-Investigator: AUK, MKP, MMI

Objective

- To design, develop, and perform an evaluation of a BRRi automatic seed sower machine for raising seedlings in a tray

Materials and Method

A BRRi automatic seed sower machine was designed and fabricated at the FMPHT divisional research workshop using locally available materials. Careful analysis of material selection and metallurgy was undertaken to ensure the quality of the product. The machine's components include the main basement, bed soil hopper, seed hopper, water tank base, topsoil hopper, reduction gear, electric housing, and driver and driven shaft.

The machine was design by the AutoCAD Engineering tools and fabricated at Uttaron Engineering workshop of Dinajpur district. The Jigs & fixtures, molds for the main basement, soil hopper base, seed hopper base, water tank base, and motor basement were developed for quick replication. The technical specification of BRRi Auto Seed Sower machine shows in Table 2. Calibration for different soil types and various sizes of paddy seeds was achieved by adjusting the lever. The prototype's performance was tested in the FMPHT divisional research workshop, Uttaron Engineering at Dinajpur, and in farmers' fields. The results of the performance tests were

satisfactory. A detailed report on the design and fabrication of the BRRRI auto seed sower machine was included in the annual report for 2021-22.



Plate 2. Laboratory trial of BRRRI Auto Seed Sower Machine

Table 2. The specification of the BRRRI Auto Seed Sower Machine.

Particulars	Unit
Model	BRRRI ASSM 2023
Dimension, mm (L*W*H)	3048×730×1135
Motor power, hp & rpm	0.5 & 1400
Bed soil hopper capacity, kg	80
Topsoil hopper capacity, kg	30
Seed hopper capacity, kg	10
Power transmission System	Chain Sprocket & Shaft
Total weight, kg	100
Speed of Sower(km/h)	Adjustable
No of Tray/min	28

Field performance of BRRRI Auto Seed Sower Machine

The machine is easy to fabricate using materials found locally in a workshop, and it can be operated by both men and women with minimal training. The distribution of bed soil is precisely adjusted using a lever. The seed distribution rate can be finely tuned with a brush adjustment meter, allowing for 120 to 160 grams of sprouted seeds to be placed in each tray. With the auto seed sower machine, a worker can sow seeds in 1680 trays per hour, a significant improvement compared to the 50-60 trays done manually. After sowing the sprouted seeds, the topsoil layer (6 mm) of each tray can be covered with loose soil. Controlling the seed sowing rate for different rice varieties is simple. The machine has a bed soil hopper, seed hopper, and topsoil hopper with capacities of 80 kg, 10 kg, and 30 kg, respectively.

Several trials were conducted at the FMPHT division of BRRRI, involving official personnel, local agricultural machinery manufacturers, and farmers (Plate 2). All participants in the field trial expressed satisfaction with the machine's effectiveness. As part of the SFMRA project, some machines have been given to the 'Mechanized Village' and regional stations of BRRRI for field-level extension and preparing seedling trays for mechanical transplanting. Introducing a community-based seedling production system using the machine could potentially create rural entrepreneurship. However, the machine should not be used if the germinated seeds are more than one day old or if the radical length is more than 2mm. In this model, the seed-sowing process is automated to reduce human effort and increase yield. A DC motor takes care of the automatic distribution of soil, water, and seeds. The BRRRI auto seed sowing machine is more efficient and less time-consuming. In the present era, all sectors, including agriculture, are progressing rapidly. To meet future food demands, farmers need to adopt new techniques that do not compromise soil texture but enhance overall crop production

The advantages of BRRRI auto Seed Sower machine are the Following

- Improved efficiency in seedlings.
- Increased yielding and reliability in crops.
- Increased cropping frequency.
- Increased speed of seed growth.
- Seed planting accuracy and uniform placement of seeds in trays.

Conclusion

The prototype of the BRRI auto seed sower machine was fabricated and tested in the FMPHT research workshop. It was adjusted for various soil textures and paddy seed sizes. The prototype performed well in tests conducted at research workshops and farmers' fields, yielding satisfactory results. Consequently, it is seen as a time-saving technology for preparing seedling trays for mechanical transplanting, potentially reducing the need for human labor. The design, creation, and automation of the model have been successful, making it suitable for large-scale use due to its minimal manpower requirements and straightforward installation process. This makes it accessible for a wide range of users. It can be concluded that (i) seed metering was accurate according to requirements, and (ii) there was no damage to the seeds during operation.

Experiment 1.3: Assessment of BRRI Whole Feed Combine Harvester (Model BRRI WCH 2021) for Mechanized Rice Harvesting

Principal Investigator: Arafat Ullah Khan

Co-Investigator: AKMSI, MKP, MGKB, MMI

Objectives

- To assess the field performance of the developed combine harvester
- To compare the performance with imported combine Harvester

Materials and Methodology

Study location

The field trial was conducted at Mithapukur upazila in Rangpur District which is located between 25°26' and 25°41' north latitudes and in between 89°06' and 89°27' east longitudes shown in Plate 3.

Crop and Soil Conditions

The condition of the crop (plant height, plant to plant distance, plant density, number of hills per square meter, hill to hill distance, and crop density, plants/m²) were determined using appropriate procedures (Table 3). The soil structure was identified for both as clay soil. The field experiment was carried out during Boro and Aman-2022.



Plate 3. Experimental field trial site.



Plate 4. Operating of paddy harvesting.

Table 3. Crop and field parameters of different paddy varieties.

Particulars	Plot-1	Plot-2	Plot-3	Plot-1	Plot-2	Plot-3
	Hybrid dhan	Hybrid dhan	BRRI dhan 74	BRRI dhan 34	BRRI dhan 93	BRRI dhan 95
Grain moisture content (w. b), %	22.3	25.5	23.4	19.4	20.7	23.6
Straw moisture content (w. b), %	24	21.5	25.7	20.3	23.1	24.2
Plant height, cm	115.6	115.2	106.8	135.3	112.3	128.5
Length of panicle, cm	107	108.4	92.3	121.7	101.5	117.2
No. of tillers per panicle, no	11.5	12.3	15.7	15.4	10.8	13.2
The number of hills/m ² , no.	14	13	14	17	14	12
No. of plants per hill	12	13	13	15	13	10
Straw grain ratio	1.24	1.27	1.45	1.40	1.56	1.61

Selected combine harvester

The BRRI whole feed combine harvester, specifically the BRRI WCH 2021 model, was selected and used for the paddy harvesting operation at the experimental site. This harvester is designed and manufactured by the Bangladesh Rice Research Institute (BRRI) as one of the SFMRA project objectives. The visual representation is in Plate 4 and detailed technical specifications are shown in Table 4.

Paddy harvesting using BRR I Combine harvester

Three plots were carefully selected to assess the operational parameters of the harvester, which included operational speed, field capacity, fuel consumption, and grain losses attributed to the combine harvester. The plot sizes were determined using a measuring tape. Additionally, three smaller areas, each measuring 1 meter by 1 meter, were randomly chosen within the plot to evaluate shattering loss. Following harvesting, three 1 meter by 1 meter plots were randomly designated, and any scattered grain/spikes within those areas were collected. It is worth noting that all tasks related to paddy harvesting, from the actual harvesting to the subsequent cleaning processes, were seamlessly executed in a single pass of the combine.

Table 4. The technical specification of the BRR I Whole Feed Combined Harvester (Model No-BRR I WCH 2021).

Particulars	Unit
Model	BRR I WCH 2021
Dimension, (L×W×H) mm	5200×1800×2600
Threshing drum (L, Φ)	2000mm, Φ620
Cutting width, mm	1500
Engine power, hp	87
Rubber track (Crawler)	400×90×51
Fuel tank, l	60
Grain tank capacity, kg	600
Power transmission	Mechanical + HST
Total weight, kg	3000
Ground clearance, mm	300
Traction load, kNm ⁻²	20.7
Traction Area, m ²	1.376 for two crawlers
Harvesting capacity, ha/h	0.45-0.5
Forward speed, kmh ⁻¹	3-4
Fuel consumption, lh ⁻¹	11-12
Total harvesting loss, %	Less than 1%

Performance representing parameters

Various parameters were considered to comprehensively assess the technical performance of the BRR I combine harvesters during the paddy harvesting process. These parameters covered the following key aspects: (i) operational time, (ii) labor required for harvesting, (iii) fuel consumption, (iv) field capacity, (v) working speed, (vi) effective harvesting time, (vii) grain yield, and (viii) grain losses. Each of these parameters played an important role in evaluating the overall efficiency and effectiveness of the combine harvester in the context of paddy harvesting operations.

Field Capacity

Several key parameters were taken into account during the paddy harvesting operation to evaluate the field capacity. These parameters included measuring the plot's area, the machine's forward speed, the cutting width of the machine, and the time taken to harvest the designated area. Here, various standard equations were used for performance evaluation.

Forward speed, $S = 3.6 \frac{D}{t}$ (i)

Where, S = Forward speed (km/h), D = Distance (m), and t = Time (sec).

Theoretical field capacity (ha/h), $FC_{Theo} = \frac{A}{E}$ (ii)

Where, E = Effective operation time (h) and A = Area of land reaping at the specified time (ha).

Effective field capacity (ha/h), $FC_{Eff} = \frac{A}{T}$ (iii)

Where, T = total time for reaping operation (h) and A = area of land reaping at the specified time.

Field efficiency (%) = $\frac{\text{Effective field capacity}}{\text{Theoretical field capacity}} \times 100$(iv)

Fuel consumption (l/ha), $F = \frac{Fa}{A}$ (v)

where, Fa = Fuel used during operation (l) and A = Area of operation (ha).

Determination of mechanical harvesting losses

Postharvest loss is a critical indicator for evaluating combine harvester performance. In assessing postharvest loss, four distinct types of losses were taken into consideration in the context of using a combine harvester. These include i) shatter loss, ii) cutter bar loss, iii) cylinder loss, and iv) separating loss. In the experimental setup, specific procedures were employed to meticulously

measure these mechanical harvesting losses. This systematic approach ensured a comprehensive evaluation of the efficiency and effectiveness of the combine harvester in minimizing these various losses during the harvesting process.

Shatter loss

Shatter losses in direct combination pertain to the heads, pods, or ears, as well as free grain, that are lost during the cutting and conveying operations. The quantification of shattering loss was carried out using below the equation. This formula provided a reliable method for evaluating the extent of shatter losses incurred during direct combining, offering valuable insights into the efficiency of the harvesting operation.

$$\text{Shatter loss, kg/ha} = \frac{D}{A} \dots\dots\dots(vi)$$

Where,

D = Average grain dropped on the ground during cutting and conveying (kg) and
 A = Area Covered (ha)

Cutter bar loss

Cutter bar loss refers to the grains that were lost because of rough handling by the cutter bar during harvesting. The calculation for determining cutter bar loss was based on the equation. This formula serves as a valuable tool for quantifying the extent of grain loss attributable to the operation of the cutter bar, providing crucial insights into the overall efficiency of the harvesting process.

$$\text{Cutter bar loss (kg/ha)} = \frac{G}{A} \dots\dots\dots(vii)$$

Where,

G = Average weight of grain lost due to rough handling of the cutter bar (kg)
 A = Area Covered (ha)

Cylinder loss

Cylinder loss in the context of combine harvesting refers to grains lost out of the rear of the combine in threshed heads. The calculation for determining cylinder loss was established by through a specific equation. This formula provides a reliable means of quantifying the extent of grain loss attributed to the operation of the cylinder, offering valuable insights into the overall efficiency of the harvesting process.

$$\text{Cylinder loss (kg/ha)} = \frac{H}{A} \dots\dots\dots(viii)$$

Where,

H = Average weight of un-threshed heads lost out the rear of the combine (kg)
 A = Area Covered (ha)

Separating loss

Separating loss in the context of combine harvesting refers to the grains lost out of the rear of the combine in threshed grain. The determination of separating loss involved the utilization of equations. These specific formulas provide a structured approach for quantifying the extent of grain loss attributed to the separating process, offering valuable insights into the overall efficiency of the harvesting operation.

$$\text{Separating loss (kg/ha)} = \frac{K}{A} \dots\dots\dots(ix)$$

Where,

K = Average weight of threshed heads lost out the rear of combine (kg)
 A = Area Covered (ha)

Total loss

The total harvesting loss was calculated by aggregating all individual losses incurred.

$$\text{Total loss, L (g)} = \text{Shutter loss (g)} + \text{Cutting loss (g)} + \text{Gathering loss (g)} + \text{Carrying loss (g)} + \text{Threshing loss (g)} + \text{Cleaning loss (g)} \dots\dots\dots(x)$$

$$\text{Loss (\%)} = \frac{Y}{L} \times 100 \dots\dots\dots(xi)$$

Where, Y = Total yield (g) and L = Total loss (g)

Results and Discussion

Field capacity of combine harvester concerning plot length

The efficiency of the BRR1 combine harvester varied depending on the plot length, mainly influenced by how often the harvester had to turn. When the plot length increased, the field capacity of the combine harvester also increased. It is noteworthy that the lowest field capacity was observed in plots with a length of 25.6 m. These findings highlight the importance of having a plot length exceeding 38.6 m for the optimal operation of the BRR1 combine harvester, especially

when it is fitted with a 1.5 m cutting width. This setup allows for fewer turning events, improving overall efficiency during the harvesting process.

Field Efficiency

The field productivity of the BRRRI combine harvester is closely connected to the size of the land it operates on. The performance of the combine harvester exhibited variation based on the land size. Specifically, field efficiency showed an upward trend with an increase in land size. The highest levels of field efficiency were observed in plots exceeding 1200 m². Conversely, plots with an area of 800 m² recorded the lowest field efficiency. These findings underscore the substantial impact that land size has on the operational efficiency of the BRRRI combine harvester, emphasizing the importance of selecting appropriately sized plots for optimal performance.

Table 5. The technical performance of combined harvester.

Plot	Forward speed	Fuel Consumption	Effective Field Capacity
	(km/h)	(l/h)	(ha/h)
1	3.00	11.25	0.00366
2	3.50	11.50	0.00263
3	4.00	11.53	0.00270
Aver.	3.5	11.43	0.00210

Field performance of BRRRI combine harvesters

The results show that the combine harvester's operational speed varied between 3.0 and 4.0 km/h during harvesting. According to ASAE Standards (2009), larger and medium-sized combine harvesters typically operate in a range of 3 to 6.5 km/h during harvesting. In the case of the mini combine harvester, the theoretical and actual field capacity were measured at 0.19 and 0.11 ha/h, respectively (Table 6). For whole-feed and head-feed combine harvesters, the theoretical and effective field capacities were found to be 0.50 and 0.36 ha/h, respectively. It is worth noting that the lowest field capacity (0.67 ha/h) was associated with the highest loss time (1.54 h) during the paddy harvesting operation, resulting in a relatively lower actual field capacity (Table 6).

Table 6. Field capacity and efficiency of combined harvester.

Parameters	Plot-1	Plot-2	Plot-3	Plot-1	Plot-2	Plot-3
	Boro/2022			Aman/2022		
Travel speed (km/h)	3.25	3.5	4.0	3.25	3.5	4.0
Working width (m)	1.5	1.5	1.5	1.5	1.5	1.5
Total work time (min)	22.35	15.32	26.07	29.08	20.41	25.2
Delivery time (min)	1.52	1.39	2.36	2.46	1.45	2.13
Operation time (min)	21.23	14.33	24.12	27.03	19.46	23.07
Turning Time (min)	9.23	5.47	8.15	9.45	6.46	8.19
EFC (ha/h)	0.12	0.10	0.07	0.08	0.11	0.09
TFC (ha/h)	0.23	0.16	0.18	0.21	0.19	0.21
FE (%)	52.17	62.5	38.9	38.2	57.9	42.85

Grain loss during harvesting and the efficiency of the harvester are illustrated in Figs. 1 and 2, respectively. Although the harvesting capacity of the BRRRI combine harvester might be considered relatively low, its standout feature is its adaptability to both smaller and larger fields, which is a significant advantage.

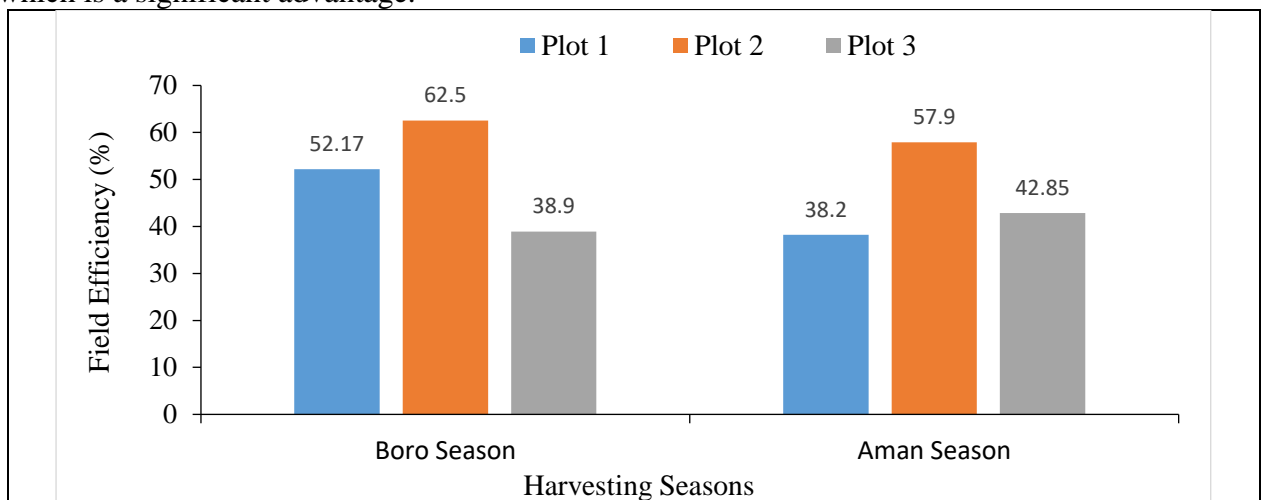


Figure 1. Field Efficiency (%) of BRRRI combined harvester regarding seasons.

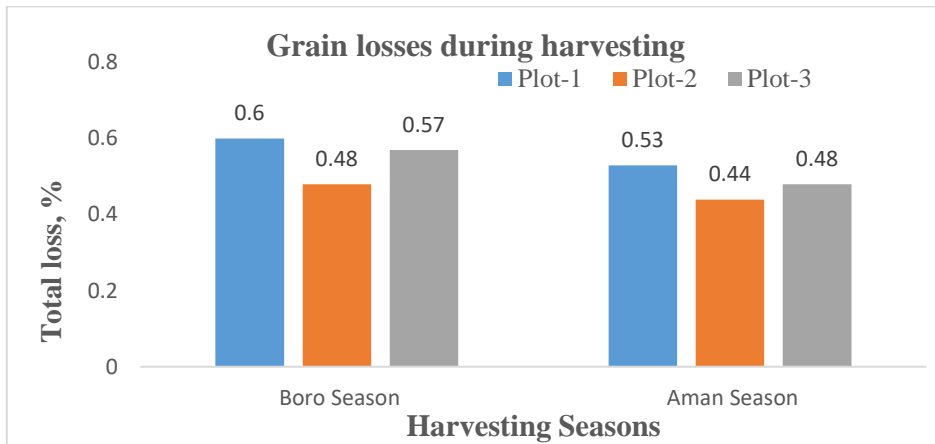


Figure 2. Grain losses during harvesting seasons shown in the graph.

Time distribution of combined harvester operation

During the harvesting operation, the time allocation for the BRRI combine harvester was distributed as follows: 58% was spent in actual harvesting, 23% in turning maneuvers, and the remaining 19% encompassed activities like repairs, idle time, and work stoppage due to rain. In contrast, medium-sized combine harvesters devoted 71.7% of their time to harvesting and the remaining 28.3% to turning, maneuvering, and unloading. Turning, reversing, and unloading are essential but time-consuming activities; the goal is to minimize the time lost, as it can account for as much as 40% of the operation's duration (Fig. 3). This unavoidable time loss can be mitigated with strategic planning and innovative practices.

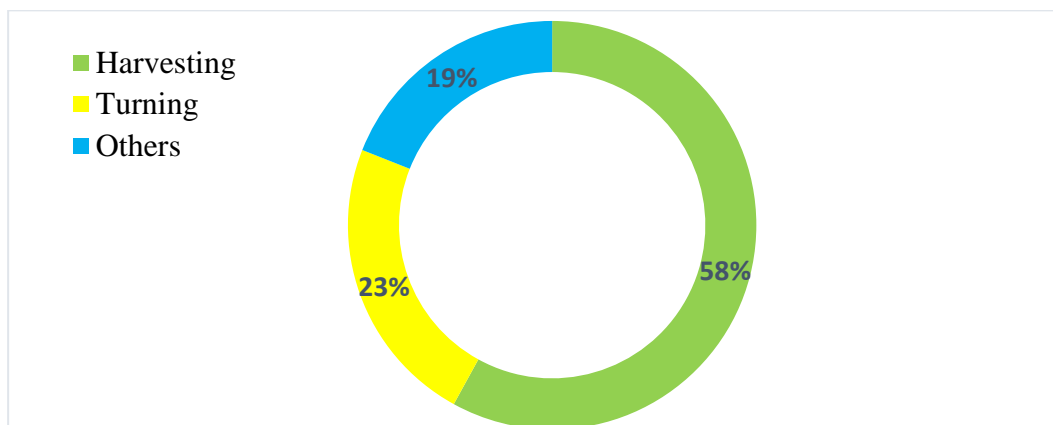


Figure 3. Time distribution of BRRI WCH operation during harvesting of paddy.

Conclusion

The evaluation of the BRRI combine harvester has concluded with very positive results, highlighting its versatility in handling both small and large fields makes it widely applicable. For optimal performance with a 1.5 m cutting width, it is recommended to operate on plots exceeding 1500 m². The harvester has a theoretical field capacity of 0.23 ha/h, with an actual capacity of 0.11 ha/h. The best grain loss rate (1.64%) was achieved under specific conditions, including a moisture content of 23.2% and a forward speed of 3.5 kg/h. The introduction of BRRI's whole feed combine harvester signifies a transformative era for Bangladesh's agriculture.

Experiment 1.4: Performance test of the BRRI developed whole feed combine harvester

Principal Investigator: Md. Durrul Huda

Co-investigator(s): SP, MGKB, AUK

Objectives

- To conduct the performance test of the developed combine harvester
- To compare the performance with imported combine

Materials and methods

Combine Harvesters

A combine harvester is an item of machinery that can harvest, thresh, clean, and bag crops in one operation. The mature rice crop is removed from the field using mechanical or mechanical harvesting. Cutting, threshing, cleaning, loading, and bagging are all aspects of harvesting. BRRI started the development of a Combine Harvester at the FMPHT Divisional Workshop in Gazipur. Using resources readily available in the local region, the FMPHT Divisional Workshop at BRRI, Gazipur, created a prototype medium-type whole feed combine harvester. The FMPHT

departmental workshop has finished the manufacture of this particular combine harvester. Specifications, known second-edition drawbacks, and recommendations are all design factors. An initial evaluation test was conducted to find any machine defects or issues. This version had a few problems discovered and fixed in the department's internal workshop. Some matters were later discovered and fixed during field testing.

The mode of operation for the whole feed combine harvester

The harvester's main operating system is divided into five sections: Reel, cutting, container, and auger units, which comprise the header. A feeder that has a powered roller and conveyor belt. The threshing drum, sieve, and blower make up the threshing unit. The transmission system unit comprises the following components: the engine, shafts, pulleys, belts, wheels, hub, brakes, suspension system, and storage unit with a grain pan and cover. This self-propelled combine harvester has a thresher with (101×61×125) cm (L×W×H) measurements and a 32-horsepower diesel engine. V-belts transferred power from the engine shaft to various machine parts. The machine's main shaft generates 32 horsepower, and its ideal operating speed is 2200 rpm. Depending on the crop and field circumstances, the machine's speed changed. The belt pulley, ideal pulley, chain, and shaft were used to transfer the main power to the driving wheel, thresher, and cutting component. Plate 5 shows an entire view of a combine harvester. The cutting and gathering process of the grain will be accrued from the reeling unit and cutting unit, which will then be conveyed from the auger to the feeder and presented to the threshing unit. As the machine moves, the divider separates the crop for cutting, the reel picks up the laid or standing crops and pushes them to the cutting mechanism, and finally, the reel pushes the crops down to the platform after cutting. The retracting fingers send the crop to the inclined conveyor chain, which feeds it into the thresher. The grain will be threshed using threshing teeth attached to threshing drums spaced along the grain's length under rotational force. These fingers, which make up the threshing combs, are thin metal rods that have each been given a short arc of carving. The grains may be separated because of the tiny space between the sieve and the comb. There, the platform auger transports in an across way. The concave and cylinder assembly of the thresher are crucial in separating most of the crop into seeds, chaffers that fall directly onto the grain pan, or a conveyor. After detachment of the grains from the ears, the sieve will separate the grains for storage, and the straw will be blown out through the straw channel to the ground. However, the general threshing problem is either over-threshed or under-threshed. Over threshing, which could damage grains due to the high speed of the thresher, is taken care of by the engine's speed but with the possibility of fine straws escaping with the grains, which can easily be cleaned later before storage. The straw and remaining seed are directed onto the straw carrier by the cylinder beater, which tends to strip the threshed material from the cylinder and aid in further separation at this point. The straw is transported rearward to be discharged from the machine while being stirred by the straw carrier, separating any leftover seed and un-threshed heads. The grain return conveyor collects the particles removed from the straw and then transports them to the grain pan in front of the chaffer sieve. Grain that has been threshed, along with some chaffer and small debris drops from the concave sieve, is combined and then sent through a vibrating sieve, cleaned by working together with a blower fan. After washing, a horizontal auger and a lifting auger transport the grain to the grain tank. Following threshing, the straw in the thresher is discharged onto the ground through the straw exit. The threshed and clean grain will be released at the bagging platform through a grain delivery spout in the bag or tank. However, all these processes cannot be achieved without the transmission system. Although the harvester does not have a standard braking system because of its speed, a provision for a stopping mechanism was provided. The entrance door beside the driver seat leads to the engine compartment so the driver can access the engine anytime in an emergency. Also, there is a provision for a hand lever near the driver seat link to the rear tires that can bring the harvester to a halt. The harvester will also have supportive components such as lightning, hitch, windows shield cover, and belt cover.

Test and evaluation process

After the prototype's fabrication, a performance test was performed, and problems were found by analyzing the test findings, leading to further modification. The initial performance test was previously performed during the Boro/2023 season to look for performance, efficiency, and operational faults. Some problems were identified by analyzing the test results, and further modification is running in the divisional workshop. The test and evaluation processes of the developed machine are shown in Figure 4.

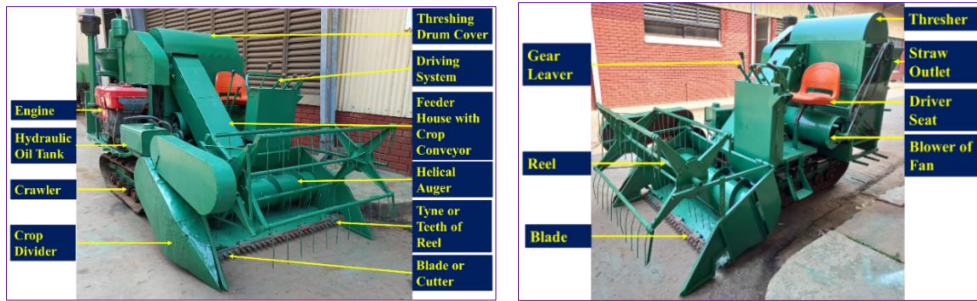


Plate 5. The complete view of the BARI whole feed combine harvester.

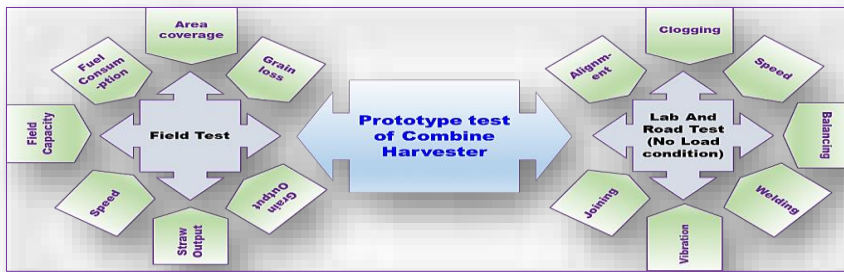


Figure 4. Test and evaluation process of the developed machine.

Tools and materials

This research was conducted at the Bangladesh Agricultural Research Institute (BARI), Gazipur. The tools used in this study BARI developed a combined harvester. The material used in this study was the rice crop.

Investigational activities

Harvest capacity calculation

Calculation and data on harvest potential and wages are obtained by first calculating the capacity and potential of each crop using an equation of harvest capacity (HC)

$$HC = \frac{\text{Crop harvest (kg)}}{\text{Area (m}^2\text{)}} \times 10000 \text{ m}^2 \dots\dots\dots(i)$$

Calculating equipment field efficiency and formulas used include

The forward speed of the combine harvester was calculated using the equation shown below.

1. Forward speed (km/hr), $S = \frac{6.3D}{t} \dots\dots\dots(ii)$

Where, D = distance (m) and t = time (s).

2. Theoretical field capacity (TFC) = $\frac{SoWc}{10}$ (ha/h).....(iii)

Where, TFC is the theoretical field capacity, ha/h; W_c is the cutting width, m; S_o is the operating speed, km/h

3. Effective field capacity (ha/hr), $EFC = \frac{A}{T_p+T} \dots\dots\dots(iv)$

Where, A = area covered (ha); T_p = productive time (hr); and T = non-productive time (hr) such as the breakdown in a field

4. Field efficiency (FE) = $\frac{TFC}{EFC} \times 100 \dots\dots\dots(v)$

Where, FE = field efficiency (%); EFC = effective field capacity (ha/hr); TFC = theoretical field capacity (ha/hr).

Fuel consumption

Fuel consumption (L/ha), $F = \frac{Fa}{A} \dots\dots\dots(vi)$

Where, Fa = fuel used during operation (L) and A= area of operation, (ha)

Moisture conversion formula

$$Wt \ 14\% = \frac{Wt_1(100 - MC_1)}{86} \dots\dots\dots(vii)$$

Where, Wt 14% = final weight at 14% moisture content, Wt_1 = initial wet weight, MC_1 = initial moisture content %

Combine harvester capacity: Included in this are the parameters of net grain output (kg/h and kg/ha), grain throughput (kg/h and kg/ha), straw output (kg/h and kg/ha), and crop throughput (tons/h).

Net grain output

Net grain output (kg/h) = (3.6 X Weight of grain sample)/ Average time for 20 m length... (viii)

Net grain output (kg/ha) = (10 X Weight of grain sample)/ Area covered in 20 m run..... (ix)

Grain throughput

Grain throughput (kg/ha) = (10 X total wt. of grain)/Area covered in 20 m run..... (x)

Grain throughput (kg/h) = Grain throughput (kg/ha) X Rate of work (ha/h) (xi)

Straw output

Straw output (kg/ha) = (Weight of straw X 10)/ Area covered in 20 m run.....(xii)

Straw output (kg/h) = Straw output (kg/ha) X Rate of work (ha/h) (xiii)

Crop throughput

Crop throughput (kg/h) = Grain throughput (kg/h) +Straw output (kg/h) (xiv)

Major Losses in Combine Harvester Operation

A combine harvester is a sophisticated, self-propelled farm machine that performs several functions. It is helpful to understand the processes in the combine before making any changes or adjustments to prevent losses. The header unit, where the grain is harvested and gathered, is where the operation of a combine harvester highlighted in Figure 5 begins. After being delivered, the material is processed, cleaned, and separated (straw walker) in a threshing unit. Straw and chaff are thrown into the field, while the cleaned grain is moved to storage tanks. The grain is bagged and moved elsewhere after the grain tank is full. Header losses (losses at the front of the harvester) and combine losses (losses at the threshing, separating, and cleaning units) or collection losses and processing losses are two categories for crop losses in the field caused by harvesting.

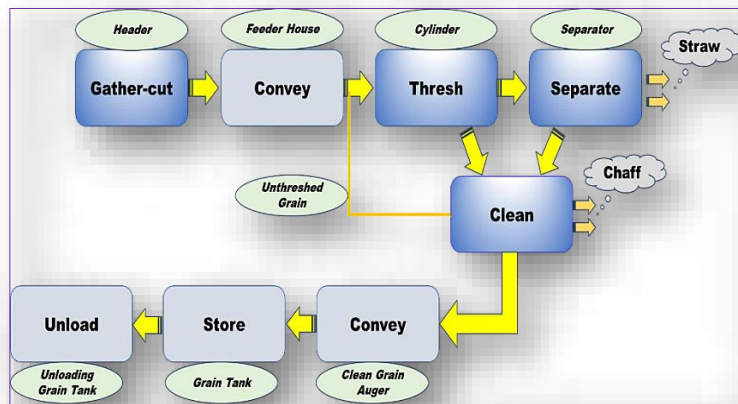


Figure 5. Procedure for operating a combine harvester indicating parts where losses occur frequently.

A good combine operation must consider the selection of the correct harvesting settings to reduce grain losses and improve grain quantity and quality. Several factors contribute to combine grain losses, including incorrect cutting height, combine forward speed, concave clearance, drum speed, fan speed, sieve opening, crop moisture content, reel speed, and the horizontal and vertical distance of the reel from the cutter bar. These variables impact the machine settings, field effectiveness, and theoretical and practical field capacity. The following are different types of grain losses in the field before and during the combining of crops during harvesting operations:

Header Losses: When the crop is fed into the machine's header before it is threshed, this is known as harvesting and is when header damage occurs. Kg/ha, a percentage of crop production, is used to measure header loss. Since the header unit severely strikes the panicles, the damage caused by the cutter bar is considered significant. Reel height, cutter/header height, the distance from the blade bar to the reel's center, and reel speed relative to machine speed all affect header loss during combined harvesting operations. When estimating grain production, reducing grain losses, and assuring maximum performance to enhance grain quality, the height at which the rice crop is harvested at harvest is crucial. Figure 6 illustrates the factors that can lead to combine harvester header damage. Cutter bar stroke, reel height, reel peripheral speed, travel speed, harvest breadth, cutting height, crop moisture, height, crop density, and crop feed rate all combine harvester header damage.

$$\text{Shatter loss, kg/ha} = \frac{\text{Avg. weight of dropped grain on the ground during cutting and conveying,kg.}}{\text{Area covered,ha}} \dots\dots(xvi)$$

$$\text{Cutter loss, kg/ha} = \frac{\text{Avg. weight of grain lost due to rough handling of cutter bar,kg.}}{\text{Area covered,ha}} \dots\dots(xvii)$$

Threshing Losses: Un-threshed grain is known as "threshing loss" when it collects in the back of the combine head and is moved to the machine's back via a straw rack. Grain damage caused by an ineffective rubbing motion between the cylinder and the concave is mechanical threshing damage. The effectiveness of the combined threshing machine has a considerable impact on grain loss due to threshing. Grain kernels are removed from a connected plant head by marking and rubbing. Threshing is influenced by cylinder speed, concave type and spacing, and equipment causes. Threshing procedures typically result in mechanical grain damage. As illustrated in Figure 7, the threshing loss of the combine depends on the feed rate, cylinder speed, and concave clearance, which is influenced by crop moisture.

$$\text{Cylinder loss, kg/ha} = \frac{\text{Avg. weight of unthreshed heads lost out the rear of combine,kg.}}{\text{Area covered,ha}} \dots\dots(xviii)$$

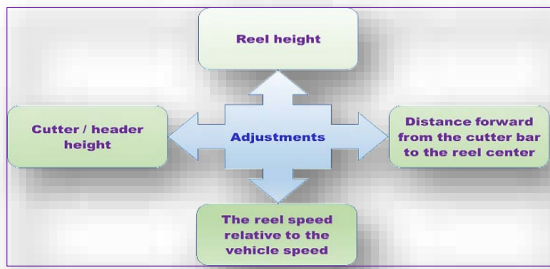


Figure 6. Machine parameters that affect combine header loss.

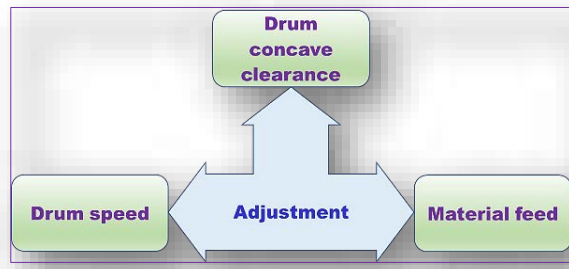


Figure 7. Machine parameters that affect threshing and separation losses.

Separation Losses: Grain separating loss is crucial when assessing a combine harvester's effectiveness. The amount of free grain that does not pass through the grate in the separation section during an axial flow is the loss due to separation. Low straw moisture causes the cylinder to break the hay down more finely, enabling more material to flow through the sieve and affecting separation. Additionally, there are significant parallels between threshing techniques and crop circumstances, machine settings, and operator preferences that influence separation efficiency.

$$\text{Separating loss, kg/ha} = \frac{\text{Avg. weight of threshed heads lost out the rear of combine,kg.}}{\text{Area covered,ha}} \dots\dots(xix)$$

Cleaning Loss: The amount of grains mixed in the screening of a combine harvester is referred to as cleaning loss, and the cleaning loss rate is typically used to measure it. Airflow while cleaning causes grains to be blown away, and damage is unavoidable. A mixture of air blasts to lift chaff and chaff and shaking motions to drive grain downward through the sieve while pushing larger particles to the bottom are used in combine cleaning systems. Again, one aspect of crop quality that will impact performance is the moisture content of harvested grain. The fan speed and sieve opening are the machine settings with the most significant impact on cleaning system losses, as shown in Figure 8.

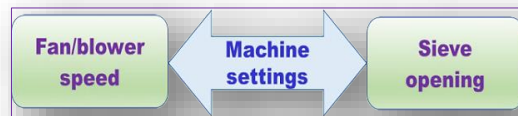


Figure 8. Machine parameters that affect grain cleaning losses.

The data to be collected

- Functional problems during operations
- Labor requirement
- Duration of the test (Working hrs.)
- Travel speed (km/h)
- Area covered
- Grain output (kg/h)
- Straw output (kg/h)
- Losses
- Fuel consumption (l/h)

Laboratory techniques

- Clean the sample
- Weight the sample
- Determine the moisture content
- Count the filled/unfilled grain.

In all procedures, the loss was estimated by dividing the grain loss by the paddy yield achieved after harvesting the study area. Field samples were collected and delivered to the FMPHT laboratory for investigation. Before loss estimates of field and laboratory data were completed, all grain weights were adjusted to the standard 14% moisture content (wet basis).

Harvesting

a. Pre-harvest losses

- ❖ Collected paddy with care in all boundary lanes between designated plots.
- ❖ Picked up all grains on the ground within the sample plot with care. It was critical not to lodge the crop.

- ❖ Placed the collected grains in the poly bag and labeled them neatly. Repeated the technique for the other plots.
- ❖ Cleaned the grain.
- ❖ Weighed and recorded the clean grains.
- ❖ Took moisture content reading and recorded it.

b. Post-harvest losses

- ❖ Laid the canvas out on the cleared boundary. Checked that the canvas was adequately secured to the ground.
- ❖ Harvested the paddy within the plot normally.
- ❖ Laid the collected crop out on the canvas record.
- ❖ Collected all grains falling to the ground due to shattering/cutter bar/header losses and separating/cylinder/rear-end losses carefully and thoroughly during harvesting.
- ❖ Cleaned the grains that have been collected.
- ❖ Weighed and recorded the clean grains.
- ❖ Took a moisture reading and wrote it down.

Information of the study field

Conducting performance tests of a complete feed combine harvester in a paddy field is essential to evaluate its performance, efficiency, and harvest loss. The choice of paddy field and its preparation for testing significantly affect the accuracy and relevance of the results. So, for conducting a complete feed combine harvester performance test in a paddy field, several important factors like paddy variety, crop maturity, field size and shape, crop uniformity, water management, soil type, weather conditions, etc., were considered. Some important information collected from the field is shown in Table 7.

Table 7. Information of the study field.

Location	Season	Variety	Date of harvesting	Plant height (cm)	Maturity of the crop (%)	The moisture content of grain (%)
BARI research field, Gazipur	Boro/2023	BRRI dhan84	10/05/2023	118.5	More than 85%	24.56

Results and Discussion

Machine performance evaluation

The data collected during field evaluation trials were used to determine field capacity, field efficiency, net grain output (kg/h and kg/ha), grain throughput (kg/h and kg/ha), straw output (kg/h and kg/ha), crop throughput (tons/h) and collectible and non-collectible harvesting losses. A combine harvester's performance was affected by size, forward speed, and grain yield.

During the Boro 2023 season, the initial performance review was carried out. The activity took place at the BARI farm in Gazipur. The machine performed well. After a long time of operation, the clogging problem occurred in the horizontal auger/screw. To address this issue, various modifications were made by switching the chain sprocket for the belt pulley. In addition to the before belt pulley, the speed of the horizontal auger/screw has been enhanced with this change. The machine worked well after the modifications. We also observed some sliding issues with the machine's blower part's belt pulley. The moisture content of the paddy plant and grain could cause this issue. The cutting, transporting, threshing, and cleaning processes were all performed satisfactorily (Plate 6). However, lowered engine performance was shown to be associated with smaller amounts of exhaust gases; thus, engine power must be increased to achieve improved capacity. The machine's fuel consumption ranged from 3.00 to 3.50 l/h, while the field capacity ranged from 0.252 to 0.262 ha/h. Table 8 summarizes the machine performance field test data.

Figure 9 illustrates the machine's capacity during operation. The machine traveled on the BARI farm at an average 2.41 km/h speed. At the BARI farm, the machine's average field capacity was measured at 0.258 ha/h, while its operational average fuel consumption was estimated at 3.22 l/h. The overall field efficiency of the machine was found to be about 71%.



Plate 6. Performance test of the developed whole feed combine harvester.

Table 8. Field performance of BARI fabricated whole feed combine harvester.

Place: BARI farm, Gazipur Sadar, Gazipur						
Plot No.	Forward speed, S (km/h)	Total operating time (h)	Effective field capacity (ha/h)	Effective cutting width, w (m)	Theoretical field capacity (ha/h)	Field Efficiency (%)
	$S=L/S*3.6$	Total time (h)	$EFC=A/h$		$TFC= (S*W)/10$	$FE= (EFC/TFC) *100$
1	2.35	0.8	0.252	1.5	0.353	71.39
2	2.50	1.0	0.259	1.5	0.375	69.07
3	2.40	0.6	0.262	1.5	0.360	72.78
Average			0.258	-	0.363	71.08

Plot section no.	Duration of test (Working hrs.)	Travel speed (km/h)	Rate of work			Fuel consumption l/h
			Grain output (kg/h)	Straw output (kg/h)	Crop throughput (kg/h)	
1	0.8	2.35	1005.50	910.40	1915.9	3.50
2	1.0	2.50	1015.65	940.20	1955.85	3.00
3	0.6	2.40	1020.50	915.60	1936.1	3.15
Average		2.41	1013.88	922.06	1935.94	3.22

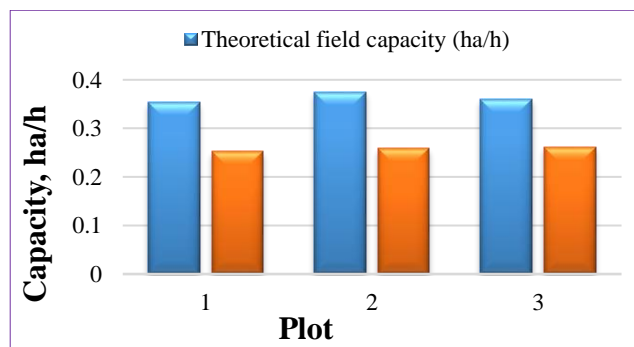


Figure 9. Capacity of the machine.

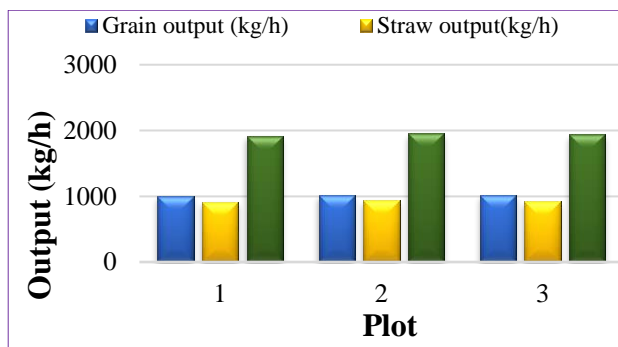


Figure 10. Grain output, straw output, and crop throughput of the machine in a different plot.

Figure 10 represents the machine's output in terms of grain and straw for the location at BARI farm, Gazipur. During its operation at the BARI farm, the machine provided an average grain output of 1013.88 kg/h. The machine's operational average straw output at the same site was 922.06 kg/h.

Table 9. Pre-harvest losses of the selected field.

Plot No	Trial No	Area		No. of collected grain	Grain weight (g)	Grain weight (kg)	Moisture content (%)	Loss= Grain wt./Area (kg/ha)	Grain loss at 14% M.C (g)	Grain loss at 14% M.C = Grain wt./Area (kg/ha)
		m ²	ha							
1	1	0.36	0.000036	42	1.040	0.001040	24.25	28.89	0.916	25.44
	2	0.36	0.000036	45	1.111	0.001111	24.25	30.86	0.979	27.19
2	1	0.36	0.000036	40	0.980	0.000980	24.25	27.22	0.863	23.97
	2	0.36	0.000036	43	1.053	0.001053	24.25	29.25	0.927	25.75
3	1	0.36	0.000036	38	0.939	0.000939	25.18	26.08	0.817	22.69
	2	0.36	0.000036	48	1.186	0.001186	25.18	32.94	1.032	28.67
Average		0.36	0.000036	42.67	1.051	0.0010515	24.56	29.21	0.922	25.62

Pre-harvest losses in a rice field refer to the loss of rice grains or panicles before harvesting begins. These losses can happen due to various factors, significantly impacting rice yield and farm profitability. Pre-harvest losses are generally measured as a percentage of the potential yield (Table 9). The average pre-harvest loss of the selected field was estimated at 14% moisture content of 27.19 kg/ha.

Table 10 shows information regarding grain shattering/cutter bar/header losses for the BRR-developed whole feed combine harvester. It varies according to the cutter bar speed, shattering tendency, and grain maturity percentages. At 14% moisture content, the average shattering loss of grain in the investigated field was estimated to be 27.79 kg/ha.

Table 10. Shattering/Cutter bar/ Header Losses of the BRR-developed whole feed combine harvester.

Plot No	Trial No	Area		No. of collected grain	Grain weight (g)	Grain weight (kg)	Moisture content (%)	Loss= Grain wt./Area (kg/ha)	Grain loss at 14% M.C (g)	Grain loss at 14% M.C = Grain wt./Area (kg/ha)
		m ²	ha							
1	1	0.36	0.000036	47	1.161	0.001161	24.25	32.25	1.023	28.42
	2	0.36	0.000036	50	1.235	0.001235	24.25	34.31	1.088	30.22
2	1	0.36	0.000036	43	1.062	0.001062	24.25	29.50	0.935	25.97
	2	0.36	0.000036	45	1.112	0.001112	24.25	30.89	0.979	27.19
3	1	0.36	0.000036	48	1.186	0.001186	25.18	32.94	1.032	28.67
	2	0.36	0.000036	44	1.087	0.001087	25.18	30.19	0.946	26.28
Average		0.36	0.000036	46.17	1.141	0.001141	24.56	31.68	1.001	27.79

Table 11 shows information regarding grain separating/ cylinder/rear-end losses for the BRR-developed whole feed combine harvester. The threshing and cleaning influence and the separating mechanism of the combine harvester. It was measured at a 12 m length of the field with the full width of the cut. At 14% moisture content, the average separating loss of grain in the investigated field was estimated to be 18.99 kg/ha.

Table 11. Separating/ Cylinder/Rear-end Losses of the whole feed combine harvester.

Plot No.	Length (m)	Width (m)	Area(m ²)	Area (ha)	Grain weight(gm)	Grain weight (kg)	Moisture content (%)	loss= Grain wt./Area (kg/ha)	Grain loss at 14% M.C (g)	Grain loss at 14% M.C = Grain wt./Area (kg/ha)	
1	12	1.5	18	0.0018	29	0.029	24.25	16.11	25.54	14.19	
2	12	1.5	18	0.0018	42	0.042	24.25	23.33	36.99	20.55	
3	12	1.5	18	0.0018	46	0.046	25.18	25.56	40.02	22.23	
Average		12	1.5	18	0.0018	39	0.039	24.56	21.67	34.18	18.99

Total losses based on the type of combine harvester

The total harvesting loss of a whole feed combine paddy harvester depends on various factors, including the efficiency of the harvester, the crop conditions, and the operator's skill. Typically, harvesting loss is measured as a percentage of the total crop left behind or lost during harvesting (Table 12).

Table 12. Total losses occurred by the developed combine harvester.

Location	Pre-harvest loss		Shattering/Cutter bar/ Header Loss		Separating/ Cylinder/Rear-end Loss		Total loss		Yield (t/ha)
	(kg/ha)	% of losses	(kg/ha)	% of losses	(kg/ha)	% of losses	(Kg/ha)	% of losses	
BARI farm	25.62	0.443	27.79	0.492	18.99	0.336	72.4	1.27	5.65

Total losses for the whole feed combination harvester, including pre-harvest loss, shattering loss, and separating loss, have been estimated to be 0.443, 0.492, and 0.336%, respectively. The developed combine harvester has total grain losses of 1.27% (Fig. 12).

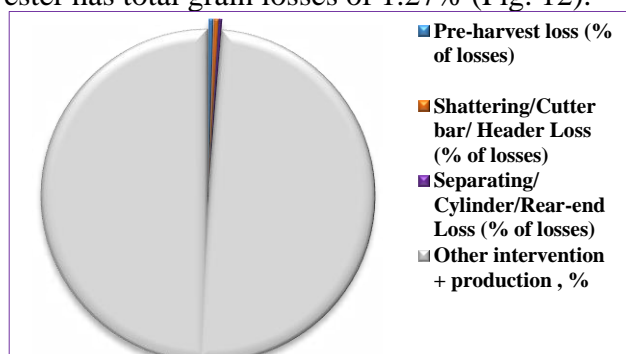


Figure 12. Different losses occurred by the developed whole feed combine harvester,

Identifying issues

Farmers, current scientists, and machine operators were asked about their impressions of the machine's general performance in the field. They provided good feedback and assessments of the developed machine's performance, emphasizing the difficulties and observations listed below.

- ❖ More engine power is needed;
- ❖ Harvesting takes more time;
- ❖ During harvest, more shattering loss of the grain in the planted crop was observed;
- ❖ The machine is difficult to move over long distances.

Conclusion

The divisional research workshop of FMPHT, located at BIRRI in Gazipur, has completed the prototype fabrication of a whole feed combine harvester using locally available materials. During the past Boro 2023 season, a preliminary performance test was conducted in the BARI research field. The results of the field tests indicate that the newly developed combine performed satisfactorily, although operator drudgery needs to be reduced for improved performance. To achieve optimum performance, engine power should be increased to 50-60 hp, or the engine quality should be improved. Additional performance testing needs to be conducted to acquire more details on the performance of the BIRRI-developed whole feed combine harvester.

Experiment 1.5: Validation and up-scaling of rice transplanting and harvesting technology in the selected sites of Bangladesh

Principal Investigator: Md. Anwar Hossen

Co-investigator(s): SP, MKP

Specific project objective(s)

- To validate and adopt mechanical rice transplanting along with fertilizer deep placement, weeding, and paddy harvesting technologies in the farmers' field.
- To minimize the cost of production of paddy cultivation and make it profitable.

Methodologies

“Validation and up-scaling of rice transplanting and harvesting technology in the selected sites of Bangladesh (VRTHB)”, a competitive Grants Program (CGP) Interim-2, 2021 Research Project under KGF-BKGET Fund, Bangladesh Agricultural Research Council (BARC) and officially launched on 04 November 2021 through the signing of the letter of agreement.

Holistic research approaches were applied to validate and up-scaling the power weeder, rice transplanter cum fertilizer applicator, and imported combine harvester (both whole feed and head feed combine harvester) in the project sites under Habiganj and Sirajganj districts during the Boro 2022-2023 and Aman, 2023 season. Demonstration and training programs were also conducted on the mentioned machinery taking the help of DAE personnel and BIRRI regional station personnel. Short brief methodologies of the main experiments that have been already initiated are given below.

I. Validation of mechanical power weeder

BIRRI-developed power weeder was used in this experiment for validation. BIRRI multi-rows power weeder was designed and fabricated in the Farm Machinery and Postharvest Technology Divisional research workshop. The basic information of the trials were presented in the Table 1.

Treatments

T₁ = One weeding by developed power operated weeder (PoW) succeeded by (sb) one hand-weeding (HaW);

T₂ = Herbicide application

T₃ = One weeding by manual weeder sb one HaW (Local practice)

T₄ = No-weed,

T₅ = Unweeded (Control);

Table 1. Basic Information of the power weeder trials.

Trial no.	Season	Location	Variety	Area covered (ha)	Date of transplanting	Date of mechanical weeding	Date of harvesting
1	Boro/ 2022-23	Habiganj	BIRRI dhan92	2.01	25/01/23	12/02/23	13/05/23
2		Habiganj	BIRRI dhan92	1.34	17/02/23	04/03/23	14/05/23
3		Sirajganj	BIRRI dhan92	1.34	10/2/2023	25/02/23	26/05/23
4		Sirajganj	BIRRI dhan92	0.27	11/2/2023	26/02/23	27/05/23
5	Aman/2023	Habiganj	BIRRI dhan95	0.40	21/8/23	06/09/23	10/11/23
6		Habiganj	BIRRI dhan87	0.27	20/8/23	25/08/23	12/11/23
7		Sirajganj	BIRRI dhan75	0.40	10/8/2023	25/08/23	05/11/23
8		Sirajganj	BIRRI dhan75	0.40	11/8/2023	25/08/23	07/11/23

Data collection

The following data were collected from each trial

- Operation speed of the weeder (km/h).
- Time of weeding (h)
- Fuel consumption (l/h)
- Actual field capacity (ha/h)
- Theoretical field capacity (ha/h)
- Field efficiency of the weeder (%)
- Weeding efficiency (%)
- Crop and yield data

Results and Discussion

Validation of mechanical power weeder in (Boro/2022-23) season

Field performance of the weeder

Field capacity of the multi-rows power weeder was measured during field operation in four locations under the project sites (Table 13). Theoretical field capacity varied with forward speed of machine operation whereas actual field capacity varied with forward speed, turning time loss, weeder placing in between rows time etc. In all cases, theoretical and actual field capacity of the power weeder varied from 0.38 to 0.66 and 0.26 to 0.43 ha/hr based on soil conditions. Field efficiency varied from 60.82 to 71.49 irrespective of soil and locations.

Table 13. Field performance of the power weeder at different project locations (Boro, 2022-23 season)

No	Time/pass in length wise (s)				Forward speed, S (km/h)	Total operating time (h)			Effective field capacity (ha/h)	Effective cutting width (m)	Theoretical field capacity (ha/h)	Field Efficiency (%)	Area covered
	1	2	3	Avg		S= L/S*3.6	Start time	End time					
1	40	35	60	45.00	4.40	1.25	1.73	0.48	0.23	0.60	0.26	86.21	4.39
2	175	77	104	80.00	3.83	3.22	4.24	1.02	0.21	0.60	0.23	91.07	4.78
3	82	72	68	74.00	3.65	1.25	2.03	0.78	0.24	0.90	0.33	72.89	4.18
4	80	75	75	76.67	3.52	1.25	2.12	0.87	0.24	0.90	0.32	76.45	4.13

Note: 1- Habiganj (1), 2- Habinag (2), 3- Sirajganj (1) and 4- Sirajganj (2)

Fuel consumption of the weeder (Boro, 2022-23 season)

The average fuel consumption rate (L/ha) of the weeding operation at the two locations in Habiganj is lower than the average fuel consumption rate (L/ha) of the weeding operation at the two locations in Sirajganj. The variation of fuel consumption was observed between different locations due to time of operation, turning time loss, mechanical error of the machine, and weed density (Table 14).

Table 14. Fuel consumption of the weeder during field operation (Boro, 2022-23 season).

No.	Area (ha)	Operating time (h)	Total fuel used (L)	Fuel consumption rate (L/ha)	Fuel consumption rate (L/hr)	Specific fuel consumption
	A	H	F	F _c =F/A	F _c =F/h	(l/hp-h)
1	0.110	0.483	0.250	2.273	0.517	0.398
2	0.213	1.017	0.550	2.588	0.541	0.416
Average	0.1615	0.75	0.4	2.4305	0.529	0.407
3	0.188	0.783	0.355	1.893	0.453	0.349
4	0.210	0.867	0.420	2.000	0.485	0.373
Average	0.199	0.825	0.3875	1.9465	0.469	0.361

Table 15. Weeding efficiency of the mechanical power (Boro, 2022-23 season).

Treatments	Habiganj-1	Habiganj-2	Sirajganj-1	Sirajganj-2	Mean
T ₁	88.97	88.80	89.10	90.00	89.22
T ₃	91.83	86.70	85.80	81.63	86.49
Mean	90.40	87.75	87.45	85.82	
CV	4.44				
LoS	L=ns, T=ns and L × T = ns				

Note: T₁ = One weeding by developed power operated weeder (PoW) succeeded by (sb) one hand-weeding (HaW); T₃= One weeding by manual weeder sb one HaW (Local practice); NS-Not significant, *-significant at 5 %, **-significant at 1 %, LoS-Level of significance, L-Locations, T- Weeding methods.

Weeding efficiency

Weeding efficiency of one weeding by developed power-operated weeder (PoW) succeeded by (sb) one hand-weeding (HaW) and one weeding by manual weeder sb one HaW (Local practice) at Habiganj and Sirajganj district are illustrated in Table 15. It was observed that the higher mean value (88.97%) and the lower mean value (88.80%) of weeding efficiency of one weeding by developed power operated weeder (PoW) succeeded by (sb) one hand-weeding (HaW) and one weeding by manual weeder sb one HaW

(Local practice) respectively. Amongst the two weeders (T_1 and T_3), the highest weeding efficiency was found at 90.00 % in T_1 at Sirajganj(1) and the lower weeding efficiency was obtained at 85.80 % in T_3 at also Sirajganj(1).

Yield

The information regarding the grain yield performance is presented in Table 16. The lower yield was obtained at the treatment of T_5 compared to the potential yield of the variety. The grain yields T_1 , T_2 , T_3 , and T_4 were significantly higher compared to T_5 . It was also noticed that the highest grain yield performance of the study was found for the treatment of T_1 and T_2 in all locations. The treatment T_1 plot gave a higher yield in all cases followed by T_2 plots in the study area of the project site. However, the treatment T_5 plot gave significantly lower yields in all cases followed by other treatment plots of the study. The operational cost of mechanical weeder and saving over traditional method is given in Table 17 & 18 respectively.

Table 16. Yield of grain (ton/ha) as affected by different weeding methods.

Treatments	Habiganj-1	Habiganj-2	Sirajganj-1	Sirajganj-2	Mean
T_1	7.89	8.4	8.25	7.85	8.0975
T_2	7.28	8.1	8.11	7.12	7.6525
T_3	7.2	7.99	7.9	7.05	7.535
T_4	6.95	7.82	7.25	6.73	7.1875
T_5	5.2	5.85	4.58	5.33	5.24
CV	4.95	6.88	8.45	9.65	-
LSD	0.48	0.41	0.38	0.35	-

Table 17. Cost calculation of the power weeder operation.

Items	Manual weeder	BRR Power weeder
Fixed cost calculation		
Purchase price (p), Tk	800.0	45000.0
Salvage value (S), Tk (10% of P)	80.0	4500.0
Working life (L), yr	5.0	5.0
Rate of Interest (I)	0.1	0.1
Avg. annual use (Au), hr/yr	480.0	480.0
Annual depreciation, $D=P-S/L$	144.0	8100.0
Interest on Investment, $I=P+S/2*i$	39.6	2227.5
Tax, insurance and shelter cost, $T=3\%$ of purchase price	24.0	1350.0
Total fixed cost ($D+I+T$), Tk/y	207.6	11677.5
Total fixed cost, Tk/h	0.4	24.3
Variable cost calculation		
Labor cost, L (Tk/h)	100.00	100.00
Fuel cost, F (Tk/h)	0.00	60.00
Lubrication oil cost per hr, $O=3\%$ of fuel cost, (Tk/h)	0.00	1.80
RPM/yr =3.5 % of purchase price	28.00	1575.00
RPM/hr =3.5 % of purchase price	0.06	3.28
Total Variable cost (Tk/h)	100.06	165.08
Total operating cost (fixed and variable cost) Tk/h	100.49	189.41

Table 18. Saving over traditional/manual weeding.

Name of Technology	Capacity, decimal/h	Capacity, hr/ha	Operating Cost, Tk/ha	Mane of technology	Cost, tk/h	Capacity, decimal/h	Capacity, hr/ha	Cost, Tk/ha	Save over traditional, Tk/ha
Weeder	10.0	24.7	2482.1	Manual	75.0	1.5	164.7	12350.0	9867.9
Power weeder	56.0	4.4	835.4	Manual	75.0	1.5	164.7	12350.0	11514.6

Conclusion

Power weeder are a common requirement for adequate agricultural instruments to raise small-scale farmers' production per unit of land. The use of a multi-row power weeder was found to be advantageous compared to conventional weeding techniques in Bangladesh's various soil conditions. Power weeders were shown to have a larger field capacity than manual weeders and other weeding techniques. The highest weeding efficiency and field capacity were enumerated in the validation of the mechanical power weeder. Therefore, power weeder was more effective and easier to operate by farmers in weed management under low land cultivation. Multi-row power weeders may be recommended for use in weeding operations due to the field capacity and increased weeding efficiency over conventional weeding techniques.



Plate 7. Photographic views of the different activities.

II. Validation and grain loss assessment of the different model of combine harvesters
Factors were considered during evaluation in Boro 2022-23 and Aman 2023 seasons

- Field Length (m)
- Cutting Height (mm)
- Plant Density (tiller/m²)

Data were collected

- Forward Speed (km/h)
- Actual Field capacity (ha/h)
- Theoretical Field capacity (ha/h)
- Specific fuel consumption (l/h-hp)

The basic information of the trials was presented in the Table 19, Table 20 and Table 21.

Table 19a. General information of the study (Aman/2022).

Trial no.	Location	Type of combine harvester	Date of purchased	Cutting height from the ground (mm)
1	Habiganj-1	Whole Feed type (FMWORLD Ruilong)	April/2022	304 (30.4 cm)
2	Habiganj-2	Whole Feed type (FMWORLD Ruilong)	April/2022	304 (30.4 cm)
3	Sirajganj-1	Head Feed Type (Yanmar AG600A)	April/2022	150 (15.0 cm)
4	Sirajganj-2	Head Feed Type (Yanmar AG600A)	April/2022	150 (15.0 cm)

Table 19b. General information of the study (continue).

Trial no.	Season	Variety	Date of harvesting	Crop height (mm)	Moisture content of grain (%)	Grain yield (t/ha)
1	Aman/2022	BRRi dhan49	27-11-2022	1146	24.61	5.47
2	Aman/2022	BRRi dhan49	27-11-2022	1122	25.66	4.82
3	Aman/2022	BRRi dhan75	01-12-2022	1032	26.84	6.14
4	Aman/2022	BRRi dhan75	02-12-2022	1038	27.69	5.39

Table 20a. General information of the study

Trial no.	Season	Location	Type of combine harvester	Date of purchased
1	Boro/2022-23	Raiganj, Srajganj	Yanmar (AG600A)	April/2022
2			Marksan (BM-608)	April/2022
3		Sadar, Habiganj	Kubota (PRO588i-G)	April/2022
4			Daedong (DXM73)	April/2022
5		Raiganj, Srajganj	Yanmar (AG600A)	April/2022
6			Kubota (PRO588i-G)	April/2022
7	Aman/2023	Raiganj, Srajganj	Yanmar (AG600A)	April/2022
8			Marksan (BM-608)	April/2022
9		Sadar, Habiganj	Kubota (PRO588i-G)	April/2022
10			Daedong (DXM73)	April/2022
11		Raiganj, Srajganj	Yanmar (AG600A)	April/2022
12			Marksan (BM-608)	April/2022

Table 20b. General information of the study (continue)

Trial no.	Variety	Crop height (mm)	Moisture content of grain (%)	Soil type	Date of harvesting	Grain yield (t/ha)
1	BRRi dhan92	980	24.16	Sandy type	13/05/23	7.89
2	BRRi dhan92	952	23.89	Sandy type	14/05/23	8.40
3	BRRi dhan92	966	23.44	Sandy loam	26/05/23	8.25
4	BRRi dhan92	980	23.31	loam	27/05/23	7.85
5	BRRi dhan92	1015	24.31	Sandy type	15/05/23	7.50
6	BRRi dhan92	985	22.89	Sandy type	16/05/23	7.85
7	BRRi87	1220	21.22	Sandy type	10/11/23	6.45
8	BRRi75	1150	20.25	Sandy type	12/11/23	4.60
9	BRRi75	1125	22.30	Sandy loam	05/11/23	4.40
10	BRRi75	1120	20.20	loam	07/11/23	4.15
11	BRRi75	1118	22.35	Sandy type	03/11/23	4.12
12	BRRi87	1225	23.25	Sandy type	04/11/23	6.85

Table 21. Design of the three factors during field evaluation.

Trials	Length of the field (m)	Crop Cutting Height (mm)	Plant Density (plant no./m ²)
T1	<20	<100	<230
T2	20-30	100-110	230-240
T3	31-40	111-120	241-250
T4	41-50	121-130	251-260
T5	51-60	131-140	261-270
T6	61-70	141-150	271-280
T7	>70	>150	>280

Results and Discussion of Combine Harvester

Aman 2022 season: Habiganj: FMWORLD Ruilong (whole feed) and Sirajganj: Yanmar AG600A (head feed)

Field performance of the head feed and whole feed combine harvester

Field performance of the studied combine harvester evaluated under different field length in the project locations (Table 22). Forward speed (km/h), Effective field capacity (ha/h), Theoretical field capacity (ha/h) and Field Efficiency (%) were measured under different conditions. All the parameters varied with the field length in all locations (Table 22).

Table 22. Field performance evaluation of the head feed combine harvester.

Category	Length, L (m)	Width (m)	Total area A (ha)	Forward speed, S (km/h)	Total operating time (h)	Effective field capacity (ha/h)	Effective cutting width, w (m)	Theoretical field capacity (ha/h)	Field Efficiency (%)
Habiganj-1									
<30	29	20	0.058	3.773	0.183	0.3164	2.2	0.830	38.11
30-40	38	20	0.076	4.188	0.167	0.4560	2.2	0.921	49.49
41-50	44	20	0.088	4.659	0.150	0.5867	2.2	1.025	57.24
51-60	55	20	0.110	4.752	0.117	0.9429	3.2	1.521	62.00
61-65	62	20	0.124	4.817	0.083	1.4880	4.2	2.023	73.54
Habiganj-2									
<30	22	20	0.044	3.600	0.150	0.2933	2.2	0.792	37.04
30-40	39	20	0.078	3.343	0.217	0.3600	2.2	0.735	48.95
41-50	47	20	0.094	3.021	0.233	0.4029	2.2	0.665	60.61
51-60	54	20	0.108	3.471	0.150	0.7200	3.2	1.111	64.81
61-65	64	20	0.128	4.114	0.100	1.2800	4.2	1.728	74.07
Sirajganj-1									
<30	24	20	0.048	2.979	0.250	0.1920	1.5	0.447	42.96
30-40	38	20	0.076	3.600	0.183	0.4145	2.5	0.900	46.06
41-50	42	20	0.084	3.844	0.217	0.3877	1.5	0.577	67.24
51-60	58	20	0.116	3.990	0.267	0.4350	1.5	0.598	72.69
61-65	65	20	0.130	4.307	0.150	0.8667	2.5	1.077	80.49
Sirajganj-2									
<30	17	20	0.034	3.166	0.183	0.1855	1.5	0.475	39.06
30-40	32	20	0.064	3.388	0.267	0.2400	1.5	0.508	47.22
41-50	45	20	0.090	3.951	0.183	0.4909	2.5	0.988	49.70
51-60	55	20	0.110	4.097	0.267	0.4125	1.5	0.614	67.13
61-65	64	20	0.128	4.608	0.150	0.8533	2.5	1.152	74.07

Field efficiency of the head feed and whole feed combine harvester in different locations

The field efficiency of both head feed and whole feed combine harvester was measured with the length of the field which is presented in Table 23. In all locations, the field efficiency of the both head feed and whole feed combine harvester increased with the increase in the field length (Table 24-29). It is observed in the liner regression curve that the field performance of the combine harvester varied relatively in line with field length in Habiganj and Sirajganj ($R^2 = 0.9665$ and $R^2 = 0.8598$ respectively) (Figure 13).

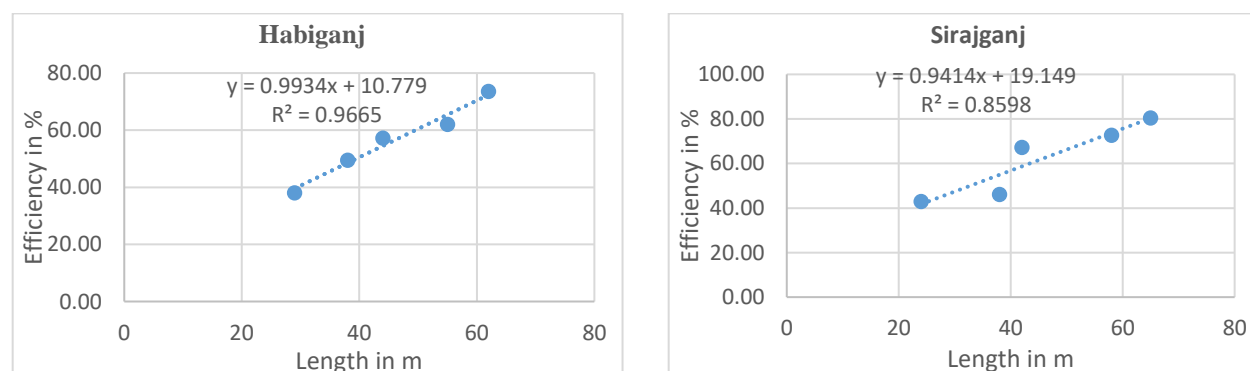


Figure 13. Influences of field length on field efficiency of the combine harvester.

2.1.3 Forward speed

It is observed in the liner regression curve that the field performance of the combine harvester varied relatively in line with field length in Habiganj and Sirajganj ($R^2 = 0.8581$ and $R^2 = 0.9199$, respectively) (Fig. 14).

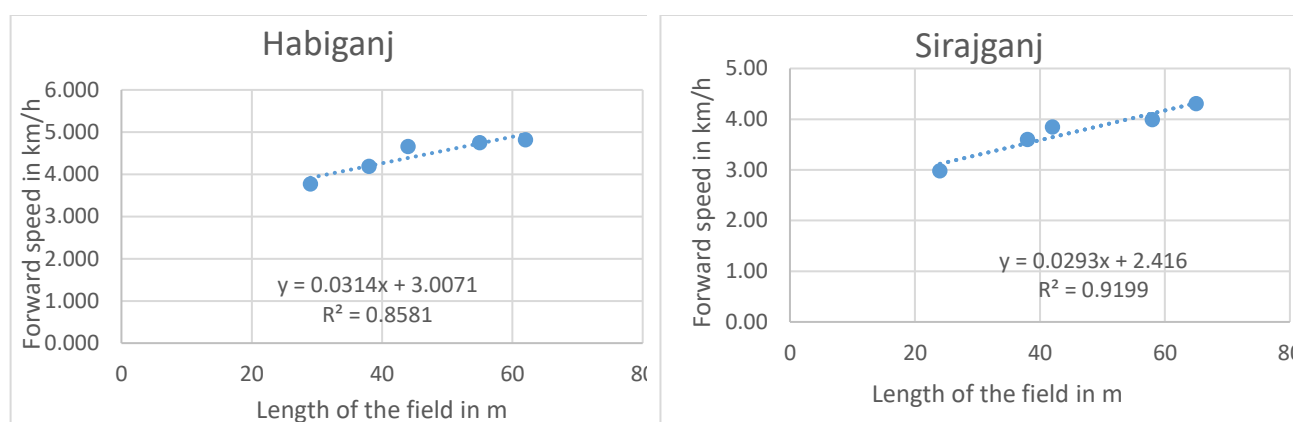


Figure 14. Influences of field length on forward speed of the combine harvester.

Table 23. Field efficiency of the combine harvester affected by the length of the field.

Length of field in m	Habiganj	Sirajganj
<30	38.11	42.96
30-40	49.49	46.06
41-50	57.24	67.24
51-60	62.00	72.69
61-65	73.54	80.49

Table 24. Total losses of grain of whole feed combine harvester in Habiganj-1.

Sl.No.	Pre-Harvest Loss, Kg/ha	Shattering loss, Kg/ha	Cylinder loss, Kg/ha	Total loss, Kg/ha	Grain yield (t/ha)	Moisture Content %	Grain loss at 14% M.C. (Kg/ha)	Grain loss in %
1	4.89	24.44	44.55	73.88	5.47	24.61	64.76	1.35
2	12.22	17.11	45.91	75.24	5.47	24.61	65.96	1.38
3	7.33	19.56	54.55	81.43	5.47	24.61	71.38	1.49
Avg.	8.15	20.37	48.33	76.85	5.47	24.61	67.37	1.41

Table 25. Total losses of grain of the whole feed combine harvester in Habiganj-2.

Sl.No.	Pre-Harvest Loss, Kg/ha	Shattering loss, Kg/ha	Cylinder loss, Kg/ha	Total loss, Kg/ha	Grain yield (t/ha)	Moisture Content %	Grain loss at 14% M.C. (Kg/ha)	Grain loss in %
1	4.89	24.40	79.55	108.83	4.82	25.66	94.08	2.26
2	2.44	27.11	72.73	102.28	4.82	25.66	88.41	2.12
3	9.78	21.69	76.36	107.83	4.82	25.66	93.22	2.24
Avg.	5.70	24.40	76.21	106.32	4.82	25.66	91.90	2.21

Table 26. Total losses of grain of whole feed combine harvester.

Sl.No.	Pre-Harvest Loss, Kg/ha	Shattering loss, Kg/ha	Cylinder loss, Kg/ha	Total loss, Kg/ha	Grain yield (t/ha)	Moisture Content %	Grain loss at 14% M.C. (Kg/ha)	Grain loss in %
1	4.89	24.42	62.05	91.36	5.14	25.14	79.42	1.80
2	7.33	22.11	59.32	88.76	5.14	25.14	77.19	1.75
3	8.56	20.62	65.45	94.63	5.14	25.14	82.30	1.86
Avg.	6.93	22.39	62.27	91.58	5.14	25.14	79.64	1.81

Table 27. Total losses of grain of the head feed combine harvester in Sirajganj-1.

Sl.No.	Pre-Harvest Loss, Kg/ha	Shattering loss, Kg/ha	Cylinder loss, Kg/ha	Total loss, Kg/ha	Grain yield (t/ha)	Moisture Content %	Grain loss at 14% M.C. (Kg/ha)	Grain loss in %
1	7.00	14.00	15.33	36.33	6.14	26.84	30.91	0.59
2	8.75	19.25	12.67	40.67	6.14	26.84	34.60	0.66
3	3.50	15.75	14.00	33.25	6.14	26.84	28.29	0.54
Avg.	6.42	16.33	14.00	36.75	6.14	26.84	31.26	0.60

Table 28. Total losses of grain of the head feed combine harvester in Sirajganj-2.

Sl.No.	Pre-harvest Loss, Kg/ha	Shattering loss, Kg/ha	Cylinder loss, Kg/ha	Total loss, Kg/ha	Grain yield (t/ha)	Moisture Content %	Grain loss at 14% M.C. (Kg/ha)	Grain loss in %
1	5.25	10.50	10.50	26.25	5.39	27.69	22.07	0.49
2	8.75	14.00	14.00	36.75	5.39	27.69	30.90	0.68
3	3.50	21.00	21.00	45.50	5.39	27.69	38.26	0.84
Avg.	5.83	15.17	15.17	36.17	5.39	27.69	30.41	0.67

Table 29. Total losses of grain of head feed combine harvester.

Sl. No.	Pre-Harvest Loss, Kg/ha	Shattering loss, Kg/ha	Cylinder loss, Kg/ha	Total loss, Kg/ha	Grain yield (t/ha)	Moisture Content %	Grain loss at 14% M.C. (Kg/ha)	Grain loss in %
1	7.00	14.00	15.33	36.33	6.14	26.84	30.91	0.59
2	8.75	19.25	12.67	40.67	6.14	26.84	34.60	0.66
3	3.50	15.75	14.00	33.25	6.14	26.84	28.29	0.54
Avg.	6.42	16.33	14.00	36.75	6.14	26.84	31.26	0.60

Boro, 2022-23: Yanmar (AG600A) and Marksan (BM-608)

Factor: Field length

Interaction and Single affect of Field Length and Machine Model on Actual Field Capacity

Interaction effect of field length and machine model showed significant effect on actual field capacity of the combine harvesters. The significantly highest forward speed was observed for field length type 7, 6 and 5 for the Yanmar model and field length type 7, 6 for Marksan model combine harvesters along with field length type 5 for Yanmar model while the lowest significant actual field capacity (0.14 ha/h) was observed for field length type 1 for Marksan model which was identical to Yanmar model combine harvester for field length type 1 as shown in Table 30.

It was observed from figure 15 and 16, the actual field capacity of the combine harvester significantly varied with field length and machine model individually. The significantly highest actual field capacity was obtained for field length type 7 followed by field length type 6 while the significantly lowest forward speed was observed for field length type 1 which was identical to field length type 2. Between the two models, Yanmar gave significantly higher actual field capacity (0.33ha/h) compared to the Marksan model combine harvester (0.23 ha/h).

Table 30. Interaction Effect of Field Length and Machine Model on Actual Field Capacity

Machine	Field Length (m)							Mean
	<20	20-30	31-40	41-50	51-60	61-70	>70	
Yanmar	0.15	0.17	0.20	0.25	0.44	0.51	0.57	0.33
Marksan	0.14	0.16	0.18	0.21	0.25	0.29	0.35	0.23
Mean	0.15	0.17	0.19	0.23	0.35	0.40	0.46	0.28
LoS	M=***, L=***, M×L=***							
CV	7.05							
LSD _{0.05}	M=0.01, L=0.02, M×L=0.03							

Note: * means $P \leq 0.05$, ** means $P \leq 0.01$, *** means $P \leq 0.001$, NS means Non-significant, LoS means level of significance, M=Machine Model, L=Field Length, M×L= Machine×Field Length

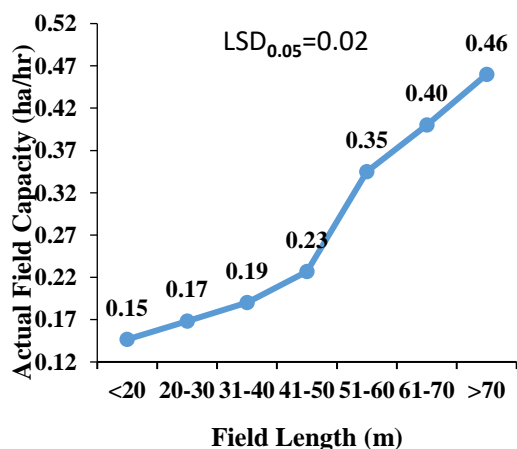


Figure 15. Effect of Field Length on Actual field Capacity

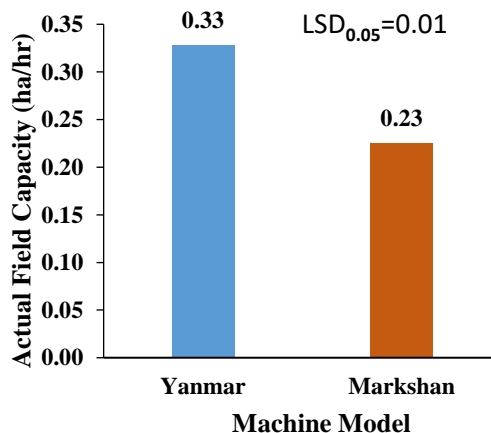


Figure 16. Effect of Machine Model on Actual field Capacity

Interaction and Single Effect of Field Length and Machine Model on Field Efficiency

Interaction effect of field length and machine model on field efficiency of the combine harvesters did not vary significantly. The highest field efficiency was observed for field length type 7 for the both model of the combine harvesters which was identical to field type 6 for Yanmar model while the lowest field efficiency (33.04%) was observed for field type 1 for Marksan model which was identical to Yanmar model (34.76%) as shown in Table 31. Figure 17 and 18 revealed that, field efficiency of the combine harvester significantly varied with field length and machine model individually. The highest significant field efficiency was observed for field type 7 followed by field type 6 while the lowest field efficiency was found for field type 1 which was identical to field length type 2. Between two models, Yanmar model (50.13%) gave significantly higher field efficiency compared to the Marksan model (45.98%).

Table 31. Interaction Effect of Field Length and Machine Model on Field Efficiency.

Machine	Field Length (m)							Mean
	<20	20-30	31-40	41-50	51-60	61-70	>70	
Yanmar	34.76	38.01	42.74	52.27	55.33	61.45	66.37	50.13
Markshan	33.04	36.21	38.80	44.15	49.66	55.45	64.52	45.98
Mean	33.90	37.11	40.77	48.21	52.49	58.45	65.45	48.05
LoS	M=***, L=***, M×L=NS							
CV	6.42							
LSD _{0.05}	M=1.95, L=3.65, M×L=5.16							

Note: * means $P \leq 0.05$, ** means $P \leq 0.01$, *** means $P \leq 0.001$, NS means Non-significant, LoS means level of significance, M=Machine Model, L=Field Length, M×L= Machine×Field Length

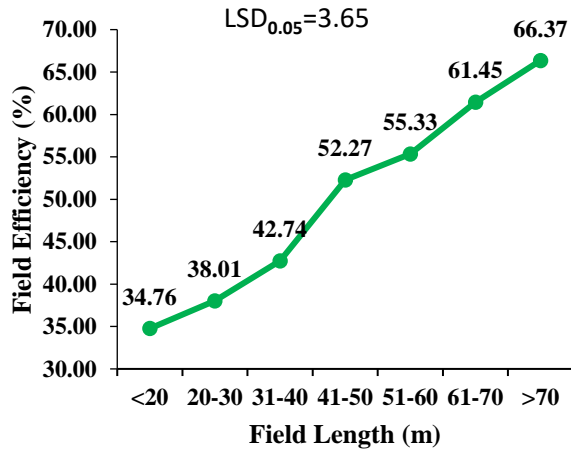


Figure 17. Effect of Field Length on Field Efficiency

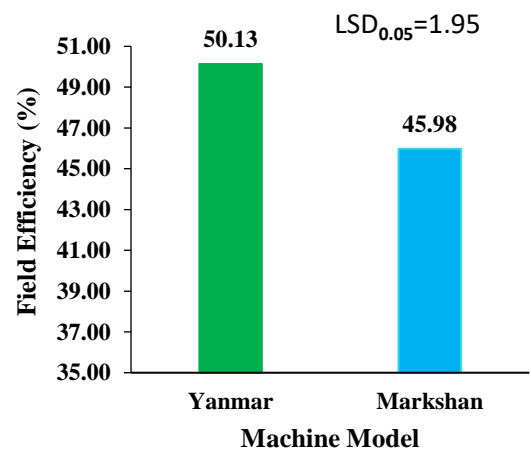


Figure 18. Effect of Machine Model on Field Efficiency.

Interaction and Single Effect of Field Length and Machine Model on Specific Fuel Consumption Rate

Interaction effect of field length and machine model on specific fuel consumption rate of the combine harvesters varied significantly. The significantly highest specific fuel consumption rate was observed for field length type 1, 2 and 3 for both model of the combine harvesters while the lowest significant specific fuel consumption was observed for field length type 7, 6 and 5 for Markshan model (0.070, 0.070 and 0.083 l/hp-hr) as shown in Table 32. It was observed from figure 19 and 20 that, specific fuel consumption (l/hp-h) of the combine harvester significantly varied with length of field individually while machine model did not vary significantly. The highest significant specific fuel consumption was observed for field length type 1 and 2 while the lowest specific fuel consumption was found for field type 7 and 6 (0.085 l/hp-h). Between the two models, the Yanmar harvester gave higher specific fuel consumption (0.104 l/hp-h) compared to the Markshan model combine harvester (0.096 l/hp-h).

Table 32. Interaction Effect of Field Length and Machine Model on Specific Fuel Consumption Rate.

Machine	Field Length (m)							Mean
	<20	20-30	31-40	41-50	51-60	61-70	>70	
Yanmar	0.110	0.110	0.103	0.103	0.103	0.100	0.100	0.104
Markshan	0.130	0.120	0.113	0.087	0.083	0.070	0.070	0.096
Mean	0.120	0.115	0.108	0.095	0.093	0.085	0.085	0.100
LoS	M=NS, L=***, M×L=*							
CV	16.44							
LSD _{0.05}	M=0.010, L=0.020, M×L=0.028							

Note: * means $P \leq 0.05$, ** means $P \leq 0.01$, *** means $P \leq 0.001$, NS means Non-significant, LoS means level of significance, M=Machine Model, L=Field Length, M×L= Machine×Field Length

Factor: Plant Density

Interaction and Single Effect of Plant Density and Machine Model on Actual Field Capacity

Interaction effect of plant density and machine model on actual field capacity of the combine harvesters did not vary significantly. The highest actual field capacity was observed for plant density range 1 for both of the combine harvesters followed by plant density range 2 while the lowest actual field capacity was observed for plant density range 7 for both of the Markshan and Yanmar model combine harvesters followed by plant density range 6 as shown in Table 33. It was observed from figure 21 and 22, the actual field capacity of the combine harvester significantly varied with plant density and machine model individually. The significantly highest actual field capacity (0.30 ha/h) was obtained for plant density range 1 followed by plant density range 2 (0.28 ha/h) while the significantly lowest actual field capacity was observed for plant density range 7 (0.16 ha/h) followed by plant density range 6 (0.19 ha/h). Between the two models, Yanmar gave significantly higher actual field capacity (0.24 ha/hr) compared to the Markshan model combine harvester (0.23 ha/h).

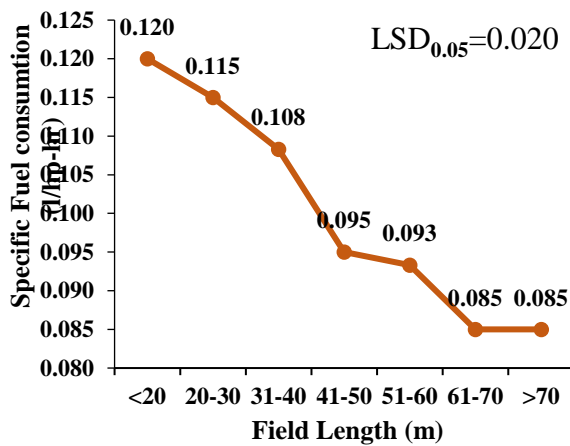


Figure 19. Effect of Field Length on Specific Fuel Consumption Rate.

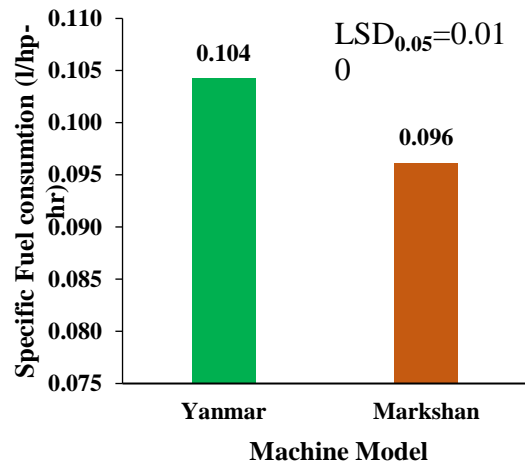


Figure 20. Effect of Machine Model on Specific Fuel Consumption Rate.

Table 33. Interaction Effect of Plant Density and Machine Model on Actual Field Capacity.

Machine	Plant Density (tillers/m ²)							Mean
	<230	230-240	241-250	251-260	261-270	271-280	>280	
Yanmar	0.31	0.29	0.27	0.24	0.22	0.20	0.17	0.24
Markshan	0.29	0.28	0.25	0.24	0.21	0.19	0.16	0.23
Mean	0.30	0.28	0.26	0.24	0.21	0.19	0.16	0.23
LoS	M=***, PD=***, M×PD=NS							
CV	2.92							
LSD _{0.05}	M=0.01, PD=0.01, M×PD=0.02							

Note: * means $P \leq 0.05$, ** means $P \leq 0.01$, *** means $P \leq 0.001$, NS means Non-significant, LoS means level of significance, M=Machine Model, PD=Plant Density, M×PD= Machine× Plant Density

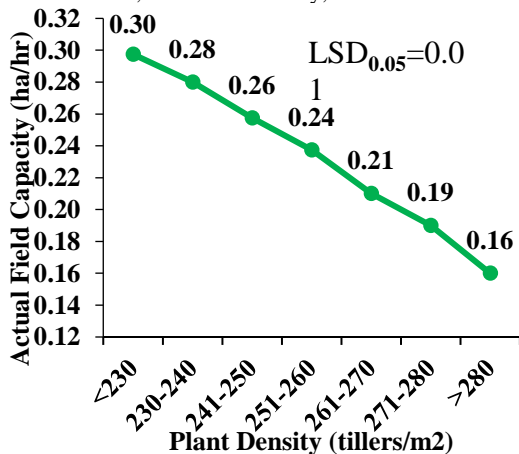


Figure 21. Effect of Plant Density on Actual Field Capacity.

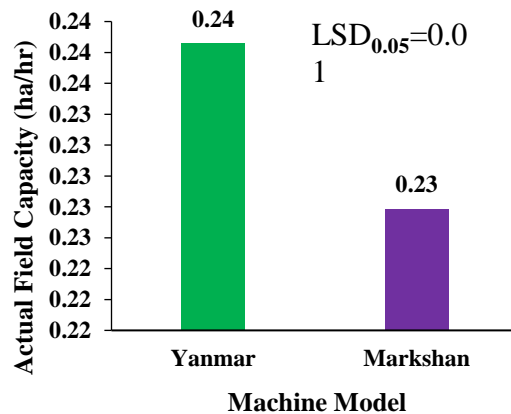


Figure 22. Effect of Machine Model on Actual Field Capacity.

Interaction and Single Effect of Plant Density and Machine Model on Field Efficiency

Interaction effect of plant density and machine model on field efficiency of the combine harvesters did not vary significantly. The highest field efficiency was observed for plant density range 1 for both of the combine harvesters followed by plant density range 2 while the lowest field efficiency was observed for plant density range 7 for both of the Marksan and Yanmar model combine harvesters followed by plant density range 6 as shown in Table 34. It was observed from figure 23 and 24, the field efficiency of the combine harvester significantly varied with plant density and machine model individually. The significantly highest field efficiency (60.64%) was obtained for plant density range 1 followed by plant density range 2 (58.00%) while the significantly lowest field efficiency was observed for plant density range 7 (37.81%) followed by plant density range 6 (44.30%). Between the two models, Yanmar gave significantly higher field efficiency (51.72%) compared to the Marksan model combine harvester (50.00%).

Table 34. Interaction Effect of Plant Density and Machine Model on Field Efficiency

Machine	Plant Density (tillers/m ²)							Mean
	<230	230-240	241-250	251-260	261-270	271-280	>280	
Yanmar	61.99	58.93	56.13	52.67	48.51	45.15	38.67	51.72
Marksan	59.30	57.07	54.56	51.88	46.81	43.45	36.95	50.00
Mean	60.64	58.00	55.34	52.28	47.66	44.30	37.81	50.86
LoS	M=**, PD=***, M×PD=NS							
CV	2.61							
LSD _{0.05}	M=1.08, PD=2.02, M×PD=2.85							

Note: * means $P \leq 0.05$, ** means $P \leq 0.01$, *** means $P \leq 0.001$, NS means Non-significant, LoS means level of significance, M=Machine Model, PD=Plant Density, M×PD= Machine× Plant Density

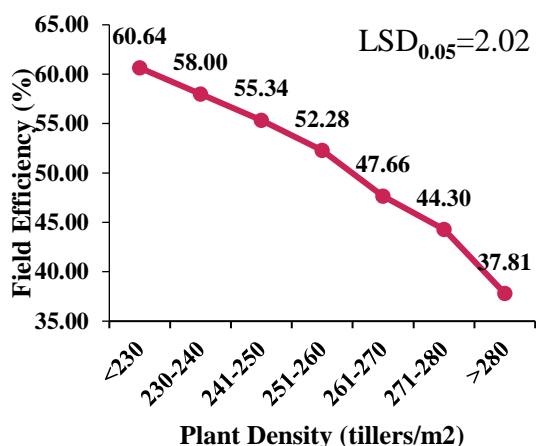


Figure 23. Effect of Plant Density on Field Efficiency.

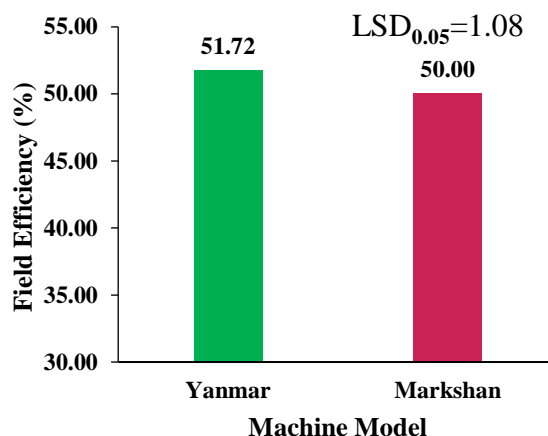


Figure 24. Effect of Machine Model on Field Efficiency.

Interaction and Single Effect of Plant Density and Machine Model on Specific Fuel Consumption Rate

Interaction effect of plant density and machine model on specific fuel consumption rate of the combine harvesters did not vary significantly. The highest specific fuel consumption rate was observed for plant density range 6 for Yanmar model and range 7 for both of the combine harvesters while the lowest specific fuel consumption rate was observed for plant density range 1 for Yanmar model combine harvester as shown in Table 35. It was observed from figure 25 and 26, the specific fuel consumption rate of the combine harvester significantly varied with plant density and machine model individually. The significantly highest specific fuel consumption rate (0.100 l/hp-h) was obtained for plant density range 7 followed by plant density range 6 (0.98 l/hp-h) while the significantly lowest specific fuel consumption rate was observed for plant density range 1 (0.088 l/hp-h) followed by plant density range 2 (0.090 l/hp-h). Between the two models, Marksan combine harvester consumed lower specific fuel (0.092 l/hp-h) compared to the Yanmar model combine harvester (0.093 l/hp-h).

Table 35. Interaction Effect of Plant Density and Machine Model on Specific Fuel Consumption Rate

Machine	Plant Density(tillers/m ²)							Mean
	<230	230-240	241-250	251-260	261-270	271-280	>280	
Yanmar	0.085	0.090	0.090	0.090	0.095	0.100	0.100	0.093
Markshan	0.090	0.090	0.090	0.090	0.090	0.095	0.100	0.092
Mean	0.088	0.090	0.090	0.090	0.093	0.098	0.100	0.093
LoS	M=NS, PD=***, M×PD=NS							
CV	3.54							
LSD _{0.05}	M=0.003, PD=0.005, M×PD=0.034							

Note: * means $P \leq 0.05$, ** means $P \leq 0.01$, *** means $P \leq 0.001$, NS means Non-significant, LoS means level of significance, M=Machine Model, PD=Plant Density, M×PD= Machine× Plant Density

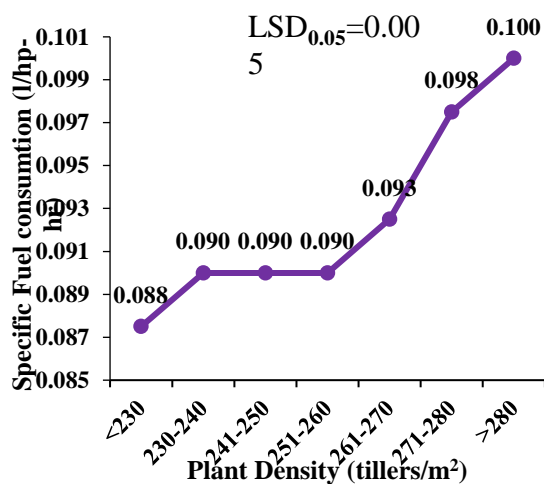


Figure 25. Effect of Plant Density on Specific Fuel Consumption Rate.

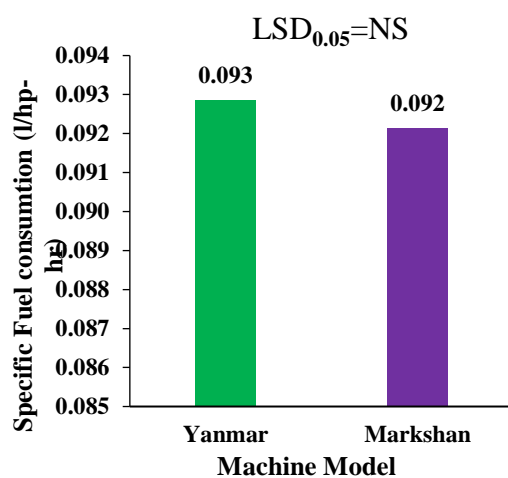


Figure 26. Effect of Machine Model on Specific Fuel Consumption Rate.

Factor: Crop Cutting Height from Ground

Interaction and Single Effect of Field Length and Machine Model on Actual Field Capacity

Interaction effect of crop cutting height and machine model on actual field capacity of the combine harvesters did not vary significantly. The highest actual field capacity was observed for crop cutting height range 7 and 6 for both of the combine harvesters while the lowest actual field capacity was observed for crop cutting height range 1 and 2 for both of the Marksan and Yanmar combine harvesters as shown in Table 36. It was observed from figure 27 and 28, the actual field capacity of the combine harvester significantly varied with crop cutting height individually while the machine model did not vary significantly. The significantly highest actual field capacity was obtained for crop cutting height range 7 (0.47 ha/h) followed by crop cutting height 6 (0.37 ha/h) while the significantly lowest actual field capacity was observed for field length type 1 and 2 (0.20 ha/h) followed by cutting range 3 (0.24 ha/h). Between the

two models, Yanmar gave higher actual field capacity (0.31 ha/h) compared to the Marksan model combine harvester (0.28 ha/h).

Table 36. Interaction Effect of Crop Cutting Height and Machine Model on Actual Field Capacity

Machine	Crop Cutting Height (mm)							Mean
	<100	100-110	111-120	121-130	131-140	141-150	>150	
Yanmar	0.21	0.20	0.25	0.30	0.32	0.38	0.51	0.31
Marksan	0.20	0.20	0.23	0.27	0.30	0.36	0.44	0.28
Mean	0.20	0.20	0.24	0.28	0.31	0.37	0.47	0.29
LoS	M=NS, CH=***, M×CH=NS							
CV	17.92							
LSD _{0.05}	M=0.04, CH=0.08, M×CH=0.11							

Note: * means $P \leq 0.05$, ** means $P \leq 0.01$, *** means $P \leq 0.001$, NS means Non-significant, LoS means level of significance, M=Machine Model, CH= Crop Cutting Height, M×CH= Machine× Crop Cutting Height

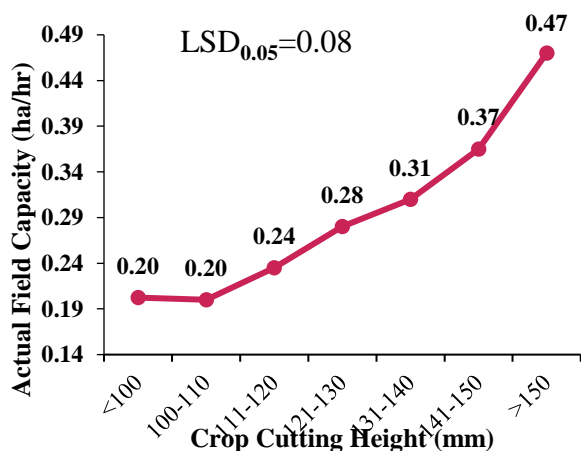


Figure 27. Effect of Crop Cutting Height on Actual Field Capacity.

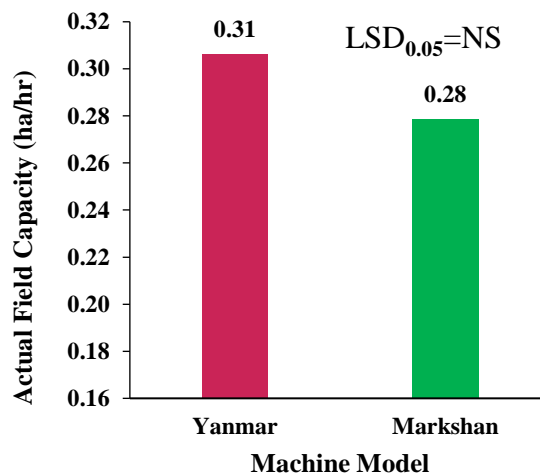


Figure 28. Effect of Machine Model on Actual Field Capacity.

Interaction and Single Effect of cutting height and Machine Model on Field Efficiency

Interaction effect of crop cutting height and machine model on field efficiency of the combine harvesters did not vary significantly. The highest field efficiency was observed for crop cutting height range 7 and 6 for both of the combine harvesters which was identical to Yanmar model for crop cutting height range 5 while the lowest field efficiency (29.34% and 29.04%) was observed for crop cutting height range 1 for both of the combine harvesters which was identical to Marksan model (43.55%) for crop cutting height range 2 as shown in table 37. It was observed from figure 29 and 30, the field efficiency of the combine harvester significantly varied with crop cutting height individually while the machine model did not vary individually. The significantly highest field efficiency (76.96 and 69.43%) was obtained for crop cutting height range 7 and 6 while the significantly lowest field efficiency was observed for plant density range 1 (29.21%). Between the two models, Yanmar gave significantly higher field efficiency (58.48%) compared to the Marksan model combine harvester (54.22%).

Table 37. Interaction Effect of Field Length and Machine Model on Field Efficiency

Machine	Crop Cutting Height (mm)							Mean
	<100	100-110	111-120	121-130	131-140	141-150	>150	
Yanmar	29.34	52.57	54.08	59.86	63.09	72.16	78.28	58.48
Markshan	29.07	43.55	50.30	54.48	59.77	66.70	75.65	54.22
Mean	29.21	48.06	52.19	57.17	61.43	69.43	76.96	56.35
LoS	M=NS, CH=***, M×CH=NS							
CV	15.08							
LSD _{0.05}	M=6.89, CH=12.89, M×CH=18.22							

Note: * means $P \leq 0.05$, ** means $P \leq 0.01$, *** means $P \leq 0.001$, NS means Non-significant, LoS means level of significance, M=Machine Model, CH= Crop Cutting Height, M×CH= Machine× Crop Cutting Height

Interaction and Single Effect of cutting height and Machine Model on Specific Fuel Consumption Rate

Interaction effect of crop cutting height and machine model on specific fuel consumption rate of the combine harvesters did not vary significantly. The highest specific fuel consumption rate was observed for crop cutting height range 1 for both of the combine harvesters which was identical to Yanmar model for crop cutting height range 2, 3, 4, 5, 6 and 7 while the lowest specific fuel consumption rate and was observed for crop cutting height range 7, 6, 5, 4, 3 and 2 for Marksan model combine harvester as shown in Table 38. It was observed from figure 31 and 32, the specific fuel consumption rate of the combine harvester did not vary significantly with crop cutting height while the machine model significantly varied individually. The highest specific fuel consumption rate was obtained for crop cutting height range 1 while

the lowest specific fuel consumption rate was observed for plant density range 7, 6, 5, 4,3, and 2. Between the two models, Marksan consumed significantly lower specific fuel (0.0104 l/hp-h) compared to the Yanmar model combine harvester (0.116 l/hp-h).

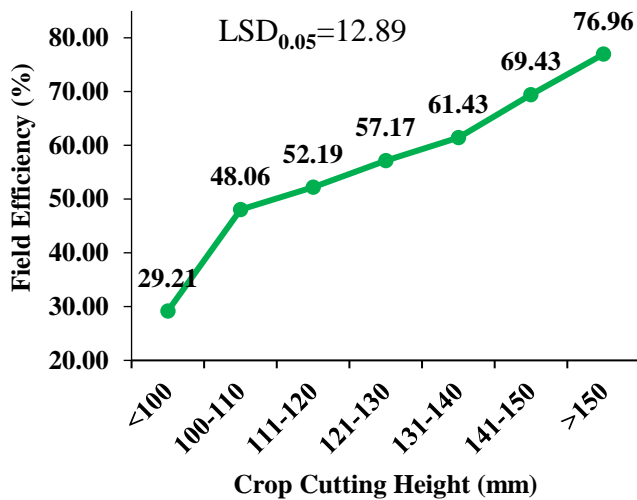


Figure 29. Effect of Crop Cutting Height on Field Efficiency.

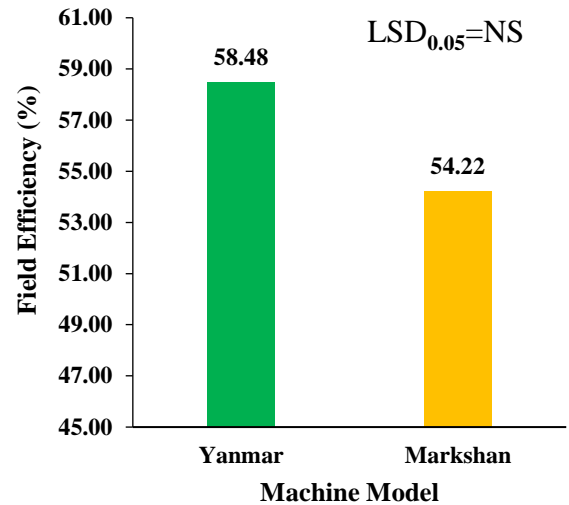


Figure 30. Effect of Machine Model on Field Efficiency.

Table 38. Interaction and Single Effect of cutting height and Machine Model on Specific Fuel Consumption Rate.

Machine	Crop Cutting Height (mm)							Mean
	<100	100-110	111-120	121-130	131-140	141-150	>150	
Yanmar	0.131	0.116	0.115	0.114	0.114	0.112	0.112	0.116
Markshan	0.129	0.101	0.104	0.101	0.099	0.098	0.099	0.104
Mean	0.130	0.108	0.109	0.107	0.106	0.105	0.105	0.110
LoS	M=*, CH=NS, M×CH=NS							
CV	10.17							
LSD _{0.05}	M=0.009, CH=0.017, M×CH=0.024							

Note: * means $P \leq 0.05$, ** means $P \leq 0.01$, *** means $P \leq 0.001$, NS means Non-significant, LoS means level of significance, M=Machine Model, CH= Crop Cutting Height, M×CH= Machine× Crop Cutting Height

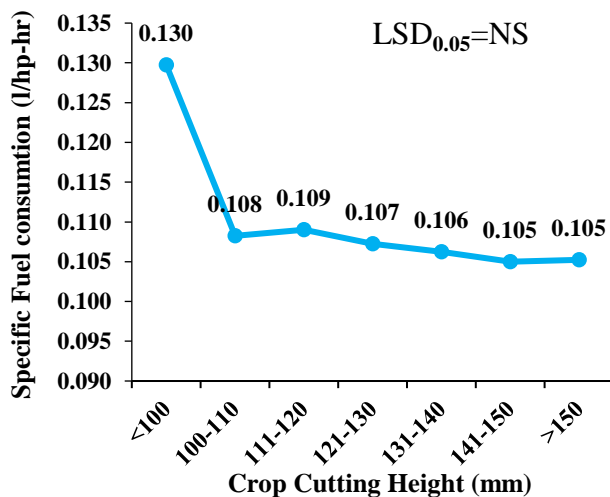


Figure 31. Effect of Crop Cutting Height on Fuel Consumption Rate.

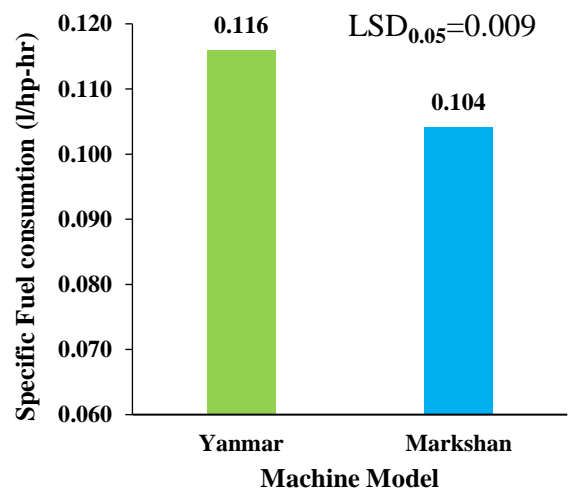


Figure 32. Effect of Machine Model on Fuel Consumption Rate.

Factor: Operator's skill

Interaction and Single Effect of Operators' Skill and Machine Model on Actual Field Capacity

Interaction effect of operators' skill and machine model on actual field capacity of the combine harvesters did not vary significantly. The highest actual field capacity was observed for those operators who had greater than two years to one year of experience for Yanmar model and greater or equal to two years of experience for Marksan model while the lowest actual field capacity was observed for those operators who had one year and no experience for Marksan model which was identical to Yanmar model for those who had no experience as shown in Table 39.

It was observed from figure 33 and 34, the actual field capacity of the combine harvester significantly varied with operators' skill and machine model individually. The significantly highest actual field capacity (0.25 ha/h) was obtained for those operators who had greater than two or two years of experience which was identical to those operators who had one year of experience (0.23 ha/h) while the significantly lowest actual field capacity (0.21 ha/h) was observed for those operators who had no experience which was identical to those operators who had one year of experience (0.23 ha/h). Between two models, Yanmer gave significantly higher actual field capacity (0.24 ha/h) compared to Marksan model combine harvester (0.22 ha/h).

Table 39. Interaction Effect of Operators' Skill and Machine Model on Actual Field Capacity.

Machine	Operators' Skill (Years)			Mean
	≥ 2	1	0	
Yanmar	0.26	0.25	0.22	0.24
Markshan	0.24	0.22	0.19	0.22
Mean	0.25	0.23	0.21	0.23
LoS	M=*, Op=*, M×Op=NS			
cv	8.07			
LSD _{0.05}	M=0.03, Op=0.03, M×Op=0.05			

Note: * means $P \leq 0.05$, ** means $P \leq 0.01$, *** means $P \leq 0.001$, NS means Non-significant, LoS means level of significance, M=Machine Model, Op=Operators' Skill, M×Op= Machine× Operators' Skill

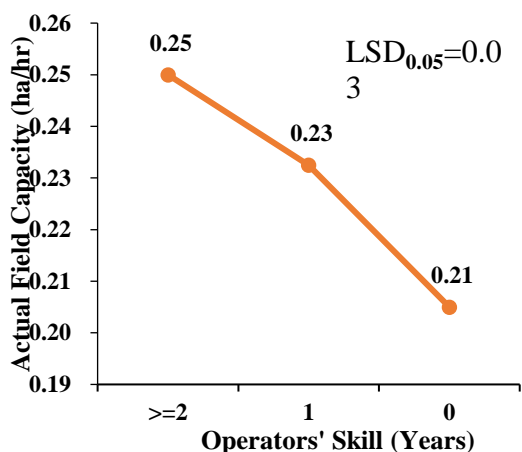


Figure 33. Effect of Operators' Skill on Actual Field Capacity

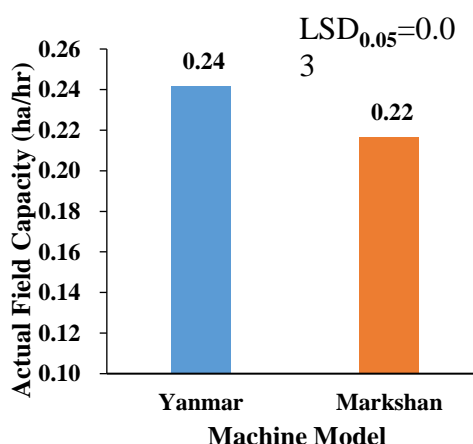


Figure 34. Effect of Machine Model on Actual Field Capacity

Interaction and Single Effect of Operators' Skill and Machine Model on Field Efficiency

Interaction effect of operators' skill and machine model on field efficiency of the combine harvesters did not vary significantly. The highest field efficiency was observed for those operators who had greater than two years to one year of experience for Yanmar model and greater or equal to two years of experience for Marksan model while the lowest field efficiency was observed for those operators who had one year and no experience for Marksan model which was identical to Yanmar model for those who had no experience as shown in **Table 40**. It was observed from figure 35 and 36, the field efficiency of the combine harvester significantly varied with operators' skill and machine model individually. The significantly highest field efficiency (51.64%) was obtained for those operators who had greater than two or two years of experience which was identical to those operators who had one year of experience (48.52%) while the significantly lowest field efficiency (43.98%) was observed for those operators who had no experience which was identical to those operators who had one year of experience (48.52%). Between the two models, Yanmer gave significantly higher field efficiency (55.55%) compared to Marksan model combine harvester (45.55%).

Table 40. Interaction and Single Effect of Operators' Skill and Machine Model on Field Efficiency.

Machine	Operators' Skill (Years)			Mean
	≥ 2	1	0	
Yanmar	53.47	51.71	46.47	50.55
Markshan	49.82	45.34	41.50	45.55
Mean	51.64	48.52	43.98	48.05
LoS	M=*, Op=*, M×Op=NS			
cv	6.24			
LSD _{0.05}	M=4.23, Op=5.19, M×Op=7.33			

Note: * means $P \leq 0.05$, ** means $P \leq 0.01$, *** means $P \leq 0.001$, NS means Non-significant, LoS means level of significance, M=Machine Model, Op=Operators' Skill, M×Op= Machine× Operators' Skill

Interaction and Single Effect of Operators' Skill and Machine Model on Specific Fuel Consumption Rate

Interaction effect of operators' skill and machine model on specific fuel consumption rate of the combine harvesters did not vary significantly. The highest specific fuel consumption rate was observed for those operators who had no experience for both of the combine harvesters while the lowest specific fuel consumption rate was observed for those operators who had greater or equal to two years of experience for both of the combine harvesters as shown in Table 41. It was observed from figure 37 and 38, the specific fuel consumption rate of the combine harvester significantly varied with operators' skill individually while the machine model did not vary significantly. The significantly lowest specific fuel consumption rate (0.086 l/hp-h) was obtained for those operators who had greater than two or two years of experience while the significantly highest specific fuel consumption rate (0.097 l/hp-h) was observed for those operators who had no experience. Between the two models, Yanmer gave higher specific fuel consumption rate (0.092 l/hp-h) compared to Marksan model combine harvester (0.090 l/hp-h).

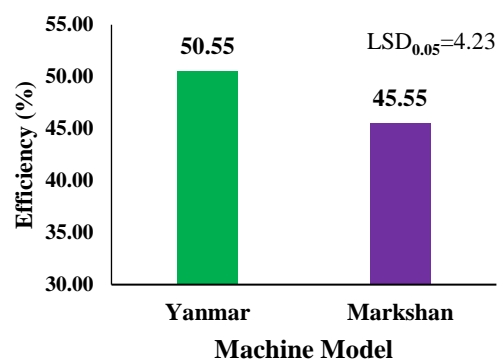
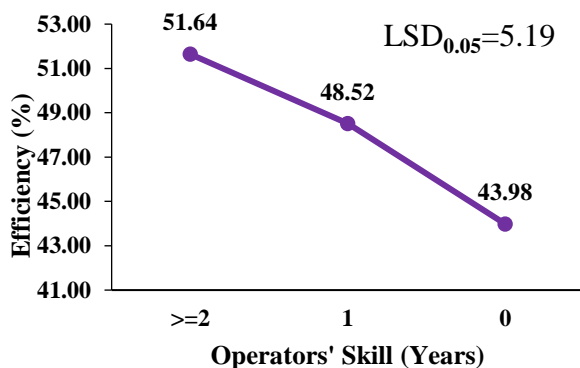


Figure 35. Effect of Operators' Skill on Field Efficiency. Figure 36. Effect of Machine Model on Field Efficiency.

Table 41. Interaction and Single Effect of Operators' Skill and Machine Model on Specific Fuel Consumption Rate.

Machine	Operators' Skill (Years)			Mean
	≥ 2	1	0	
Yanmar	0.086	0.093	0.097	0.092
Marksan	0.086	0.090	0.096	0.090
Mean	0.086	0.091	0.097	0.091
LoS	M=NS, Op=***, M×Op=NS			
CV	1.88			
LSD _{0.05}	M=0.002, Op=0.003, M×Op=0.004			

Note: * means $P \leq 0.05$, ** means $P \leq 0.01$, *** means $P \leq 0.001$, NS means Non-significant, LoS means level of significance, M=Machine Model, Op=Operators' Skill, M×Op= Machine× Operators' Skill

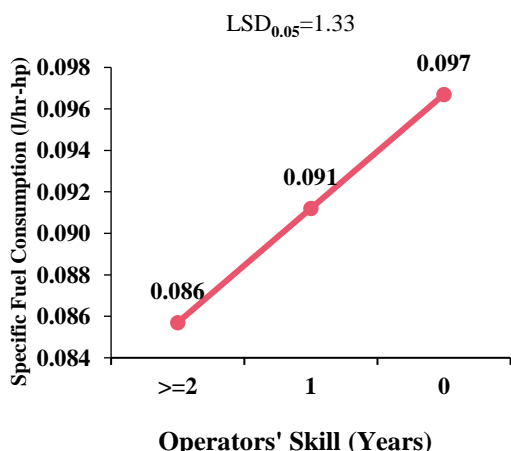


Figure 37. Effect of Crop Operators' Skill on Specific Fuel Consumption.

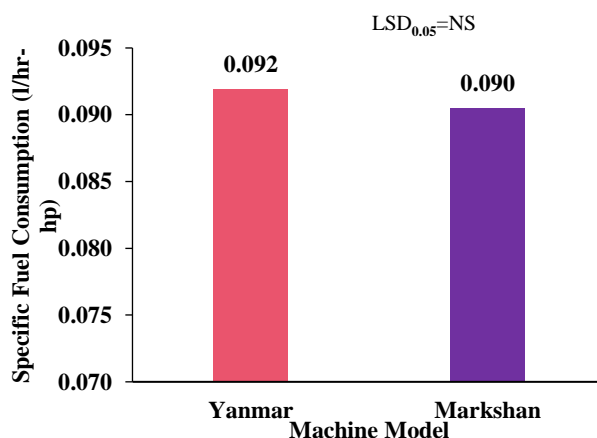


Figure 38. Effect of Machine Model on Specific Fuel Consumption.

Economic Performance Evaluation

Break-Even Use

Figures 39 and 40 illustrate the break-even use for mechanized harvesting with the Yanmar & Markshan model combine harvester. To cover yearly fixed costs, the break-even area for mechanized harvesting using a Yanmar combine harvester is 29 hectares of rice land, while a Markshan model is 26 hectares. Because the Markshan model's overall operational cost is lower, it requires less area coverage to cover the yearly fixed costs than the Yanmar model. After harvesting 26 ha of paddy fields at an initial cost of Tk 29,50,000 and 29 ha of paddy fields at an initial cost of Tk 31,50,000, respectively, and at harvesting rates of 0.24 ha/h and 0.28 ha/h, it becomes economically feasible to own the Yanmar and Marshan model combine harvesters. The data show that as the annual field area covered by harvesting increases, so does the overall operational cost for harvesting paddy with a combine harvester. The outcomes additionally demonstrated that the combine harvester is financially advantageous to end users when the annual harvesting area coverage surpasses the size of the rice field.

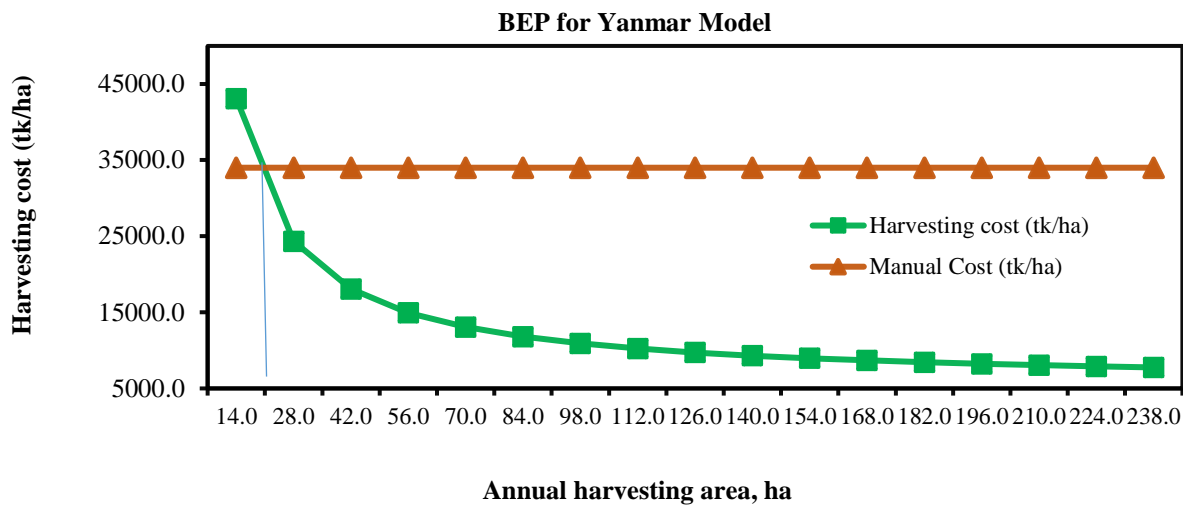


Figure 39. Break Even Use for Yanmar Model Combine Harvester.

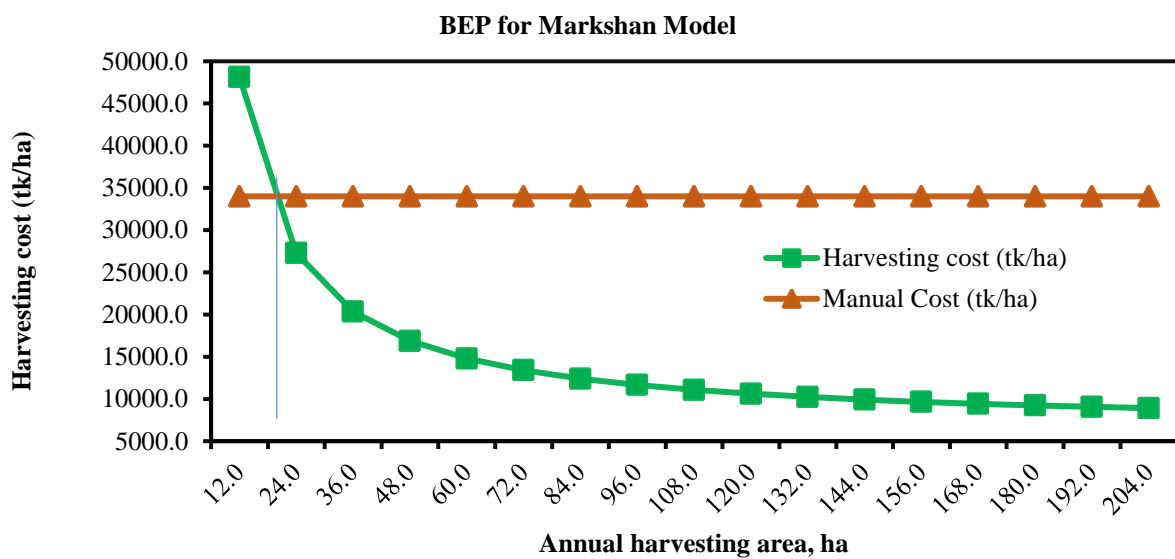


Figure 40. Break Even Use for Markshan Model Combine Harvester.

Conclusion

Field performance, more specifically forward speed, effective field capacity, and field efficiency of both head feed and whole feed combine harvester varied relatively in line with the length of the field. It is also varied inversely with the crop density, positively with the cutting height and operators' stillness. The field length must be more than 40 m for getting 50% field efficiency of the machine. However, grain loss of the head feed combine harvester is less than 1% while it was about 1.80% for the whole feed combine harvester.

III. Validation of rice transplanter cum mixed fertilizer applicator with existing practices

BRRRI-developed rice transplanter cum mixed fertilizer applicator was used in this experiment for validation. It was designed and fabricated in the Farm Machinery and Postharvest Technology Divisional research workshop. The major specification and features of the machine are given in Table 42. The photographic view of the rice transplanter cum mixed fertilizer applicator is also shown in Plate 8.



Plate 8. BRRRI developed rice transplanter cum mixed fertilizer applicator.

Table 42. Description of the rice transplanter cum mixed fertilizer applicator.

Country of origin and Model		South Korea and ARP-4UM
Type		Walk behind type
Dimensions	Overall length × width × height (mm)	23505×1480×800
	Overall weight (kg)	175
	Maximum output kW rpm ⁻¹	3/1800
	Starting method	Recoil
Travelling Section	Steering	Hydraulic power steering mode
	Wheel type	Rubber lug wheel (Dia.: 60 cm)
	Gearshift: Forward× Reverse	2 speeds and 1 speed
Transplanting Section	Transplanting mechanism	Rotary
	Number of rows	4
	Row-to-row distance (mm)	300 (fixed)
	Plant-to-plant distance (mm)	110 to 150
	Transplanting speed, m s ⁻¹	0.3 to 0.7
Fertilizer application section	Dispensing mechanism	Screw conveyor type associated with flexible pipe, furrow opener, and closer mechanism
	Fertilizer dose	Simple lever
	Operation	Engage and disengage the lever
	Fertilizer placement depth control	Mechanical
	Hopper capacity (kg)	8-10
	Power transmission	Engine to screw conveyer through belt-pulley and gear mechanism

Treatments

T1: Machine transplanting with 100% urea fertilizer

T2: Machine transplanting with 80% urea fertilizer

T3: Machine transplanting with 70% urea fertilizer

T4: Machine transplanting without fertilizer

T5: Farmers practice

The location of the trials, the farmer's address, and basic information about the trials were presented in Table 43.

Table 43. Basic Information of the rice transplanter cum fertilizer applicator.

Trial no.	Season	Location	Variety	Area covered (ha)	Date of sowing	Date of transplanting
1	Boro/2022-23	Habiganj	BRR1 92	2.01	19-12-22	25-01-23
2		Habiganj	BRR1 92	1.34	20-12-22	17-02-23
3		Sirajganj	BRR1 92	1.34	22-12-22	10/2/2023
4		Sirajganj	BRR1 92	0.28	22-12-22	11/2/2023
5	Aman, 2023	Habiganj	BRR195	0.40	10/7/2023	22/8/23
6		Habiganj	BRR187	0.27	10/7/2023	21/8/23
7		Sirajganj	BRR175	0.40	15/7/2023	10/8/2023
8		Sirajganj	BRR175	0.40	15/7/2023	11/8/2023

Results and Discussion***Validation of rice transplanter cum mixed fertilizer applicator with existing practices*****Field performance of the rice transplanter cum mixed fertilizer applicator (Boro 2022-23)**

The field capacity of the developed rice transplanter cum mixed fertilizer applicator was also measured with and without fertilizer deep placement mechanism in four locations during Boro 2022-23 seasons (Table 44). The actual field capacity of the rice transplanter varied from was found 0.15 to 0.22 ha hr⁻¹ with fertilizer deep placement while it varied from 0.22 to 0.25 hah⁻¹ without fertilizer deep placement mechanism in Boro 2022-23 season, respectively. Field efficiency varied from 63 to 86% with fertilizer deep placement while it varied from 60 to 84% without fertilizer deep placement mechanism. Field capacity was found higher to some extent without fertilizer deep placement mechanism during transplanting due to extra fertilizer re-filling time and slow operation.

Table 44. Field performance of the rice transplanter cum mixed fertilizer applicator Boro 2022-23 Season

Locations	Treat	Area (Decimal)	Length (m)	Operation time (hr)	Operation time (min)	Width of cover (m)	FS (km/h)	AFC (ha/h)	TFC (ha/h)	Efficiency (%)
Sirajganj-1	T ₁	55	65	1.48	89	1.2	1.62	0.15	0.1944	77.22
	T ₂	45	62	0.97	58	1.2	2.1	0.19	0.252	74.79
	T ₃	48	48	0.95	57	1.2	2.2	0.20	0.264	77.48
	T ₄	42	50	0.73	44	1.2	2.5	0.23	0.3	77.29
	T ₅	40	42	16.00	2500	0	0	0.010	0	76.70
Sirajganj-2	T ₁	49	68	1.23	74	1.2	1.95	0.16	0.234	68.74
	T ₂	50	70	1.18	71	1.2	2.1	0.17	0.252	67.88
	T ₃	50	62	1.10	66	1.2	2.3	0.18	0.276	66.68
	T ₄	48	60	0.87	52	1.2	3.1	0.22	0.372	60.28
	T ₅	45	55	21.67	1300	0	0	0.008	0	65.89
Habiganj-1	T ₁	120	85	2.53	152	1.2	2.52	0.19	0.3024	63.42
	T ₂	85	85	2.20	132	1.2	2.03	0.16	0.2436	64.21
	T ₃	80	80	1.45	87	1.2	2.8	0.22	0.336	66.48
	T ₄	75	75	1.30	78	1.2	2.9	0.23	0.348	67.12
	T ₅	35	72	12.67	760	0	0	0.011	0	65.31
Habiganj-2	T ₁	120	128	2.65	159	1.2	1.78	0.18	0.2136	85.83
	T ₂	100	120	2.20	132	1.2	1.95	0.18	0.234	78.64
	T ₃	75	101	1.53	92	1.2	2.2	0.20	0.264	75.01
	T ₄	35	95	0.57	34	1.2	2.5	0.25	0.3	83.35
	T ₅	30	90	11.23	674	0	0	0.011	0	80.71

Field efficiency vs field length

The field efficiency of the rice transplanter cum mixed fertilizer applicator varied with field length. It is observed in the liner regression curve ($R^2 = 0.90$) that the field performance of the rice transplanter cum mixed fertilizer applicator varied relatively in line with field length in an average of 04 locations (02 locations in Sirajganj and 02 locations in Habiganj) where 90% variable explained the prediction of field efficiency varied with the field length (Fig. 41).

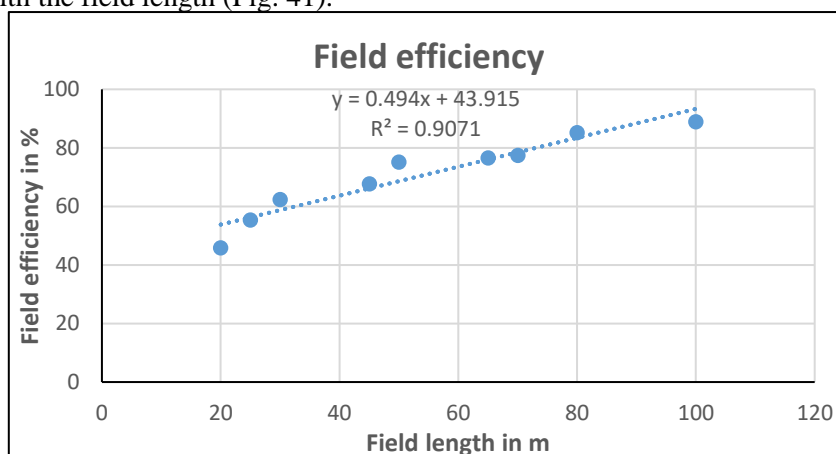


Figure 41. Influences of field length on field efficiency of the rice transplanter.

Yield and TWG of Boro 2022-23 season

Grain yield under different treatments of mechanical rice transplanting along with fertilizer deep placement at different rate varied significantly with the mechanical transplanting and farmers practices (Table 45).

Table 45. Grain yield and 1000 grain weight as affected by different treatments.

Location	Treatments	Yield (t/ha)	TGW (g)
Habiganj-1	1	7.81 a	23.57
	2	7.43 b	23.20
	3	7.27 bc	23.20
	4	7.13 c	23.23
	5	6.49 d	23.0
	% of CV value	4.32	3.80
	LSD0.05	0.1794	0.6459
Habiganj-2	1	7.57 a	22.13 b
	2	6.98 b	22.30 ab
	3	6.90 b	22.50 ab
	4	6.81 bc	22.63 ab
	5	6.31 c	22.80 a
	% of CV value	4.45	5.62
	LSD0.05	0.5789	0.6371
Sirajganj-1	1	7.38 a	22.03
	2	6.79 ab	22.10
	3	6.71 bc	22.33

Location	Treatments	Yield (t/ha)	TGW (g)
	4	6.62 bc	22.46
	5	6.13 c	22.63
	% of CV value	4.67	3.60
	LSD0.05	0.6025	0.6819
Sirajganj-2	1	7.12 a	21.83
	2	6.60 b	21.9
	3	6.52 b	22.17
	4	6.44 bc	22.30
	5	5.96 c	22.47
	% of CV value	5.52	4.85
	LSD0.05	0.5071	0.6504

Note: T1: Machine transplanting with 100% urea fertilizer, T2: Machine transplanting with 80% urea fertilizer, T3: Machine transplanting with 70% urea fertilizer, T4: Machine transplanting without fertilizer (fertilizer used as per farmers practice) and T5: Farmers practice

Conclusion

BRRRI already incorporated the mixed fertilizer deep placement mechanism in the existing walking-type rice transplanter. The developed rice transplanter cum mixed fertilizer applicator was used in the study entitled “Validation and comparative analysis of rice transplanter cum mixed fertilizer applicator with existing practices” for validation. The developed technology were evaluated in both Aman, 2022 season and Boro 2022-23 season. In all cases, the actual field capacity of the rice transplanter varied from was found insignificant less with fertilizer deep placement compare with the without fertilizer deep placement mechanism in both the seasons. It is observed in the liner regression curve that the field performance of the rice transplanter cum mixed fertilizer applicator varied relatively in line with field length. BCR of rice production is found more transplanting with the developed technology at 80% less of recommended urea fertilizer because of significantly higher yield.

Experiment 1.6: Modification of power transmission system of BRRRI hydro-tiller

Principal Investigator: Mohammad Afzal Hossain

Co-Investigator: MGKB, HR, MA

Objectives

- To detect the causes of frequent tearing of hydro-tiller chain
- To modify the power transmission system for increasing longevity of hydro-tiller

Materials and method

Hydro-tiller was tested at BRRRI West byde to find out the causes of frequent tearing of hydro-tiller chain. The reason associated with the fault of hydro-tiller chain tearing was identified and necessary modification was done using M/S sheet, different types of gear, sprocket, bearing, chain etc. The complete design of the modified hydro-tiller was done with the help of Solid works tool. After that, the modified hydro-tiller was tested at BRRRI west byde, Gazipur.

Theoretical field capacity

Theoretical field capacity is the rate of field coverage of an implement that would be obtained if the machine were performing its function 100% of the time at the rated forward speed and always covered 100% of its width.

$$TFC = W \times S$$

Where,

TFC=Theoretical field capacity ($m^2 hr^{-1}$)

W=Operating width of the machine (m)

S= Speed (mhr^{-1})

Actual field capacity

Actual field capacity is the ratio of actual rate of field coverage by the machine to the total time during operation.

$$AFC = \frac{A}{T}$$

Where,

AFC= Actual field capacity ($m^2 hr^{-1}$)

A= Area (m^2)

T= Operating time (hr)

Field efficiency

It is the ratio of effective field capacity to the theoretical field capacity of a machine under field conditions and the theoretical maximum productivity and it can be calculated by the following equation:

$$\eta = \frac{C}{C_o} \times 100$$

Where,

η = Field efficiency (%)

C = Actual field capacity ($\text{m}^2 \text{hr}^{-1}$)

C_o = Theoretical field capacity ($\text{m}^2 \text{hr}^{-1}$)

Fuel consumption

Before starting the operation in the test plot, the fuel tank of the engine was filled up to its top. The quantity of fuel required to fill the tank fully after puddling the plot was measured to determine the quantity of fuel consumed for puddling the test plot.

Results and Discussion

Shortcomings and faults of the hydro-tiller

Failure of the transmission chain occurred repeatedly. Stopping of engine arose occasionally due to overloading. The reason associated with the fault of hydro-tiller chain tearing was identified as the followings:

- Thickness of the chain is not sufficient to bear the load.
- Strength of the bearing of the rotary box is not sufficient to bear the load.

To overcome the problem, the following modification was done.

Modification of the power transmission system of the hydro-tiller

To increase of the strength of the power transmission elements of the Hydro-tiller, thickness of the sprocket and width of the chain was increased.

- Thickness of the sprocket (9 mm) was increased to 11 mm (Fig. 42).
- ASME #60 chain was used instead of ASME #50 chain. Width of the ASME #60 chain is 23 mm (Fig. 43).
- Two bearing was set in combine to the rotary box shaft instead of single bearing to increase the strength of the Hydro-tiller in smooth operation at full load condition. Size of each bearing was 62 mm x 16 mm (Fig. 44 & 45).

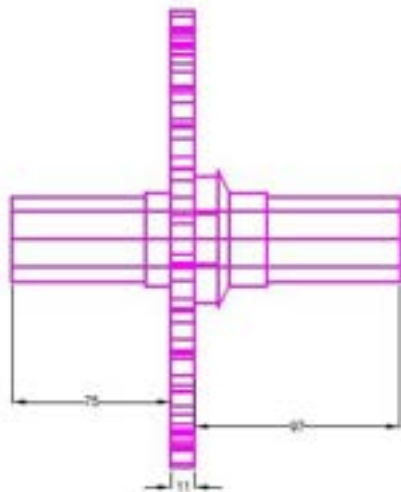


Fig.42. Sprocket



Fig. 43. Chain ASTM #60



Fig. 44. Arrangement of double bearing in gearbox

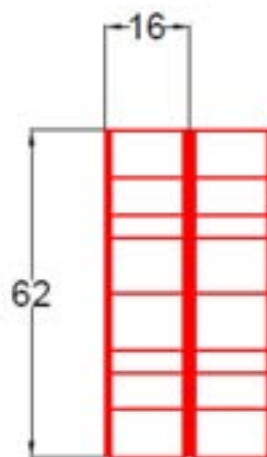


Fig. 45. Combination of two bearing

Developed hydro-tiller

Hydro-tiller is a floating rotary tiller, puddle the low lying fields uniformly with less operations. It is suitable for both primary and secondary tillage when the field has been soaked for at least half a day to soften the soil. The modified hydro-tiller is more suitable for water-logged, marshy lands. It consists of an engine, gear box, pontoon, cage wheel, clutch lever etc. Its' specification is given in Table 46 and depicted in Fig. 46.

Table 46. Specification of the hydro tiller.

Physical dimensions	Transmission	Engine
Length, 195 cm Width at front, 160 cm Width at rear, 85 cm Height, 75 cm Cage wheel dia, 270 cm	Belt pulley between engine and primary transmission load Enclosed chain and sprocket between primary transmission load to cage wheel	Robin EY 40B Max. power: 8.2 kw Revolution per minute (rpm): 3600

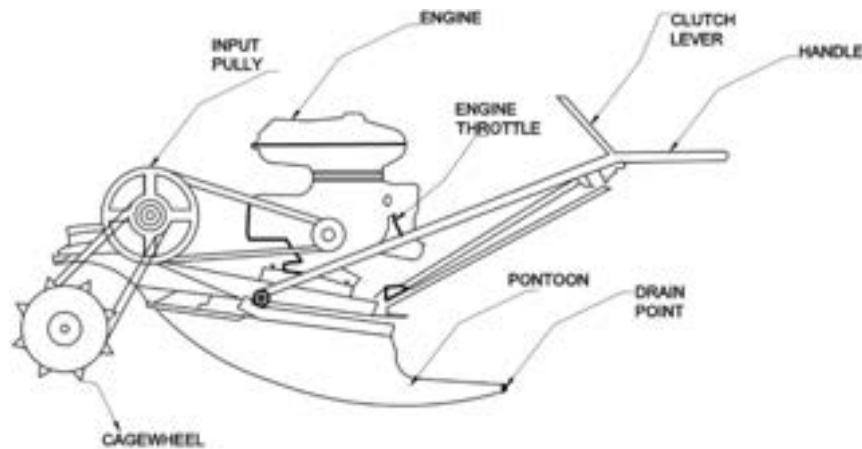


Fig. 46. A schematic diagram of the modified Hydro tiller.

Power transmission system of hydro-tiller

A 8.2 kw engine was used to increase the capacity of the Hydro-tiller. RPM of the engine is 2800. It was step down to 2400 rpm in the gear box shaft through the power transmission elements i.e. v belt, pulley. Again, it was step down to 1800 rpm in the cage wheel shaft through the power transmission elements i.e. chain, sprocket, bearing. A flow sheet diagram of power transmission system of the modified hydro-tiller is depicted in Fig. 47.

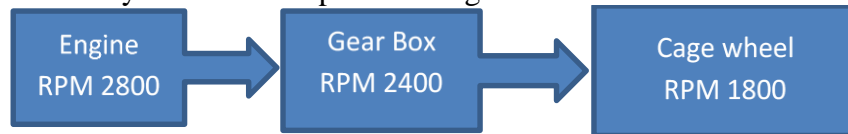


Fig. 47. Flow sheet diagram of power transmission system of the modified hydro-tiller

Cage wheel

Cage wheels till and soften the marshy land. Two cage wheel was attached in the gear box shaft. Length of each cage wheel is 478 mm. Diameter of each cage wheel is 270 mm. An exploded view of power transmission elements of hydro-tiller is presented in Fig. 48 and 49.

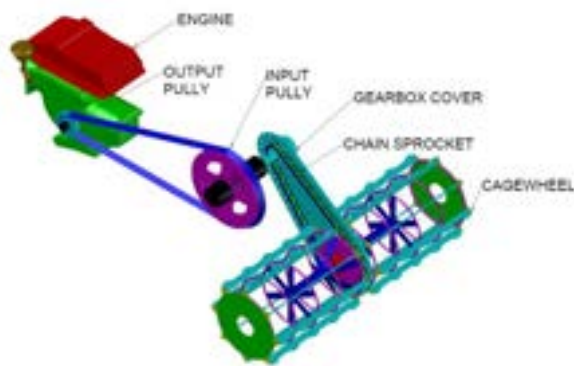


Fig. 48. Power transmission system of Hydro tiller.

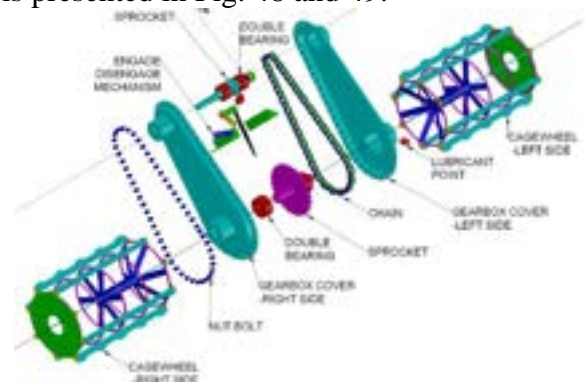


Fig. 49. Exploded view of power transmission system between gearbox and cage wheel

Performance of modified hydro-tiller

Existing hydro-tiller was tested (Plate 9) and its capacity was found 0.023 ha/h. After modification, the capacity of the hydro-tiller was increased to 0.039 ha/h. Average fuel consumption of the modified hydro-tiller was 2.01 l/h (Table 47).

Table 47. Field performance of the modified hydro-tiller.

Location	No. of trail	Actual rate of area coverage (ha/h)	Theoretical rate of area coverage (ha/h)	Field efficiency (%)	Fuel consumption (l/h)
BRR West	1	0.037	0.061	64.0	1.97
Byde	2	0.039		61.7	2.00
Gazipur	3	0.041		67.4	2.05



Plate 9. Test of modified hydro-tiller at BRRRI west byde, Gazipur.

Before modification of the hydro-tiller, the average number of chain and belt tearing was about 20 and 16 per year, respectively. The number of chain and belt tearing of the hydro-tiller has been decreased to below 8 per year after the modification. On an average 150 number engine stopping event due to overloading was found every year in the existing hydro-tiller. After modification of the hydro-tiller, this number sharply fall to around 10 last year. No event of engine stopping due to overloading arose during land cultivation this year. This is depicted in Fig. 50.

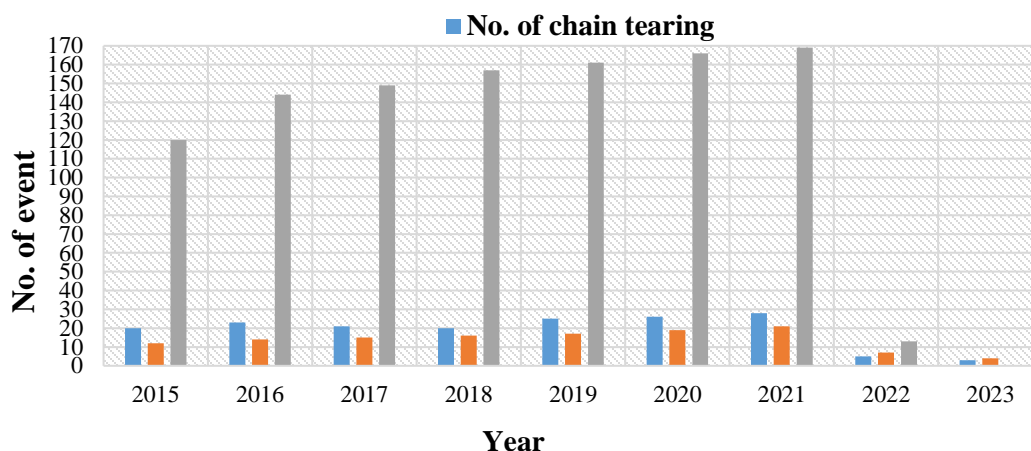


Fig. 50. Chain, belt tearing and engine stopping scenario of the hydro-tiller.

Conclusion

The fault of BRRRI hydro-tiller chain tearing was identified i.e. thickness of the chain is not sufficient to bear the load, strength of the bearing of the rotary box is not sufficient to bear the load through a field test at BRRRI West Byde. The existing BRRRI Hydro-tiller was modified accordingly at BRRRI research workshop and tested at BRRRI west Byde, Gazipur. Its' capacity was found 0.039 ha/hr. Its' capacity increased 0.016 ha/hr. than that of the existing one. The number of chain and belt tearing of the hydro-tiller has been decreased sharply after modification. No engine stopping event due to overloading occurred during land cultivation.

1.7: Experiment: Design and Development of a manually operated Briquetting Machine.

Principal Investigator: Md. Mahir Shahriyar

Co-Investigator(s): MMR, HR, M.R Karim, MI

Objectives

- To design and develop a manually operated briquetting machine.
- To evaluate the performance of the briquetting machine.
- To determine the physical and combustion properties of the briquette.

Materials and method

Design consideration

- This machine should be suitable for household-level use.
- The briquette machine design should prioritize simplicity and manual operation.
- Unlike existing pressing machines that pose environmental hazards, this machine must be smoke-free and environmentally friendly.
- It should be fabricable and repairable using locally available materials.
- The cost should be within reach for smallholder farmers, enabling them to fulfill their daily cooking fuel needs easily.

Design Steps

- According to the design, the material was collected from the local market.
- The frame forms the briquette machine's basic structure and supports other components. The frame serves as the briquette machine's foundational structure, crafted using angle bars for durability, robustness, and resistance to deformation during the pressing process.

- A square-shaped cylinder was meticulously designed, taking into account the appropriate size for the briquette.
- A scissor-pressing mechanism was employed to facilitate the compression of raw materials within the pressing chamber, utilizing four pistons.
- The components, including the frame, basement, square-shaped cylinder, scissor pressing unit, pistons, and handle, were manufactured and assembled at the FMPHT divisional workshop (Fig. 51).
- After prototype fabrication, a lab test was conducted using charcoal and rice husk.

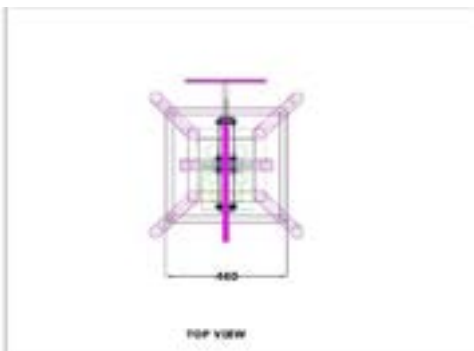

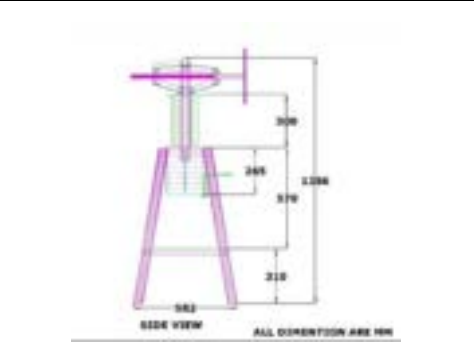

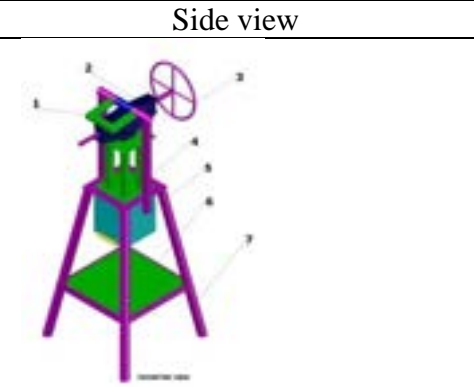
Operation of manual pressing briquette machine

- Raw materials are gathered and thoroughly dried to minimize moisture content. They are then mixed in the appropriate ratio to achieve optimal bonding strength, ensuring effective briquette formation.
- The dried and well-mixed raw materials are manually loaded into the pressing chamber of the briquette machine.
- Using a handling wheel, the operator applies mechanical pressure, compressing the biomass. This pressure causes the individual particles of biomass to bind together, creating a cohesive and solid briquette.
- Once the briquette is formed and has achieved the desired size and density, it is manually ejected from the machine.

Benefits of manual briquette machine

- Manual briquette machines are cost-effective and demand minimal initial investment.
- Well-suited for small-scale operations and remote locations, these machines offer practical solutions in areas with limited infrastructure.
- Manual operation eliminates the dependency on electricity, making it feasible for regions with restricted or no access to power.
- Manual briquette production creates income-generating prospects for local communities and individuals.
- By utilizing agricultural waste, the machine reduces the disposal of these materials, contributing to overall waste reduction efforts.

Descriptions of the developed machine

 <p>TOP VIEW</p> <p>Top view</p>	 <p>FRONT VIEW</p> <p>Front view</p>
 <p>SIDE VIEW</p> <p>ALL DIMENSIONS ARE MM</p> <p>Side view</p>	 <p>Manual pressing briquette machine</p>
	<ol style="list-style-type: none"> 1. Scissor pressing unit holder 2. Scissor pressing unit 3. Handle wheel 4. Pressing Piston 5. Square-type Pressing chamber 6. Receiving tray 7. Basement frame
<p>Fig. 51. Isometric view of Manual pressing Briquette machine</p>	

Scissor pressing unit holder

The apex point of the machine serves as the anchor for the suspended pressing unit, functioning as a basement for the scissor pressing mechanism.

Handle wheel

This wheel is designed to control the pressing unit, and it is linked to the screw of the scissor pressing mechanism. Turning the wheel in a clockwise direction generates pressure within the square-type pressing chamber through pistons, while turning it anti-clockwise releases the pressure.

Receiving tray

The tray is intended to collect the produced briquette (final product).

Basement frame

This component serves as the primary structure, providing support for the entire machine to stand firmly on the ground. It has a height of 35 inches from the ground, with the lower portion measuring 23 inches in breadth and the upper portion measuring 12 inches in breadth (Plate 10).



Plate 10. Base frame

Square-type Pressing chamber

The pressing chamber is the section where raw materials are loaded and compressed to produce briquettes. It takes on a square shape and is specifically designed to withstand the pressure and forces encountered during the compression process. Its dimensions are 4 inches in length, 4 inches in breadth, and 10.5 inches in height (Fig. 52).

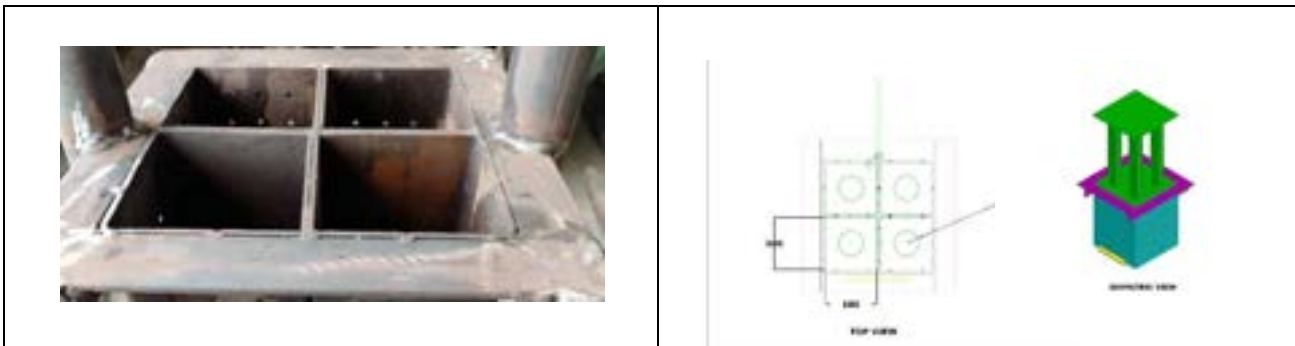


Fig. 52. Square-type Pressing chamber

Pressing piston

Pressing pistons were designed in a way that sufficient compression strength can develop during pressing. The length of the piston rod is 11.5 in and the area of the piston head is 4in × 4in (Fig. 53).

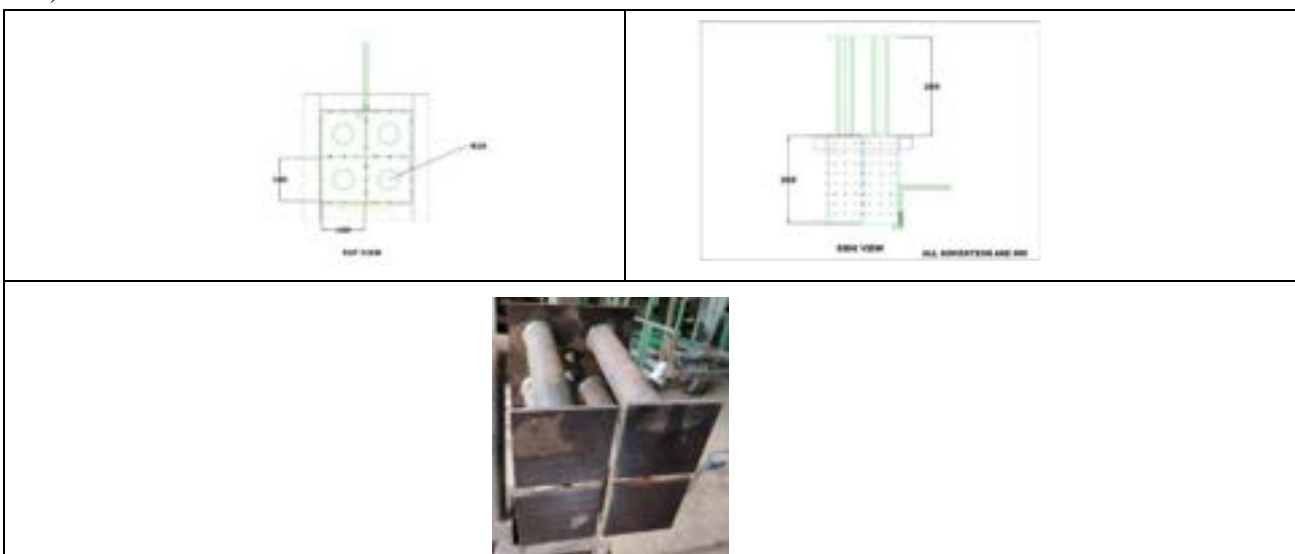


Fig. 53. Pressing piston.

Scissor pressing unit

The scissor-pressing unit operates through a simple yet effective mechanical principle ((Plate 11)). When force is applied to the actuating mechanism, it is transmitted to the scissor mechanism, causing the arms to close. This closure generates a powerful pressing at the point of contact. The pressing capacity of this scissor-pressing unit is about 1 to 1.5 tons.



Plate 11. Scissor pressing

Table 48. Detail specifications and materials used for manufacturing the machine.

Sl. No.	Items	Specification	Material
	Overall dimension (L*W*H)	138*56*56	Mild steel pipe, plate, sheet and angle
1.	Total height	138 cm	
2.	Total weight	43.5 Kg	
3.	Piston:		Mild steel pipe and plate
	➤ Area of piston head	9.6*9.6 cm ²	
	➤ Total length	28.5 cm	
	➤ Stroke length	14.5 cm	
	➤ Total clearance	11 cm	
4.	Square Cylinder		Mild steel plate
	➤ Diameter	10*10 cm ²	
	➤ Length	25.5 cm	
5.	Pressing unit (Scissor jack)		Mild steel round rod
	➤ Diameter of the power screw	2 cm	Mild steel rod
	➤ Diameter of hand wheel	26.5 cm	
	➤ Operating length	40 cm	
	➤ Height of the jack from cylinder	47 cm	

Lab Test

- A prototype of the machine has already been developed preliminary observational trial was done in the divisional workshop. There was no fault in the machine.
- Initially manually operated briquette machine tested in research workshop using charcoal and rice husk.
- Charcoal-briquette can be formed without using any binding material under the developed pressure mentioned above diagram while rice husk did not bond ((Plate 12)).



Plate 12. Charcoal Briquette.

- The final trial of this machine used rice husk, grinded maize stem, and cassava stretch as raw material and binding material respectively (Fig. 54 & 55).
- The following mixing ratio of raw materials (Table 49) used next to find optimum bonding strength.

Table 49. Mixing ration of raw materials used in trails

	Raw materials	2kg mixture
Trail 1	Rice husk	1000g
	Grinded maize stem	400g
	Cassava stretch	200g
	Water	400g
Trail 2	Powdered Rice husk	1000g
	Grinded maize stem	100g
	Cassava stretch	200g
	Water	700g









Raw Materials	
Trail 1	Trail 2
	
Rice Husk	Powdered Rice Husk
	
Grinded maize stem	Grinded maize stem
	
Cassava stretch	Cassava stretch
	
Water	Water



Fig.54. Unboned substance from trail 1



Fig. 55. Briquette from trail 2

Result and Discussion:

The manual briquette machine emerges as a practical and accessible solution for biomass briquette production in resource-constrained areas lacking electricity. Despite challenges associated with manual operation, our study's findings underscore its potential in generating clean and efficient fuel sources. Positioned as a promising tool for community development and sustainable energy, the developed briquette machine measures approximately 138×56×56 (L×W×H) with a weight of 43.5kg, subject to variation based on the material used. Detailed specifications of its components are outlined in Table 48.

The critical factor influencing briquette performance is bonding strength. A robust bond ensures structural integrity, rendering briquettes resilient to handling, transportation, and usage forces. Heightened bonding strength contributes to increased durability, allowing briquettes to withstand external forces and friction, leading to extended burning times and enhanced efficacy as a fuel source.

However, the primary challenge in employing a manually operated briquetting machine lies in achieving optimal bonding strength while economically utilizing binding materials. Our research addresses this concern through laboratory test trials, specifically the second iteration (Table 49), revealing the essential mixing ratio for achieving the ideal bonding strength among individual biomass particles.

Trial one unequivocally demonstrates that attaining the minimum bonding strength for briquette production using a manual pressing machine is nearly impossible without incorporating powdered rice husk into the raw material. This emphasizes the pivotal role of specific materials, such as powdered rice husk, in ensuring successful briquette production. The subsequent section will delve into the physical and combustion properties of the produced briquettes, providing further insights into the implications of our research findings.

PROJECT 2: MILLING AND PROCESSING TECHNOLOGY

Experiment 2.1: Test, evaluation and modification of rubber roll de-husker and friction type polisher

Principal Investigator: Md. Golam Kibria Bhuiyan

Co-investigator(s): MDH, BCN, SI, AKMSI

Objectives

- To modify and development of a rubber roll de-husker
- To evaluate the performance of paddy de-husker

Rubber rollers for de-husking paddy are formed of rubber holdings that are identical in diameter but operate at various speeds to remove the husk from the paddy. One of the two rubber rollers is fixed in place, while the other is adjustable to meet the needs of the desired clearance. The adjusted rice rubber roller operates at a slightly lower speed, while the fixed roller operates at a higher speed. An aspirator is attached to the base of both rice rubber rollers to separate the hulls or husk from the brown rice. This ensures that the entire husk is collected at one end after the rice rubber roller operation. FMPHT division modified a rubber roll de-husker that runs with a 4 kW (3-phase 4 wire 1440 rpm) electric motor. The diameter and length of the both fixed and adjustable rubber rolls are 230 mm and 154 mm, respectively. The fixed and adjustable rubber rolls have rpm of 1048 and 789, respectively. The blower's rpm is 1020. A stairway made of 16 BWG sheet and 50 x 50 mm angle bar was built to help transport paddy in the hopper. A pipe connects to the husker's end to a husk aspirator (dia. 200 mm). The aspirator fan has a diameter of 330 mm and is powered by a 1.5 kW (2840 rpm) motor ((Plate 13)). To collect husk, a cyclone separator was modified and attached to the de-husker. Previously, husk was collected directly from the aspirator discharge outlet with a gunny bag, resulting in a large amount of dust in the working area. The aleuronic layer of paddy is not damaged by rubber roll de-husker. An airstream is blown over the grains, and immature grains are discharged into a separate hopper. Paddy and husk were discharged separately. In this experiment, BRRRI dhan104 (un-parboiled) was used. The moisture content (wb.) was 11.20%, and each sample weighed 20 kg. To evaluate the commercial value of milling parameters, de-husked paddy was processed in an MNMP-15 model friction type polisher. The different milling parameters were calculated with the following formula:

Husking efficiency

The percentage of total mass of milled rice (head and broken rice) recovered from the mass of the corresponding input paddy to the rice mill (husker or huller and whitener). It is also called total milling recovery.

$$\text{Husking efficiency}(\%) = \frac{\text{Weight of milled rice}}{\text{Weight of rough rice}} \times 100$$

Percentage head rice

The main aim of milling process is to get maximum head rice yield. The rice kernels which are three quarters or more in length as compared to length of original kernels obtained after complete milling is termed as head rice. Head rice is 2 to 3 times costlier than broken rice. Head rice yield (HRY) can be defined as the ratio of weight of milled rice kernels obtained in percentage of the weight of rough rice or paddy.

$$\text{Percentage head rice} (\%) = \frac{\text{Weight of head rice}}{\text{Weight of rough rice}} \times 100$$

Percentage broken rice

The percentage of broken rice recovered from the mass of the corresponding input paddy to the rice mill.

$$\text{Percentage broken rice} (\%) = \frac{\text{Weight of broken rice}}{\text{Weight of rough rice}} \times 100$$

Percent husk

The percentage of husk recovered from the mass of the corresponding input paddy to the rice mill.

$$\text{Percent husk} (\%) = \frac{\text{Weight of husk}}{\text{Weight of rough rice}} \times 100$$

Degree of milling (DoM)

Milled rice quality is determining its degree of milling. It can define either by measuring the remaining amount of bran on the surface of milled rice kernels or by determining the extent of removal of the germ or layers of bran from brown rice kernels during various milling operations. A gravimetric measuring of DoM is done by using equation 1 (Mohapatra and Bal, 2007).



Plate 13. Modified de-husker

$$\text{Degree of milling} (\%) = \left(1 - \frac{\text{Weight of milled rice}}{\text{Weight of brown rice}}\right) \times 100$$

Moisture content of grain was determined by a moisture meter (Rice Ter D, Kett). Thousand grain mass (TGM) was determined by counting 1000 grains with machine and hand counting for each variety and weight with a precision digital balance.

For BRR1 dhan104 the average de-husking capacity of the husker was found 769 kg/h and husking efficiency was about 90.97 % (Table 50). Closing the adjustable roller husking efficiency can be increased however, it increases the broken rice percentage (brown rice). Brown rice percentage was about 77.88% and rest of was husk and embryo. Average fixed and adjustable rubber roll rpm was found 1048 and 789 respectively.

Table 50. Performance of developed husker for BRR1 dhan104.

Sl. no.	Capacity (one pass) Kg/h	Husking Efficiency (one pass) %	Brown Rice, % (based on input paddy)	Adjustable roll speed (rpm)	Fixed roll speed (rpm)	Ratio of fixed and adjustable roller
1.	780	91.50	77.80	785	1045	24.88
2.	768	90.90	78.20	794	1052	24.52
3.	760	90.10	77.65	788	1048	24.81
Av.	769	90.97	77.88	789	1048	24.74

Fixed rubber roll rotates at an average rpm of 1048 which is 24.80 % more rpm than the adjustable rubber roll. The difference in peripheral speed subjects the paddy grain falling between the rolls to a shearing action that strips off the husk. The clearance between the rolls depends on the thickness of the paddy and it should be less than the thickness of the grain.

Evaluation of milling parameter of BRR1 dhan104 processed in friction type polisher

Brown rice was polished in friction type polisher (MNMP-15) and average capacity of the polisher for BRR1 dhan104 was 740 kg/h and the average milling recovery was 61.8 % ((Plate 14)). The average head rice recovery (based on input paddy) was 52.67 % and head rice recovery (based on total milled rice) was 85.27% (Table 51).

Table 51. Milling parameter of BRR1 dhan104 processed in friction type polisher.

Sl. No.	Capacity of Polisher Kg/h	Milling yield %	Head rice % (Based on input paddy)	Head rice % (Based on total milled rice)	Broken rice % (Based on input paddy)	Broken rice % (Based on total milled rice)
1.	740.0	62.0	52.00	83.87	10.00	16.13
2.	742.0	61.8	52.60	85.11	9.20	14.89
3.	738.0	61.5	53.40	86.83	8.10	13.17
Av.	740.0	61.8	52.67	85.27	9.10	14.73

The broken rice percentage was 9.10 % (based on input paddy) and 14.73 % (based on total milled rice).



Plate 14. MNMP-15 friction type polisher in operation

Recommendations for increasing the life of the rice rubber roller

For optimum life and the performance of the rice rubber rollers, the following instruction should be followed:

- The moisture content in the paddy should be below 14%.
- The alignment of both the rubber roll huskers should be maintained before the start of the operation.
- The clearance should be adjusted to nearly 0.5mm or the rolls should be exactly touching each other and not overlapping.
- The hulling efficiency should be checked immediately after the start of the machine. If the efficiency is less than 90% then the hulling efficiency has to be decreased until it reaches a value of 90-95%, else the rolls are not locked in its position.
- The feed gate has to be fully open so as to ensure that the rollers wear out uniformly.
- The hulling efficiency of the rubber rolls should be checked at regular intervals, otherwise, the rubber rollers will wear out.
- The axis of the roller must be in complete alignment with the hub and the shaft.
- The uneven rolls can be made uniform and smooth with the help of a lathe machine.
- The side baffles of each side of the rice rubber rollers should be checked before the operation so as to ensure that there is no leakage in between the paddy plates and the rubber roll surfaces.
- The end faces of both the rollers should be always facing each other.

Husking efficiency and milling recovery was found around 90.97 % and 61.8 % respectively for BRR1 dhan104 polished in friction type polisher followed by de-husking. The average head rice recovery based on input paddy was 52.67 %, which is encouraging for processing of quality rice. Steel engelberg huller may replace with one rubber roll de-husker and a polisher for better quality rice. De-husker also separate husk and polisher separate bran. Separately collected husk and bran is suitable for briquette and edible oil production.

PROJECT 3: RENEWABLE ENERGY

Experiment 3.1: Design and development of a solar seed dryer

Principal Investigator: Subrata Paul

Co-investigator(s): MDH, MGKB, MAfH

Objectives

- ❖ To design, develop, and fabricate a solar seed dryer
- ❖ To compare with traditional sun drying of paddy

Materials and Method:

Drying is a critical process after harvesting to prevent decay and extend the storage life of paddy. There are two primary ways to dry paddy - open sun drying and mechanical drying, which involves using various dryers. Although open sun drying is inexpensive, it is labor-intensive and can compromise the quality of the product. On the other hand, mechanical dryers, designed for various crops like maize and rice, protect freshly harvested paddy from deterioration, reduce wastage due to bacterial action, and shorten drying time. However, farmers have not yet adopted these improved drying techniques (dryers) to dry their paddy seeds. With the increasing need for better and higher quality seeds and more efficient post-harvest operations, rice drying by farmers may pose a challenge in terms of processing techniques and the preservation of seed quality.

Design consideration

Designing a solar paddy seed dryer requires careful consideration of various factors to ensure efficiency and effectiveness. Here are some essential design considerations:

Solar Collector Type: The appropriate type of solar collector would be selected based on the available solar radiation.

Drying Capacity: The dryer could process 80-100 kg of rice seeds per batch or day.

Drying Time: The average drying time of rice seed should be considered so that the required throughput is within the dryer's capacity.

Airflow and Ventilation: Dryers must be appropriately designed to facilitate airflow and ventilation to remove moisture effectively. Adequate ventilation should be ensured.

Insulation: During the drying process, the heat loss should be as low as possible, and a consistent temperature should be maintained inside the dryer.

Temperature Control: Keeping a temperature control system to control the drying temperature and prevent overheating from preventing damage to rice seeds.

Material of Construction: Use durable, weather-resistant materials suitable for high-temperature applications so that the machine is not damaged even after the dryer is exposed to various weather conditions.

Orientation and Tilt: Solar collectors should be appropriately oriented towards the sun to maximize solar exposure throughout the day. The tilt angle should be easily adjustable based on location for optimal solar capture.

Economic Feasibility: Economic viability has to be ensured so that the overall cost of the system, including installation, maintenance, and operational costs, will be within the purchasing power of the farmers.

Local Conditions: Considering specific climatic conditions such as temperature, humidity, and solar radiation levels where the dryer will be installed.

Accessibility and Mobility: If the dryer needs to be moved or transported, it should be easily disassembled and assembled at a new location.

Maintenance and Cleaning: Ease of maintenance and periodic cleaning.

The solar dryer was developed according to the following considerations at a glance:

- The dryer would be conceived as low-cost.
- Easy-to-fabricate and easy-to-operate equipment.
- Using available local materials to minimize the fabrication cost.
- To make it suitable for most farmers with little or no formal education.
- It should be designed well so that uniform grain drying may occur.
- The cost of the dryer must be within the capacity of small and medium farmers.
- It should be suitable for drying seeds 80-100 kg.

Materials and method

- ❖ Solar collector: To collect heat from the sun.
- ❖ Drying chamber: Construction of a well-insulated chamber to hold rice seeds during drying.

- ❖ Air circulation system: Fans or blowers ensure uniform airflow inside the drying chamber.
- ❖ Thermocouple: Temperature sensors to monitor and control drying temperature.
- ❖ Control system: Designing a control system for thermal control
- ❖ Support structure: Make a metal frame to hold the solar collector and drying chamber.
- ❖ Ventilation system: Making openings or vents for air exchange to maintain proper humidity level.

Needs Assessment: Understood the local context and specific requirements for rice seed dryers, including targeted drying capacity, weather conditions, available space, and production costs.

Literature Review: A literature review of current solar rice seed dryers and related drying technologies was performed. Information on successful designs and best practices was collected.

Conceptual Design: A solar rice seed dryer design was developed based on demand assessment and literature review. The overall layout, size of the drying chamber, air circulation system, and control system were considered.

Material Selection: Appropriate materials for drying chambers, solar collectors, fans, and other components were selected considering thermal conductivity, durability, and cost-effectiveness.

Detailed Engineering Design: Prepared detailed engineering drawings and specifications for each component of the solar paddy seed dryer.

Prototype Development: A solar paddy seed dryer prototype was developed using a detailed engineering design. Its effectiveness was evaluated by testing the prototype with paddy seeds. Problems with the prototype were identified, and the machine was subsequently modified.

Solar Energy Assessment: The solar energy potential at the installation site was analyzed to determine the optimal solar collector capacity required for the drying system.

Air Circulation System Design: Developed the air circulation system including fan size and placement to ensure efficient and uniform airflow throughout the drying chamber.

Field Testing and Evaluation: Installed solar paddy seed dryer and conducted field trials over an extended period. Data were collected on drying performance, energy consumption, and seed quality.

Deployment and Monitoring: After installing the solar paddy seed dryer, monitor its performance regularly. Ongoing support and maintenance were provided to ensure continued functionality and efficiency.

Working principle

The dryer's design was based on the concept of batch-type dryers. The primary working principle of the solar-assisted paddy dryer was to raise the ambient air's temperature as it passed through the solar collector by absorbing solar heat energy from the sun and then using this heated air to dry the moist grains. Using locally available materials, a solar-assisted grain dryer was developed and fabricated in the Farm Machinery and Post-harvest Technology division of Bangladesh Rice Research Institute (BRRI), Gazipur. The solar-assisted dryer consists of the following components: a flexible PVC sheet that acts as a solar air collector (collector stand, inlet of the collector, outlet of the collector), drying chamber (drying chamber inlet, drying chamber outlet), air distribution model, and a blower, flexible pipe, etc. A schematic diagram of the total drying system developed for this experimental work is shown in Figure 56.

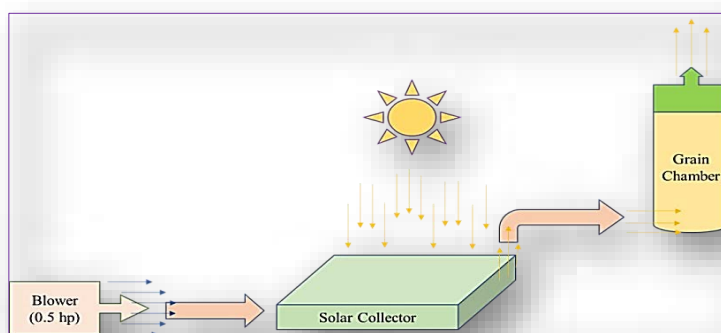


Figure 56. Schematic diagram of the drying process of the dryer.

How it works:

Solar Energy Capture: Solar collectors absorb sunlight and convert it into heat energy. The collected solar energy is then transferred to the drying chamber.

Seed Placement: Freshly harvested rice seeds are poured inside the drying chamber. Seeds inside the chamber are placed at equal heights to ensure even drying.

Drying Process: Solar energy heats the air inside the drying chamber, creating a warm and dry environment. Aeration systems circulate this heated air through the seed, facilitating moisture evaporation from the seed.

Moisture Evaporation: As warm air passes through the seed, it absorbs moisture, causing the rice seed moisture to decrease gradually.

Completion of Drying: The drying process is complete once the rice seeds reach the desired moisture content. The seeds are then ready for storage or further processing.

Data was collected

- Moisture content of the grain, %
- Ambient temperature of the dryer, °C
- Drying time, hr.
- Drying Capacity per batch, kg

Description of the dryer

Using locally available materials, a solar-assisted grain dryer was developed and fabricated in the Farm Machinery and Post-harvest Technology division of Bangladesh Rice Research Institute (BRRI), Gazipur. The solar-assisted dryer consists of the following components: a flat plate solar air collector (collector stand, inlet of the collector, outlet of the collector), drying chamber (drying chamber inlet, drying chamber outlet), air distribution model, and a blower, flexible pipe, etc. A solar-assisted seed dryer is a machine specially designed to dry paddy seeds using solar energy as the main heat source. This use will reduce reliance on fossil fuels and conventional electricity for drying agricultural produce, resulting in cost savings and improved seed quality.

Solar Collector: The solar collector is the heart of the solar-assisted rice seed dryer. It is a PVC flexible plastic sheet collector made of materials with high solar absorption properties. A PVC flexible plastic sheet solar collector for a solar rice seed dryer is a simple and low-cost solar thermal collector (Figure 57). It was designed to harness solar energy and convert it into heat. The solar collector was set on a metallic frame. A dark-colored absorbent material was attached inside the frame as a black dark-colored coating. The absorbent material is responsible for absorbing solar radiation and converting it into heat energy. This allows solar radiation to pass through while minimizing heat loss from the collector to the surrounding environment. The back and sides of the collector frame are insulated to reduce heat loss. Insulation helps retain absorbed solar energy within the collector and prevents heat from escaping. When sunlight falls on the PVC flexible plastic sheet, it transmits solar radiation to the dark-colored absorbent material underneath. Absorbent material absorbs solar energy and converts it into heat. As the absorber material absorbs solar energy, it heats the air trapped between the PVC sheet and the absorber. The air gains thermal energy and increases in temperature as it circulates within the confined space. This circulation process helps in efficient heat transfer and distribution. Warm air inside the PVC flexible plastic sheet solar collector was forced into the drying chamber of the rice seed dryer in force mode. The heat exchanging system in the drying chamber transfers heat from the warm air to the surrounding air, facilitating the drying process of rice seeds.



Figure 57. Solar collector of the dryer.

Heat Absorption: When sunlight falls on a solar collector, it absorbs solar radiation and is converted into heat. The design of the collector was efficient in capturing and retaining this heat.

Heat Transfer Air: A heat transfer air is circulated through the collector chamber. This air absorbs the heat generated by the solar collector and increases in temperature as it flows through the collector.

Heat Exchange System: The heated air flows through a solar collector chamber, increasing the air temperature. The purpose of the heat exchanger was to transfer heat from the air inside the drying chamber to the surrounding air.

Drying Chamber: A drying chamber is an enclosed space to hold rice seeds during drying. The cylindrical drying chamber in a solar rice seed dryer efficiently utilizes the heat generated by the

solar collector. The cylinder-shaped drying chamber used an MS sheet to transport heat well. It consists of a cylinder-shaped body in a semi-closed condition to create a controlled environment for the drying process. It was designed to hold a certain amount of rice seed to ensure easy drying. The drying chamber is located vertically; between it, another section of cylindrical shape is vertically through which the hot air passes from the bottom to the top of the drying chamber, and the hot air is spread around. The heated air from the solar collector is connected to an exchanger inside the cylinder-shaped drying chamber through which the air is transferred. This natural convection ensures adequate air circulation, distributes warm air among rice seeds, and initiates drying. The rice seeds are evenly distributed inside the cylindrical drying chamber. The drying chamber has a temperature control system to maintain the desired drying temperature. The cylinder-shaped drying chamber was designed with access points for loading and unloading rice seeds (Figure 58). Easy cleaning and maintenance measures were included to ensure system longevity and optimal performance.



Figure 58. Drying chamber of the dryer.

Air Circulation: The air circulation system of this solar rice seed dryer ensures the even distribution of the heat by spreading heated air within the drying chamber and facilitating the rice seed drying process. It plays a vital role in increasing the efficiency of solar-assisted rice seed dryers. Air circulation was usually done with fans or blowers (Figure 59). The fan was responsible for creating airflow within the drying chamber. It can be powered by electricity or, in some cases, by solar energy. The fan or blower was placed behind the solar rice seed dryer's solar collector. In this position, the fan forces the air inside the solar collector into force mode. Warm air was evenly distributed inside the drying chamber. The fan or blower was designed to create airflow from one direction to the solar collector chamber. The continuous flow of warm air over the rice seeds facilitates the evaporation of moisture from the seeds and accelerates the drying process. As the moisture evaporates, the rice seeds gradually reach the desired moisture content for safe storage.



Figure 59. Blower of the dryer.

Fabrication of the solar dryer

Structure a solar-assisted seed dryer involves several steps, from manufacturing the individual components to assembling them into a functional system. Appropriate materials were selected to construct the solar collector, drying chamber, and air circulation system. Fabrication of a PVC flexible plastic sheet solar collector for a solar rice seed dryer involves fabricating the collector and integrating it into the dryer system. The rectangular metal frame was made in this case, and a flexible PVC plastic sheet was placed on it. The frame was made by combining PVC flexible plastic sheets. The inside of the frame was coated in dark black as a heat-absorbing material. PVC flexible plastic sheets are stretched over the frame. The edges of the PVC sheet were sealed so that no air escaped from the collector. It was painted black to absorb more solar heat to heat the inside of the collector. The drying chamber was constructed using an MS sheet based on the design and size requirements. Proper insulation was included to reduce heat loss and maintain internal temperatures. A fan or blower was installed behind the solar collector chamber to create controlled

airflow. A blower forced hot air into a grain chamber with a height of 87 cm and a chamber diameter of 57 cm. The cylinder sieve of the drying chamber has a hole size of 3 mm, which was selected according to the size of the rice grain (Plate 15). The solar collector, drying chamber, and air circulation system are integrated into one interconnected unit. All components must be connected, ensuring proper sealing and compatibility between systems. Figure 60 shows the drawing view with the actual picture of the solar-assisted paddy dryer, and Figure 61 shows the flow behavior of drying air within the drying chamber.

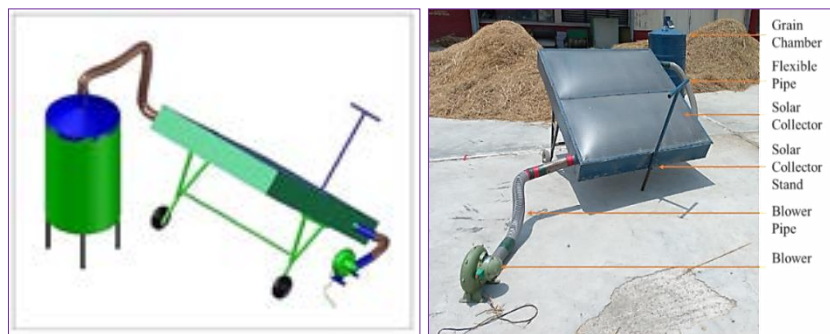


Figure 60. Complete view of the developed dryer.



Plate 15. Photographic views of the perforated cylinder of the drying chamber.

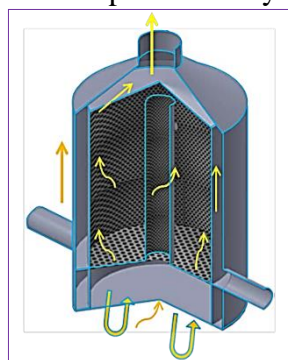


Figure 61. Flow behavior of drying air within the drying chamber.

Technical specification

Here are some standard technical specifications of solar paddy seed dryer follows:

Drying Capacity: The drying capacity refers to the amount of paddy seeds the dryer can handle at a time. It was usually measured in kilograms (kg). The capacity of the dryer was found to be 90 kg.

Solar Collector Type: A 3 mm thick PVC flexible plastic sheet is used as the solar collector in the dryer. The dimension of the solar collector chamber was 148 cm x 130 cm x 20 cm for absorbing solar heat from the sunshine.

Solar Collector Area: The total area of the solar collector, measured in square meters (m²), determines the amount of solar energy it can capture. The total area of the solar collector was found to be 1.92 m².

Heat Exchanger: The heat exchanger transfers heat from the solar collector to the drying chamber. The heated air passes to the drying chamber through a flexible pipe. The diameter of the flexible pipe was 72 mm.

Drying Chamber Size: The height of the drying chamber from the soil surface was 1449 mm, whereas the stand height of the dryer was 320mm. The main dryer chamber height was 906 mm. The drying chamber diameter was 570 mm. A perforated cylindrical vessel with a diameter of 93 mm was fitted inside the large-diameter cylinder. Another wire-made net cylinder had a diameter that was 469 mm.

Heat Transfer media: The heat transfer media was air. Hot air was generated from the solar collector and transferred to the drying chamber by force mode air blowing.

Air Circulation System: Hot air was passed through a duct to a grain drying tank. A centrifugal blower of 0.5 hp was used to circulate the air through the solar-assisted dryer. 94 mm diameter flexible pipe was attached to the blower.

Temperature Range: The range of drying temperatures was 30-40°C.

Power Source: The dryer's blower was operated by electric energy, but it can be used by solar

energy.

Results and Discussion

Performance test of the machine

The machine's preliminary performance test was done to identify faults in the dryer's functional elements ((Plate 16)). Conducting a performance test for a solar paddy seed dryer involves evaluating its efficiency, effectiveness, and overall functionality.



Plate 16. Performance test of the developed dryer.

Test Planning: It was clearly understood that performance parameters were to be evaluated. It included factors such as drying time, temperature, and moisture control. It would include energy consumption, seed quality after drying, temperature control, and overall ease of use.

Setup and Calibration: First, ensure the solar rice seed dryer is installed correctly. According to the design specifications, the various parts of the machine should be placed perfectly and checked for any defects in the unloading condition. Then, the instrument was initially calibrated.

Measurement Instruments: Necessary equipment for data collection are temperature sensors, moisture meters, timers, etc.

Baseline Data: Before starting the experiment, baseline data were recorded for comparison. The initial moisture content of the rice seeds used for the investigation was measured.

Test Conditions: The test must be performed under different weather conditions (sunny, partly cloudy) to observe the dryer's performance under varying solar radiation levels.

Drying Test: The rice seeds were loaded into the dryer according to its recommended capacity. Then, the drying process was started. Temperature, moisture content, and drying time were carefully monitored.

Data Collection: Data were recorded at regular intervals throughout the drying process. An attempt was made to include ambient temperature, moisture content, and time during the process. The ambient air temperature of the solar seed dryer was measured throughout the drying process (Table 52). This information was obtained through a moisture meter. Before starting the drying process, a sample of rice seeds was taken, and their initial moisture content was measured using a moisture meter. The total time taken to reach the desired moisture content of the rice seeds during the drying process was recorded. The energy consumption of the solar rice seed dryer was not measured during the experiment.

Seed Quality Assessment: After the drying process, the final moisture content of the dried rice seeds was measured. Seed quality was not assessed by examining uniformity, germination rate, and any signs of damage or discoloration.

Variation of moisture content and temperature during the drying operation

The moisture content of Paddy seeds was initially recorded as over 28%. The aim was to reduce it to less than 15%, which required over 10 hours of drying in a newly developed solar dryer. The ambient temperature ranged from 27-34.8°C, and the test sample used was BRRI dhan89. The solar dryer effectively initiated the drying process, gradually reducing moisture content levels. As the day progressed, the solar radiation and heat from the sun intensified, causing the ambient temperature to rise. By noon, the moisture content had dropped to 24-26%. By mid-afternoon, the ambient temperature was around 34.8°C, and the moisture content of the rice seeds had further reduced to about 17-19%. As evening approached, the ambient temperature dropped to around 31°C, and the solar drying process continued until 6:00 PM. During this period, the moisture content of the rice seeds rose slightly before finally reaching levels below 15% (Fig. 62).

Table 52. Moisture content and ambient temperature with daytime.

Drying Time (am/pm)	Moisture content (10 cm distance from the upper bin), %	Moisture content (40 cm distance from the upper bin), %	Moisture content (70 cm distance from the upper bin), %	Average Moisture content, %	Ambient Temperature, °C
09.30 am	28.1	27.2	26.6	27.30	27
10.00 am	28	28.1	26.8	27.63	28.5
10.30 am	28.1	27.9	26.9	27.63	30.6
11.00 am	27.9	27.2	25.1	26.73	31.4
11.30 am	26.5	26.1	25.1	25.90	31.7
12.00 pm	26.8	26.6	24.5	25.97	31.9
12.30 pm	24.6	25.4	22.9	24.30	32.0
01.00 pm	23.1	24.6	20.7	22.80	32.3
01.30 pm	21.7	20.2	20.1	20.67	32.6
02.00 pm	19.8	19.1	18.1	19.00	33.2
02.30 pm	20.1	19.3	16.9	18.77	33.8
03.00 pm	18.2	18.3	16.1	17.53	34.8
03.30 pm	16.6	15.1	14.4	15.37	34.5
04.00 pm	15.3	15.3	14.2	14.93	34.3
04.30 pm	14.1	16.4	15.4	15.30	34.0
05.00 pm	15.9	14.9	15.3	15.37	33.0
05.30 pm	15.1	17.4	15.6	16.03	33.0
06.00 pm	15.9	17.1	16.3	16.43	31.0

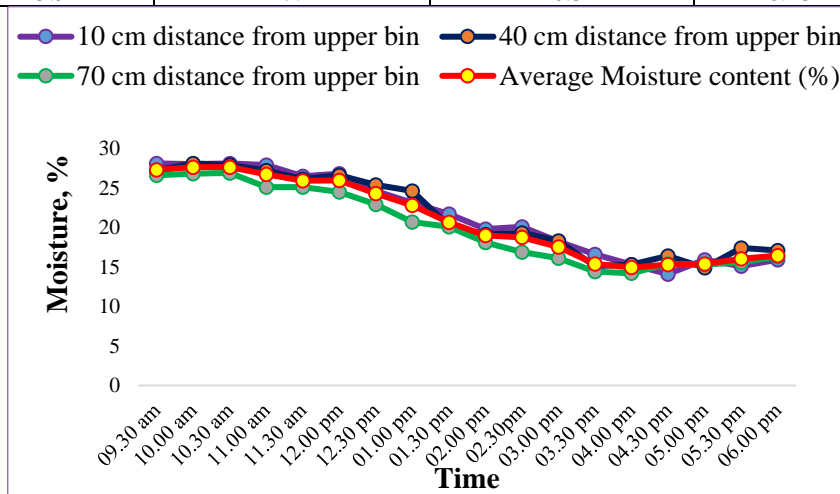


Figure 62. Variation of moisture content with drying time.

The ambient temperature surrounding a solar paddy seed dryer can vary significantly based on several factors, including geographical location, time of day, season, weather conditions, and local climate patterns (Figure 63). The ambient temperature directly influences the drying process inside the solar paddy seed dryer and affects the system's overall efficiency. The temperature range found during the operation was 27-34.8 °C. At the start of the drying operation (9:30 a.m.), the ambient temperature was 27 °C.

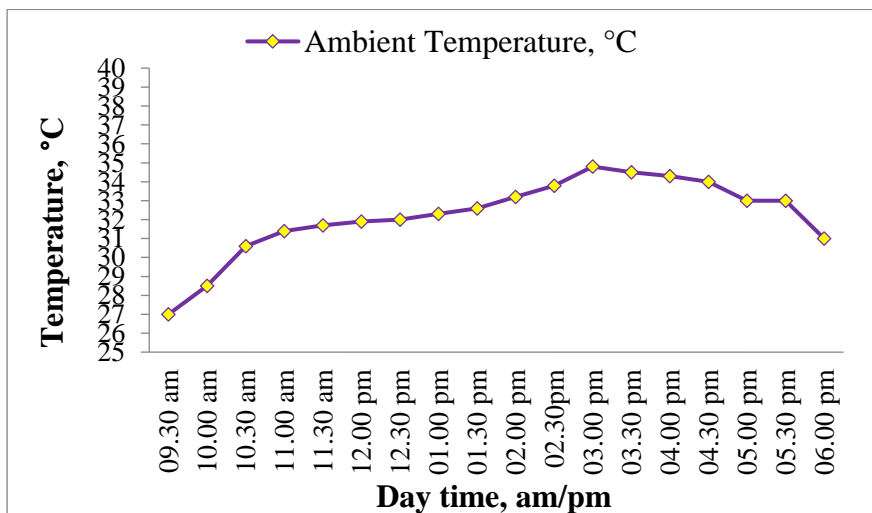


Figure 63. Variation of temperature with daytime.

Limitations and challenges:

Here are some common limitations and challenges of a solar rice seed dryer:

Dependence on Sunlight: The primary limitation of solar paddy seed drying was their dependence on sunlight. It can only work efficiently on sunny days with ample sunlight. Cloudy or rainy weather significantly reduces drying capacity.

Seasonal Variation: Solar grain seed dryers were less effective during certain seasons with low solar radiation levels, such as winter or monsoon.

Drying Capacity: The drying capacity of solar seed dryers was limited compared to large-scale conventional dryers. This limitation makes it challenging to meet the drying requirements of large rice harvesters.

Drying Time: Solar seed dryers take longer to dry rice seeds than conventional dryers, especially during periods of low solar intensity.

Moisture Control: Maintaining precise moisture control in a solar dryer was challenging. Over-drying or under-drying affects the quality and storage life of dried seeds.

Backup Heating: A backup heating system will be needed to ensure continuous drying in areas with limited sunlight or unpredictable weather patterns. However, incorporating such a system adds complexity and cost.

Storage Capacity: The storage capacity of the drying chamber was limited; frequent loading and unloading of rice seeds was required to dry large quantities of rice.

Despite these limitations and challenges, solar seed drying is an environmentally friendly and sustainable technology for drying rice seeds, especially in areas with abundant sunlight.

Identification of problems and recommendations

The key themes of the discussions were the perceptions of existing scientists and machine operators regarding the machine's overall performance, emphasizing the problems and observations listed below.

- ❖ The solar collectors are fixed in place to take advantage of the incoming solar radiation. The rays falling on the collectors cannot be in the ideal direction since the sun's location always changes due to the earth's rotation and revolution around the sun.
- ❖ It takes more time to dry the seed.
- ❖ Electricity supply is always to be needed without any interruptions.
- ❖ A backup heating system could be attached to the dryer.

Conclusion

A solar-assisted dryer was developed, fabricated, and tested primarily for paddy seed drying. The dryer is powered by a 0.5 hp single-phase electric motor and can reduce the moisture level of the paddy from 28.1% to less than 15%. The dryer can be scaled up for commercial drying of paddy seed. It is recommended for use on a small scale with inadequate sun-drying space. This is because sun drying can mix up dust, inert matter, or other seeds, attract birds or other pests, and have the potential for microbial contamination. Based on the findings, solar-assisted paddy dryers offer significant seed drying and handling advantages. The developed solar-assisted dryer is easy to handle, operates comfortably, and has an optimal capacity. Solar-assisted paddy seed dryers provide a sustainable and environmentally friendly alternative for agricultural communities, especially in areas with plenty of sunlight. By efficiently drying paddy seeds with solar energy, farmers can improve seed quality, reduce post-harvest losses, and promote sustainable agricultural practices.

Recommendations

- ❖ High-quality solar collectors with high heat absorption efficiency must be used to capture solar energy effectively.
- ❖ A well-insulated drying chamber should minimize heat loss and maintain a consistent temperature.
- ❖ Adequate space and proper arrangement of rice seeds would be ensured for airflow and efficient drying.
- ❖ An aeration system should be applied to facilitate proper airflow over the rice seeds so that drying is uniform.
- ❖ Depending on the size and design of the dryer, consideration may be given to using natural convection or forced convection systems.
- ❖ Thorough tests need to be conducted under various conditions to ensure the effectiveness and efficiency of the solar seed dryer.

Experiment 3.2: Study on solar energy utilization for small agricultural machinery

Principal Investigator: Subrata Paul

Co-investigator(s): MDH, MGKB, MAH, MMR, HR

Objectives

- To design a mechanism for solar energy utilization.
- To assess the effectiveness of solar power integration in small agricultural machinery.
- To evaluate the performance of the developed system and machines.

Materials and methods

A solar panel carrier must be developed and fabricated for solar energy for small agricultural machinery and other multifunctional applications to carry out this study or research. The research begins with analyzing existing solar panel carriers to identify their limitations and explore potential improvements. Factors such as weight, portability, ease of assembly, and compatibility with different solar panel sizes and types were considered during the design process. A new design concept was proposed, incorporating lightweight materials, foldable structures, and efficient mechanisms for easy transportation. Auto CAD engineering drawing tools/ software was utilized to generate detailed 3D models of the self-propelled mobile solar panel carrier, enabling optimization of the carrier's structural integrity, weight distribution, and availability. Prototyping and testing were conducted to evaluate the performance and functionality of the developed carrier. Various aspects were assessed, including stability, ease of use, and compatibility with different terrains. The carrier's ability to withstand environmental factors such as wind, rain, and temperature fluctuations was also examined. The development process also involved integrating smart features, such as optimizing the solar panel orientation for maximum sunlight exposure. This enables the carrier to adapt to changing solar angles and improve energy generation efficiency.

Design consideration

Several major aspects should be taken into account while developing a self-propelled mobile solar panel carrier for multipurpose use in addition to handling small agriculture machinery:

Compatible with small agricultural machinery: The carrier should be designed to work effectively with small agricultural machineries such as BIRRI open-drum threshers, BIRRI winnowers, Mini rice mills, BIRRI chopper machines, solar seed dryers, automated seed sower machines, water pump domestic electric instruments, machinery, ensuring compatibility and efficiency.

Load capacity and structural design: The carrier structure must be strong enough to support the weight of multiple solar panels and additional equipment or payload. It should distribute the load evenly to ensure balance when moving.

Mobility and maneuverability: The carrier should be designed to be compact to handle narrow farm paths and confined places that are frequent in small-scale farming operations. Mobility is essential for effective transportation.

Power source and energy efficiency: A dependable energy source, such as a rechargeable battery system or solar panels, should be added to save energy and reduce reliance on fuel/electricity to enable self-propelled movement. It will also be featured as an energy source, allowing small agricultural machinery to run on energy from rechargeable batteries or solar panels, reducing dependence on external energy sources.

Safety and control systems: Carriers have to include safety measures, such as emergency stop buttons and apparent markings, to protect the safety of employees and equipment during transport.

Size, weight, and portability: To ensure ease of transportation and storage, the carrier should be compact, lightweight, and easily fold up if necessary.

Ease of attachment, detachment, folding, and unfolding: The carrier should be designed for quick and easy attachment to small agricultural machinery, allowing farmers to switch between tasks faultlessly. It also should have an easy folding and unfolding mechanism.

The design of the movable/self-propelled solar panel carrier was based on several crucial considerations:

- The power supply should be stable during the operation
- The battery will supply the power, ensuring a stable power source during machine operation.
- The rpm of the rotating parts should be the same as the designed machine

- The device shall be such that two people can easily insert and remove the panel frame into and out of the main body frame
- Weight should be favorable
- Using available local material
- Easy to down the solar panel
- Easily movable of solar panel carrier or trolley
- Alternative use of traditional energy.

Materials

The following materials were used during the study period for the execution of the study.

Lightweight and durable materials such as MS angle, MS flat bar, and MS box were suitable for the frame and structural components. High-quality metal hinges and joints were used to ensure stability, flexibility, and ease of folding or unfolding. The carrier accommodated 150 watts of 20 solar panels (Size: 1490mm*660mm*30mm). High-quality, durable wheels suitable for different road conditions, such as rubber tires, were employed for mobility. Light weight yet strong axles and wheel supports were necessary for load-bearing capacity. Stainless steel nuts-bolts, MS nuts-bolts, and screws were used for assembly and securing components. The charge controller regulates the flow of electricity from the solar panels to the battery bank. It prevents overcharging and ensures optimal charging efficiency. The battery bank stores the excess electricity the solar panels generate for later use. It provides a steady power supply to the carrier's components, even when sunlight is unavailable. In alternating current (AC) cases, a power inverter converts the DC electricity directly from the solar panel into AC electricity.

Methods

The following methods were considered during the study period for the execution of the study.

Requirement Analysis: The specific requirements for the portable solar panel carrier were identified. Weight, size, compatibility with different solar panel types, ease of assembly and disassembly, transportation considerations, and stability were also considered.

Research and benchmarking:

- Conducted a comprehensive literature review of existing literature, scientific articles, and research papers on solar power utilization in agriculture and small machinery.
- Identified key design requirements, including weight, portability, compatibility, ease of assembly, and positioning.

Design and selection of agricultural machinery:

- Identified and selected small agricultural machinery (powered by a diesel engine not exceeding 4 hp) suitable for solar power integration based on the study's specific objectives.
- Considered power requirements, operating conditions, and compatibility with solar power systems.

Conceptualization and design:

- Generated multiple design concepts based on the identified requirements.
- Utilized Auto-CAD engineering drawing tools/software to generate detailed 3D models of the selected design concepts (Figure 64).
- Optimized the designs for structural integrity, weight distribution, and user-friendliness.
- Considered the use of lightweight materials and foldable structures for improved portability.

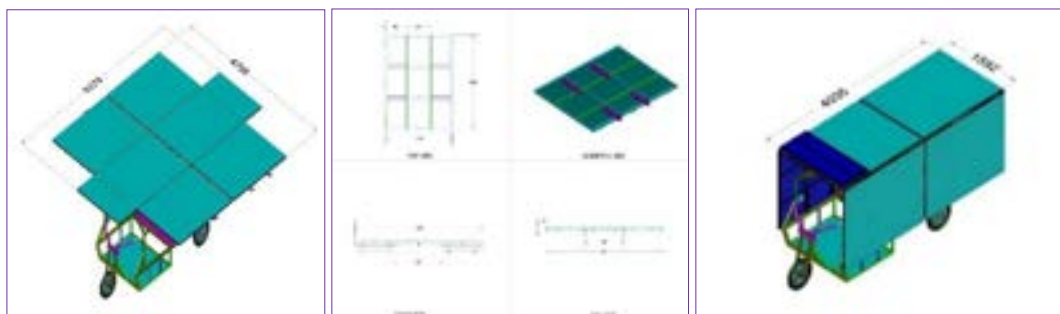


Figure 64. Drawing views of the solar panel carrier.

Material selection:

- Identified suitable materials based on the specific requirements and design constraints.

- Considered strength, durability, weight, corrosion resistance, and cost-effectiveness factors.
- Chosen lightweight materials that maintain structural integrity.

Solar power system design:

- Designed solar power systems that can meet the power demands of the selected agricultural machinery.
- Determined the optimal configuration of solar panels, battery storage, charging mechanisms, and power management systems.
- Considered factors such as solar panel type, capacity, orientation, battery technologies, charge controllers, and inverter.

Prototyping and testing:

- Fabricated prototype of the selected design concept(s) using the optimized 3D models.
- Determined the manufacturing process based on the selected materials and design requirements.
- Collaborated with manufacturers to ensure the production of high-quality components.
- Evaluated the prototypes for stability, ease of use, and compatibility with different grounds.
- Tested the prototype under various environmental conditions, such as wind, rain, and temperature fluctuations.
- Assessed the prototypes' ability to withstand transportation and positioning stresses.
- Integrated the solar power system with the selected agricultural machinery.
- Ensured the solar power components' proper installation, connection, and functionality.

Iterative design refinement:

- Analyzed the test results and user feedback to refine the design.
- Made necessary modifications to improve performance, durability, and user experience.
- Repeated the prototyping, testing, and evaluation process as needed.
- Some modifications need to be made to develop the carrier further.

Performance testing:

- The performance of solar-powered farming machinery will be evaluated through performance tests (Figure 65).
- Power generation, battery charging, and utilization efficiency will be measured and recorded under various operating conditions.
- Field trials of solar-powered agricultural machinery (BRRRI open drum thresher, BRRRI winnower, BRRRI solar dryer, mini rice mill, seed sower machine, power chopper, etc.) will be conducted.
- Assessed the system's reliability, durability, ease of use, and ability to withstand varying weather conditions and terrain.

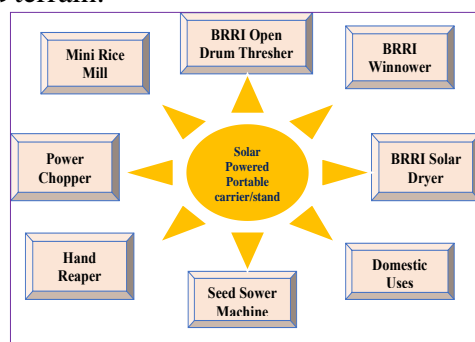


Figure 65. Flow Diagram of solar power utilization for small agricultural machinery.

Manufacturing process

The manufacturing process involved several stages in designing and developing a solar panel carrier for using solar energy in agricultural machinery.

Conceptualization and design: Identified the requirements and specifications for the solar panel carrier, considering factors such as size, weight capacity, mounting mechanism, and compatibility to integrate solar energy into the different agricultural machinery. A reverse engineering method was applied to develop the prototype of a solar panel carrier. 3D models of the carrier were completed after its development (**Figure 66**).

Material selection and procurement: Identified suitable materials for the carrier based on strength, durability, weight, and cost. Required materials were procured from the local markets.

Fabrication of structural components: Used metal fabrication techniques like cutting, bending, and welding to shape and assemble the structural elements of the carrier, such as the frame and support structures.

Attachment mechanism integration: Designed and fabricated the attachment mechanism that securely attached the solar panels to the carrier. It tested the mounting mechanism to ensure sufficient stability, adjustability, ease of installation, and inclination.

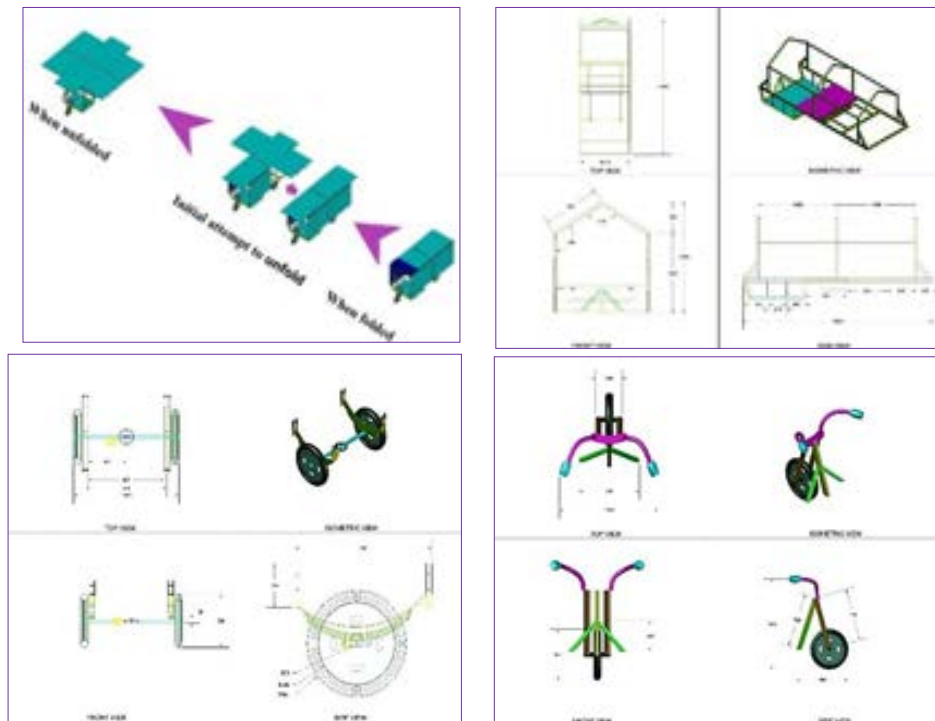


Figure 66. Some drawing view of the solar panel carrier.

Painting: The first time, red oxide paint was applied to protect it from moisture. Another protective color was used to achieve the desired performance characteristics.

Electrical integration: Electrical components such as wiring cables, connections, junction boxes, and control boxes were planned for and incorporated into the carrier. Electrical connections must be adequately protected to avoid damage and provide safety.

Testing and quality assurance: The solar panel carrier has been extensively tested to evaluate its performance under various conditions, including load-bearing capacity, vibration resistance, and exposure to environmental factors.

Installation and field testing: Folders containing solar panel carriers were opened to use solar power in agricultural machinery. Initial field tests assessed the carrier's performance in optimum conditions.

Result and discussion

Chronological development of the prototype of the solar panel carrier

Solar panel array (arrangement) upon the panel carrier (model 1(Previously designed)): For the first time, five foldable panel combinations were included in the carrier as a solar panel mounting system (Figure 67). However, there were specific problems with this panel arrangement technique. Panels were organized into five folders. Opening the folders was a complex task that required a large number of personnel. When the folders were opened, the folder's frames tended to bend slightly. With so many folders open at once, the support bar below them got slightly unstable as it carried the load of the panels and the folders.



Figure 67. Solar panel array (arrangement) model 1(Previously designed)

Solar panel array upon the panel carrier (model 2): For the second time, three foldable panel combinations were introduced and included in the carrier as a solar panel mounting system instead of five foldable panel combinations (Plate 17). Panels were organized into three folders. Opening folders was as difficult as earlier (previous five foldable panel combinations); now, opening folders was much less complicated with three folders. Only now two workers are required to open the folders. In the case of trained workers, one worker is enough to open the folders. Folders were no longer curved when the three foldable panel combinations were opened. As there are three folders, the support bar under the folder does not make it difficult to carry the load of the folders.



Plate 17. Solar panel array model 2

Key features of the movable/self-propelled/mobile solar panel carrier

A mobile/self-propelled solar panel carrier for utilizing solar energy in small agricultural machinery and multipurpose use has several key features to enhance its efficiency and effectiveness ((Plate 18)).



Plate 18. Solar-powered self-propelled mobile solar panel carrier

Solar panel mounting system: The Solar Panel Carrier has a sturdy and adjustable mounting system for solar panels. The panel specification is given in Table 53. This system offers ease of installation, adjustment, and position of the panels to expose them more to sunlight ((Plate 19)). Efforts were made to create a strong frame to make the carrier light durable, withstanding environmental conditions sufficient for the solar panels.



Plate 19. Solar panel array of the carrier.

Table 53. Features of solar panel

Serial No.	Items Description	Value
1.	Rated Max Power, Pmax (Model: XH150P (36))	150Wp
2.	Tolerance	0-3%
3.	Voltage at Pmax (Vmp)	18. 0V
4.	Current at Pmax (mp)	8. 34A
5.	Open-Circuit Voltage (Voc)	22. 1V
6.	Short-circuit Current (Isc)	9.05A
7.	Nominal Operating Cell Temp (NOCT)'	47°C ±2°C
8.	Maximum System Voltage	1000 VDC
9.	Maximum Series Fuse Rating	10A
10.	Dimensions, mm	1490*660*30

Wheel or track system: The carrier was equipped with a reliable wheel that ensures stability, traction, and smooth movement across different environments ((Plate 20)). This carrier used a spring-type shock absorber and plate-type suspension (leaf spring) for shock absorption ((Plate 21)).

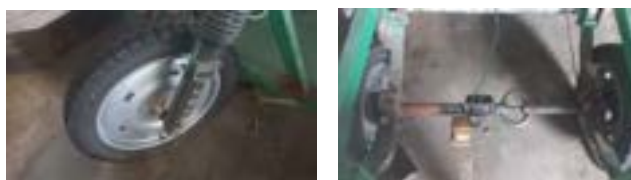


Plate 20. Wheels of the solar panel carrier



Plate 21. Suspension/shock absorber of the carrier	Plate 22. Motor of the solar carrier	Plate 23. Steering system of the panel carrier.
--	--------------------------------------	---

Self-propulsion: The carrier becomes self-propelled when equipped with a dependable propulsion system, such as an electric motor, eliminating the need for external pulling or pushing ((Plate 22). This allows it to move freely across roads and fields, increasing mobility, reducing farmers' workload, and maximizing solar energy collection.

Steering mechanism: An effective steering system enables accurate control and mobility, allowing the carrier to travel through challenging roads and confined locations. The carrier features a responsive and efficient steering mechanism, enabling precise control and maneuverability, even in confined spaces within the agricultural site ((Plate 23).

Tracking mechanism: This solar panel carrier does not have a solar tracking system that would allow it to track the sun's movement throughout the day. As the solar panel carrier is self-propelled, it has three wheels. The solar panel array could be easily rotated manually with the sun's direction so that solar panels always face the sun at an optimal angle, maximizing energy generation.

Adjustable panel angles: The carrier allowed for adjusting solar panel angles to optimize energy generation based on the sun's position ((Plate 24). This feature ensured the panels captured sunlight at the most effective daytime angles.



Plate 24. Adjustable panel angle with the carrier

Battery or power storage: The carrier has an integrated energy storage system, such as batteries, to store excess energy generated during peak sunlight hours. These batteries were used to power solar panel carriers and small agricultural machinery during sun-shining periods, ensuring continuous operation and reducing reliance on the electrical grid (Plate 25).



Plate 25. Battery/power Storage of the carrier



Plate 26. Solar Battery charger



Plate 27. Solar inverter

Charging system: For easy recharging and longer operation times, the carrier was fitted with a charging system that runs on solar or conventional power sources (Plate 26).

Power distribution: The power outlets or ports to distribute solar energy to small agricultural machinery and others (Plate 27). were included with the carrier. These outlets were conveniently located for easy access and connection to the equipment.

Safety features: Safety was the priority in designing the solar panel carrier. Safety mechanisms, including braking systems, were integrated to ensure the safe movement of the carrier and protect both the equipment and personnel (Plate 28).



Plate 28. Braking system of the carrier.



Plate 29. Control box and controller of the carrier.

Control system: A control system will be incorporated to monitor energy generation, storage levels, and power distribution. This feature enables efficient operation and maintenance of the carrier. A simple operating control system was attached to the solar panel carrier (Plate 29).

Easy maintenance: The carrier was designed for easy maintenance and servicing. Accessible components, user-friendly interfaces, repairs, and upgrades reduce interruption. Features such as

batteries, motors, and control systems should be easily accessible for inspection, repair, or replacement.

Integration with agricultural machinery: The carrier will be integrated with small agricultural types of machinery such as BRR open-drum threshers, BRR winnowers, Mini rice mills, BRR chopper machines, solar seed dryers, automated seed sower machines, domestic electric instruments, and machinery, as well as the solar pump. This allows for directly utilizing solar energy to power this machinery, reducing dependence on fossil fuels and lowering operational costs.

Technical specifications

A Self-Propelled mobile solar panel carrier designed to utilize solar energy for small agricultural machinery would typically have the following technical specifications:

Solar panel capacity: In this case, the solar panel carrier linked all panels in series. The carrier has enough surface area to hold 20 solar panels. Each solar panel is capable of producing 150 watts. The array of the 3kW panel meets the energy requirements of the small agricultural machinery (driven by no more than a four-hp diesel engine).

Solar panel mounting system: This system allowed for easy sloping and angling of the panels to maximize solar energy capture based on the sun's position. This adjustable mounting mechanism maintained a 23-degree angle to direct as much sunlight as possible toward the panel. The solar panels would consist of photovoltaic cells capable of converting sunlight into electrical energy.

Battery capacity: The carrier incorporated a battery system to store solar energy generated during daylight hours. The battery capacity was adequate to provide power to the carrier and the small agricultural machinery during non-daylight hours or when additional power was required. Energy storage systems such as batteries store the generated solar energy. The solar panel carrier used four (04) 12-volt (130AH) batteries. The batteries were charged through a charge controller with solar power drawn from the panels. Inverter systems convert harvested DC energy into AC energy suitable for powering agricultural machinery. The carrier has energy storage devices such as batteries to ensure continuous power supply. The carrier is a feature of a battery or energy storage system to store the energy generated by the solar panels.

Charger and inverter capacity: It has an MPPT battery charger (48 Volt, input=300 V (MPPT), Charging Current=10 Amps) for charging 04 batteries. The purpose of the charger was to regulate the current from the solar panels to prevent the batteries from overcharging. A solar charger was used to sense when the batteries were fully charged and to stop the current flowing into the battery. It has a solar 3-phase pure sine wave with MPPT and VFD inverter. Input voltage and output power were 300V (MPPT) and 3000VA, respectively.

Electric motor: The carrier was equipped with an electric motor (1000W) to enable self-propulsion. The motor's power and torque were moderately good but insufficient for moving the carrier through the varied environments encountered in agricultural operations. However, the power and torque of the motor must be increased. The more powerful the motor, the higher its torque, which improves the conveyor's load and movement capacity.

Control system: A sophisticated control system manages to move the carrier. The carrier has a control system that manages the charging and discharging of the battery, monitors the power output of the solar panels, and controls the movement of the carrier.

Wheels/tracks: Depending on the terrain and mobility requirements, the carrier was designed with three wheels. The wheel diameter was 580 mm, and the width was 90 mm. The distance between the two rear wheels was about 1096 mm. The distance between the front wheel and rear wheel was about 2951 mm. The distance from the basement to the center of the wheel was about 360 mm. The spring-type shock absorber and plate-type suspension (leaf spring) were adjusted upon the rear axle (Fig.5).

Frame and structure: The carrier was fabricated with a sturdy frame and system capable of supporting the weight of the solar panels, batteries, and machinery while ensuring durability and resistance to environmental conditions.

Size and dimensions: If necessary, the carrier's size and dimensions were optimized for easy maneuverability within transportation on roads and agricultural fields. The overall dimension of the solar panel carrier is 538 cm X 491 cm X 228 cm (LxWxH). The overall area covered 26.42 m² by the solar panel carrier when the folders were opened.

The overall specification of the self-propelled mobile solar panel carrier for utilizing solar energy is shown in Table 54.

Table 51: Overall specification of the mobile solar panel carrier for solar energy utilization.

Section/ unit	Components	Particulars			
		Materials and accessories	Size	Number	Description and remarks
Moving parts	Wheel	✓Tire ✓Tube ✓Rim	✓ Wheel ✓ Dia: 580mm; ✓ Width: 90mm	03	<ul style="list-style-type: none"> ➤ The distance between the two rear wheels was about 1096mm ➤ The distance between the front wheel and rear wheel was about 2951 mm ➤ The distance from the basement to the center of the wheel was about 360 ➤ Plate-type suspension (leaf spring) adjusted upon the rear axle. ➤ Spring-type shock absorber adjusted upon the front wheel.
	Axle (Small) (For the front wheel)	MS Shaft	L:150mm, Dia: 30 mm	01	➤ The length of the axle shaft was about 150 mm. (Procured from the market)
	Long axle Shaft adjusted with two rare wheels	MS high carbon and MS Pipe	L: 1188 mm, Dia: 35 mm	01	➤ The axle shaft was covered by MS pipe. (Procured from the market).
Driving parts	Handle-type steering system	Accelerator	Grip-type	01 set	Available in the market
		Front Light	Inbuilt in the Controller	01	Available in the market
		Controller meter for operating	Oval shape	01	High-capacity controller set-up, which is available in the market
		Front shocker & T SET	-	01	Available in the market
		Hubs	-	02	Available in the market
		Bearing	6005	06	Available in the market
		Mudguard	-	01	Available in the market
		Wiring cable	DC cable	01 set	Customized wire cables can be purchased readily on the market.
		Flexible pipe	Plastic-made flexible pipe (20 m)	01 set	Available in the market
		MS Pipe	Dia: 30mm; L:6m, Dia: 40mm; L: 6m	01 01	Available in the market
Power transmission system	Motor	DC motor	48 V, 1000W	01	Available in the market
	Battery	Solar Battery	48 V, 130 Ah	04	Available in the market
	Drum	MS	W:160mm	02	Two drums containing the brake saw were attached to the rear wheel. This drum has four nut bolts through which the rear wheel is connected to the axle
	Foot brake	Brake Show		04	
Basement /platform (4800mm X1370mm)	Main body frame	MS box	75mm*45mm	04 (20 ft long)	The main body was about 20m long and made of boxes (75 mm X 45 mm). For making the main body, an additional 5m long box (50mmX50mm), 06m long box (40mmX40mm), and 03m long box (25mmX25mm) were required to make the other parts of the body.
		MS box	50mm*50mm	01 (20 ft long)	
		MS box	40mm*40mm	01 (20 ft long)	
		MS box	25mm*25mm	01 (10 ft long)	
		MS box	50mm*25mm	01 (10 ft long)	
	Base	MS sheet	1.5m*1.5m	02 piece	It was used as the base of the platform
	Trailer leaf spring	MS plate	Thickness:5mm	02 set	Each set contains 5 plates that were used for the shock absorber. Available in the market.
	Trailer leaf spring holder	MS flat bar	Thickness: 5mm	08 pieces	Making the trailer leaf spring holder and other additional works, a 03 m long flat will be required.
Stand for supporting panel with frame.	Pentagonal shape frame	MS Box	100mm* 50mm	02 pieces	About a total of 100m long MS box was required. According to the size, it will be cut to make two stands for supporting the panels. About 920 mm X 1530 mm size 01-piece plates were required. A total of 10 m long shaft was required. A 4mm thick flat bar about 02m long was used to make a half-moon shape to keep the frame at the desired angle. The pipe supported the main frame of the panel.
			45mm*45mm	01 pieces	
		MS plate	Thickness: 5mm		
		MS Shaft	Dia: 25mm		
		Flat bar	Thickness: 4mm, L:2M		
Pipe	L: 2001 mm; D=65mm	02 pieces			
Frame for panel holding	Rectangular shape panel holding frame	MS angle	38mm*38mm	-	A 36m long box was required to make a panel frame. A 15-meter long (25mm X 25mm) angle was required.
			25mm*25mm		
		MS box	25mm*25mm 38mm*38mm	-	About 15m long box was required for making panel frame.
Bearing	Dia: 42mm; Number:6201	40 pieces	About 50 pieces required bearing size were incorporated into the main panel		

Section/ unit	Components	Particulars			
		Materials and accessories	Size	Number	Description and remarks
					frame for moving down in the main body frame.
		MS Shaft	Dia: 12mm	-	About 05m long MS shaft was required
		Handle	Dia:20-30mm		The handle was used for up-and-down solar panels in the main panel frame.
	Big size frame	MS angle	1992mm*1593mm	06 pieces	03 panels arranged in this frame
	Small size frame	MS angle	1593mm*666mm	02 pieces	Single panel arranged in this frame
	Frame connecting and pushing box with a hand gripper	MS box	38mm*38mm L:2241mm	08 pieces	This box helps to connect with the frame, and this box maintains panel inclination.
	Holding box	MS box	50mm*50mm L:470mm	24 pieces	This box holds the pushing box
	Box	MS box	25mm*25mm L:470mm	12 pieces	This box gives additional strength to the frame
Solar power utilization	Solar panel	-	200w Dimensions, mm: 1330*990*40	14	Available in the market. A total 2800-watt panel carrier was developed.
	Inverter	3 phases with MPPT	Input: 300V(MPPT) Output power: 3000VA	01	Available in the market. 3phase with MPPT Solar inverter was used to convert solar energy to AC.
	Charge controller	MPPT	48V	01	Available in the market. A 48-volt charge controller was used to charge the battery.
Development, modification, and accumulation of small agricultural machinery for solar-powered operation	BRRRI Winnow, BRRRI open drum thresher, BRRRI Chopper, Solar dryer, Rice Mill, Seed Sower, etc., and domestic electric instruments or accessories.	Developed machines Rearrange the belt-pulley system to synchronize the rpm of the machines.	0.5 hp motor-operated winnower and solar dryer, 01 hp operated chopper, 02 hp motor-operated open drum thresher, and rice mill.	01 set of machinery	The mentioned small agricultural machinery can be performed using solar energy generated by the movable solar panel carrier system. The developed solar system worked a maximum 2hp motor-operated machine. This solar panel carrier will also be used for net metering to the grid system.

Conclusion

The FMPHT divisional research workshop in BRRRI, Gazipur, has completed the prototype fabrication of a self-propelled mobile solar panel carrier using locally available materials. The initial test was carried out in the workshop of the FMPHT division. During the trial, the solar panel carrier generated energy using solar panels that could power 0.5, 1.0, and 2 horsepower motors. Only the motors were driven throughout the day for the initial test. This 3-kW panel could initially power a 2-horsepower motor all day. The developed solar panel carrier will be thoroughly tested to ensure its optimal performance, with further adjustments needed to reduce operator fatigue and improve overall performance. To achieve optimal performance, the motor power should be increased. Extensive performance testing is required to acquire additional details on the performance of the developed solar panel carrier. The design and development of a movable/self-propelled solar panel carrier offers an efficient and sustainable solution to address the challenges associated with solar panel transportation. The findings can contribute to advancing portable solar panel technology, enabling the widespread adoption of renewable energy solutions.

Recommendations

- Optimize the carrier design for performance while considering space and weight distribution.
- A simple gear mechanism may be attached to the carrier to open and close the solar panel frames more easily.
- Conduct structural studies to ensure long-term durability and resistance to dynamic loads.
- Measure the carrier's center of gravity (CG).
- Load-bearing capacity and weight balance need to be improved.
- A tracking mechanism might be added for further improvement.
- Self-propelled solar panel careers may be designed and developed with panels of different sizes and capacities.
- Analyze cost-effectiveness and affordability, taking scaling and savings into consideration.
- Conduct field tests to evaluate performance and obtain feedback from users.
- Encourage stakeholder collaboration to take advantage of knowledge and industry alignment.

PROJECT 4: PRECISION AGRICULTURE

Experiment 4.1: Evaluating the Effects of Climate Change on Thermal Bioclimatic Indices in Bangladesh Using Climate Projections from Bias-Corrected CMIP6 Models

Principal Investigator: Dr. Mohammad Kamruzzaman

Co-Investigator(s): Dr. Md. Sazzadur Rahman, PSO, Plant physiology division, Md. Mizanur Rahman, SO, FMPHT division

Objectives

- Assess the effects of climate change on Thermal Bioclimatic Indicators (TBIs) in Bangladesh using bias-corrected CMIP6 models.
- Examine climate projections under three Shared Socioeconomic Pathways (SSPs) for near, mid, and far future periods to understand variations in TBIs.
- Identify how climate change impacts TBIs across different regions of Bangladesh, focusing on temperature changes and their implications for rice cultivation.
- Provide insights into climate change impacts on biodiversity and ecosystems, supporting the development of adaptation and mitigation strategies for rice cultivation.
- Offer evidence-based recommendations for policymakers and stakeholders to safeguard food security and promote sustainable agricultural practices in the face of climate change.

The bioclimate plays a fundamental role in the interaction between climate and biota. It provides critical information on annual and seasonal climate averages, changes, and variations. Understanding bioclimatic indicators is crucial for assessing species distribution, cropping suitability, thermal comfort zones, and vulnerability to climate change. Climate change has complex effects on climate variables, impacting biological distributions, and posing risks to ecosystems and human health. Global climate models (GCMs), especially CMIP6, have improved accuracy in projecting future climate scenarios. However, uncertainties in modeling call for a Multi-Model Ensemble (MME) approach to provide robust assessments.

Bangladesh, a tropical monsoon region, faces severe climate change impacts, including rising temperatures, threats to rice production, and public health challenges. TBIs are valuable for evaluating climate change effects, but there is limited research in tropical regions like Bangladesh. This study aims to fill this gap by assessing TBIs across Bangladesh using CMIP6 models and employing bias correction and multimodal ensemble techniques. The research findings will offer insights into climate change impacts on biodiversity and ecosystems in Bangladesh, informing adaptation and mitigation strategies. Policymakers must consider these projected changes to protect agriculture, ecosystems, and public well-being in the face of a changing climate. The study's contribution to understanding climate change's effects on tropical regions underscores its importance in climate change research and policy-making.

Material and methods

Data for the study were obtained from 28 meteorological stations in Bangladesh, including observed daily rainfall, maximum temperature (T_{max}), and minimum temperature (T_{min}) data for the period 1985 to 2014. Additionally, 18 CMIP6 Global Climate Models (GCMs) were used to project future climate scenarios for the years 2015 to 2100 under different Shared Socioeconomic Pathways (SSPs): SSP1-2.6, SSP2-4.5, and SSP5-8.5.

The study analyzed 11 Thermal Bioclimatic Indicators (TBIs) across Bangladesh to understand their current and projected changes under different future scenarios. These indicators represent various aspects of the thermal environment and are critical for assessing the impacts of climate change on biodiversity and ecosystems. The downscaling and bias-correction techniques were applied to GCM simulations using the observed station data. A multi-model ensemble mean approach was used to average the results from the 18 GCMs, reducing uncertainties and providing a more comprehensive representation of the TBIs. The spatiotemporal change analysis compared the multi-model ensemble mean values of the TBIs for near future, mid-future, and far future periods under different SSP scenarios. This analysis aims to provide insights into how these bioclimatic indicators may vary over time and across regions, helping policymakers and stakeholders develop effective climate adaptation strategies.

Results and discussion

The study examined the projected climate changes and their impacts on Bangladesh using multiple climate scenarios (Shared Socioeconomic Pathways, SSPs) and future periods. Here are the key findings from the study:

Annual Indicators

- Mean Annual Temperature (Bio-1): Projections show an increasing trend in Bio-1 across all scenarios and future periods. The highest increases are observed in the far future under SSP585. Southeastern and central southern to southeastern regions of Bangladesh are expected to experience the most significant temperature increases.
- Diurnal Temperature Range (Bio-2): All projected periods and SSPs indicate a negative change in Bio-2, indicating a decrease in temperature variability. The most substantial decreases are anticipated in the northern, central, southern, and southeastern parts of Bangladesh.
- Isothermality (Bio-3): The data indicate a consistent trend of decreasing isothermality percentages, indicating a more uniform annual temperature range with fewer differences between warmest and coldest months. The greatest decline in Bio-3 is projected in the eastern and southern regions of Bangladesh.
- Temperature Seasonality (Bio-4): Projections show minor fluctuations in Bio-4 values for all future periods and scenarios. The largest decline in Bio-4 is projected in the northwestern to southwestern regions of Bangladesh.
- Annual Temperature Range (Bio-7): Bio-7 is expected to undergo more significant increases or decreases in the far future compared to the near or mid-future. A slight increase in Bio-7 is projected in the northeastern and southeastern regions, while a more substantial decrease is projected for the northwestern, central, and southwestern parts of Bangladesh (Fig. 68).

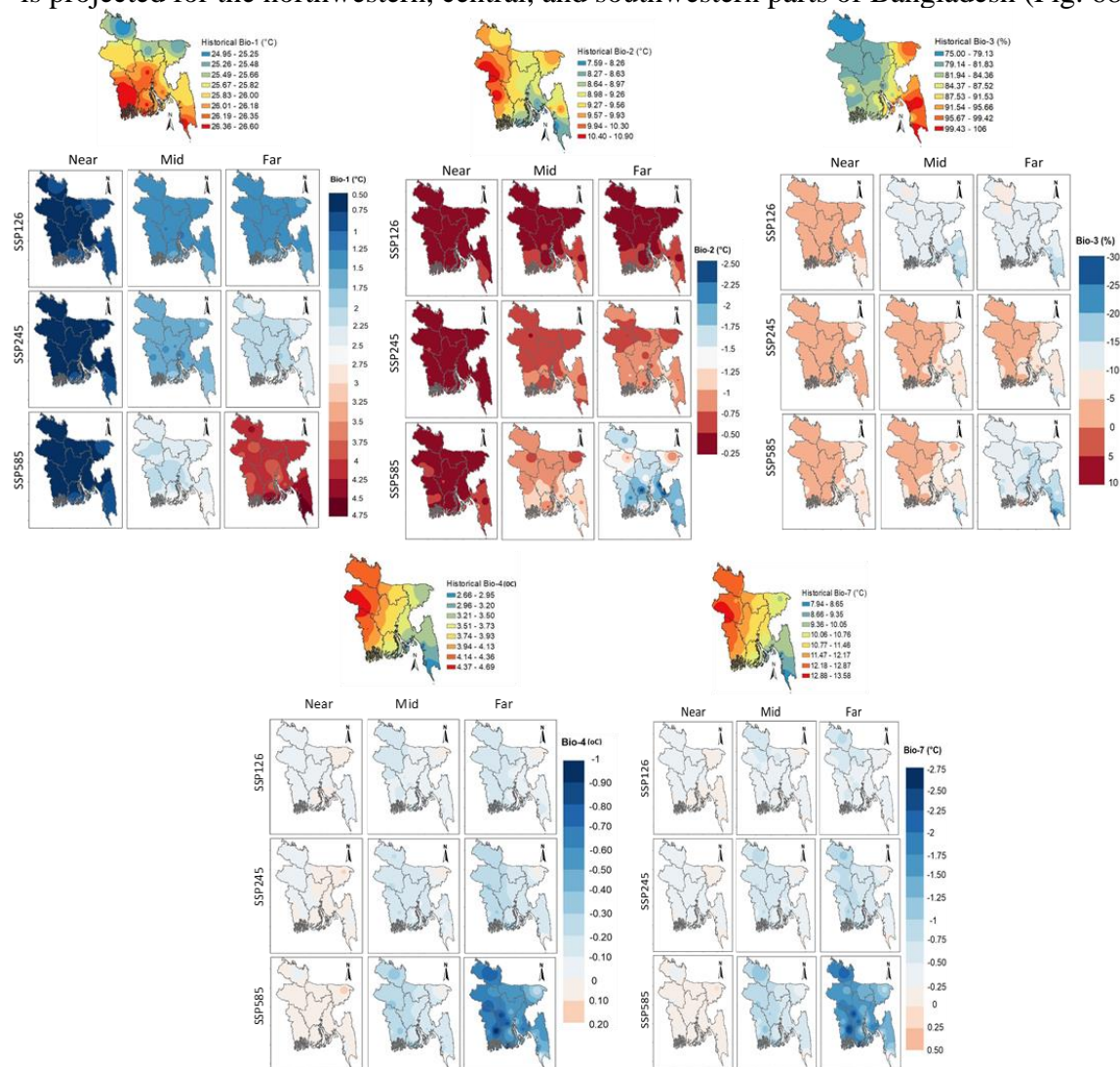


Figure 68: Annual Indicators.

Seasonal Indicators:

- Mean Maximum and Minimum Monthly Temperature (Bio-5, Bio-6): Projections show increasing trends in both Bio-5 and Bio-6 for all future periods and scenarios. The monthly minimum temperature (Bio-6) is projected to increase at a faster rate compared to the monthly maximum temperature (Bio-5).
- Mean Temperature of Warmest and Coldest Quarters (Bio-10, Bio-11): Both Bio-10 and Bio-11 are expected to increase under all three SSPs. The temperature increase during the warmest quarter (Bio-10) is projected to be more significant than in the coldest quarter (Bio-11).

- Overall, the study highlights the potential climate impacts on Bangladesh, including rising average temperatures, decreasing diurnal temperature ranges, and changes in temperature variability, which could have significant consequences for the environment and ecosystems in the region. These findings provide valuable insights for climate adaptation and mitigation strategies in Bangladesh.
- This study's findings reveal that changes in Thermal Bioclimatic Indicators (TBIs) due to climate change may significantly impact rice cultivation in Bangladesh. As the study suggests, an increase in average annual temperature (Bio-1) could increase evapotranspiration rates and reduce soil water storage, leading to higher irrigation demands and potentially reducing groundwater reserves. Furthermore, increased Bio-1 might negatively affect soil carbon, soil organic matter, and soil fertility, potentially resulting in decreased rice production. The projected decrease in diurnal temperature range (Bio-2, DTR) can also impact rice cultivation. DTR plays a crucial role in the development and growth of rice. Studies have shown that a decrease in DTR negatively affects rice output, thereby potentially impacting food security and livelihoods in Bangladesh where agriculture plays a crucial role.
- In terms of the decrease in isothermally (Bio-3), it could influence the distribution and behavior of various species, including crops like rice. Alterations in temperature patterns could affect crop phenology and yields, with potential implications for food security in the region. Moreover, the delay in the onset of summer from winter due to reduced temperature seasonality (Bio-4) might lead to prolonged cooler conditions, delaying the start of the growing season and affecting rice planting schedules. This delay can result in shorter growing periods and potentially reduced rice yields (Fig. 69).

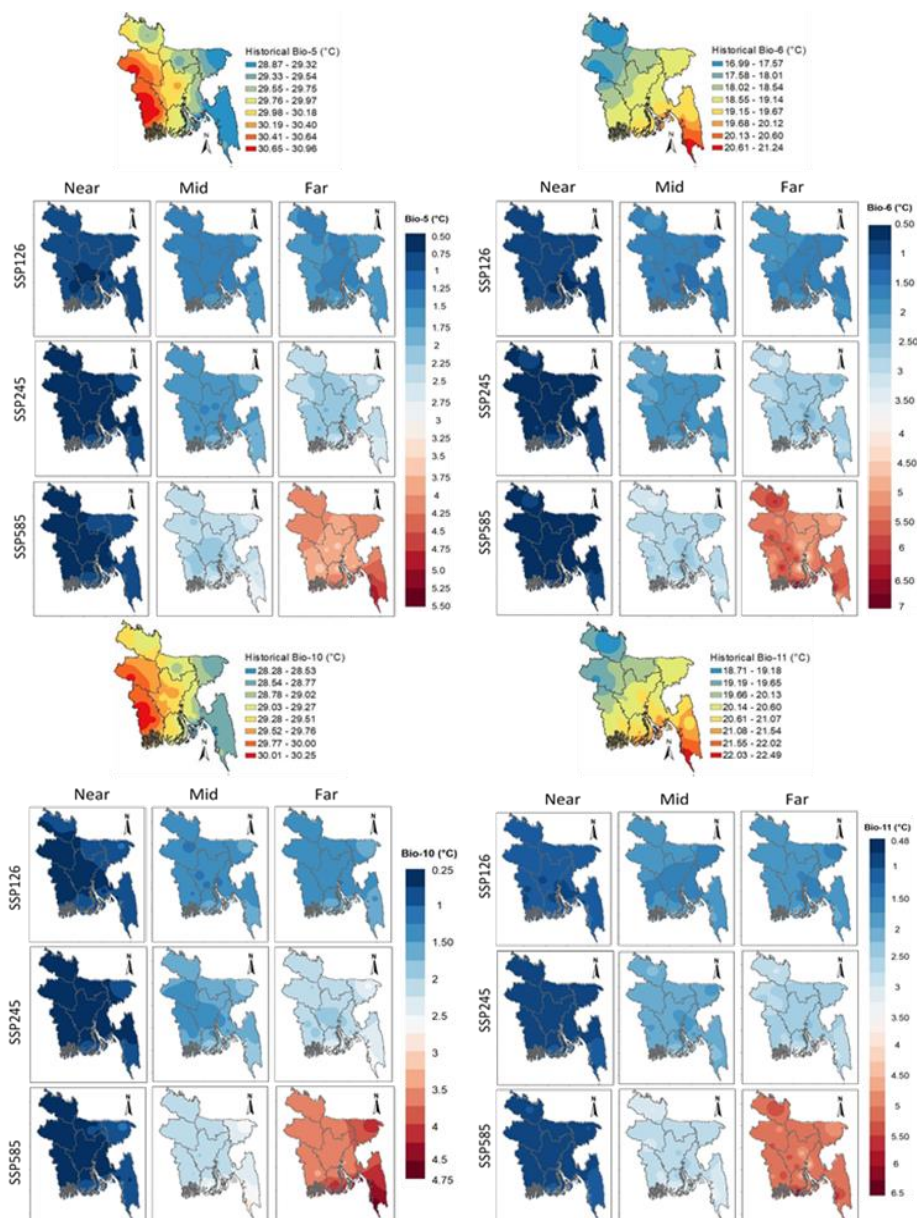


Figure 69. Seasonal Indicators

Conclusion

The changes in TBIs due to climate change could significantly influence rice cultivation in Bangladesh through various direct and indirect effects on water resources, soil fertility, crop growth, and agricultural schedules. These impacts highlight the importance of implementing climate-adaptive measures in agriculture, such as developing heat-tolerant crop varieties,

improving water-efficient irrigation methods, and promoting sustainable agricultural practices, to ensure food security in the face of climate change.

Experiment 4.2: Compound Precipitation and Temperature Extremes in the coastal region of Ganges Delta: A 50-Year Analysis (1971-2021)

Principal Investigator: Dr. Mohammad Kamruzzaman

Co-Investigator: Dr. Md. Sazzadur Rahman, Md. Mizanur rahman

Objectives

- Examine the frequency, spatial extent, and changes over 50 years (1971-2021) of compound precipitation and temperature extremes in the coastal region of the Ganges Delta, including dry/cold, dry/hot, wet/cold, and wet/hot combinations.
- Evaluate how these compound climate extremes have impacted rice cultivation, considering the increasing hot extremes and decreasing cold extremes and their implications for agricultural practices.
- Investigate the relationship between compound extremes and large-scale atmospheric circulation modes, to improve early warning systems and inform climate adaptation strategies.
- Provide evidence-based insights for policymakers, farmers, and stakeholders to develop targeted strategies for climate resilience, disaster preparedness, and sustainable agricultural production.

The coastal region **of Ganges Delta**, is exposed to various extreme weather events, including heatwaves, heavy rainfall, and droughts, threatening the ecosystem, human health, and vital socio-economic sectors such as agriculture. The recent rise in compound extremes - co-occurring or sequential extreme events - exacerbates these threats due to their potential for more severe impacts.

Despite this region's vulnerability, comprehensive research on compound precipitation and temperature extremes remains scant. Such research is critical to enhance disaster risk reduction, agricultural resilience, and sustainable development planning. Additionally, an improved understanding of the relationships between large-scale atmospheric circulations and compound climate extremes could significantly enhance early warning systems.

Therefore, this study, aims to fill these knowledge gaps. The study provides a comprehensive analysis of the spatiotemporal changes in compound precipitation and temperature extremes, including dry/hot, dry/cold, wet/hot, and wet/cold combinations. It further examines the relationship between these compound extremes and large-scale atmospheric circulations, offering valuable insights for enhancing early warning systems and informing climate adaptation strategies. By analyzing the data over a period of 50 years, the study also reveals the historical trends and changes in compound extremes, thereby offering a solid basis for future projections and mitigation plans.

Materials and Method

The study utilizes monthly precipitation and temperature data from the Climatic Research Unit (CRU) dataset for the period 1971-2021. Additionally, large-scale atmospheric circulation indices, including the Niño 3.4 Sea Surface Temperature (SST) index, Pacific Decadal Oscillation (PDO) index, and North Atlantic Oscillation (NAO) index, were used to examine their influence on compound extremes.

Compound extremes were defined as simultaneous occurrences of extreme precipitation and temperature events, categorized into four types: dry/cold, dry/hot, wet/cold, and wet/hot. The thresholds for defining compound extremes were based on the 25th and 75th percentiles of precipitation and temperature for each season. The study employed the linear regression method is used to estimate the slope. The positive slope value indicates an increasing trend, while a negative value indicates a decreasing trend. to assess trends in the spatial extent of compound extremes. F-test used to measure the level of significance.

The analysis aims to provide insights into the changes and impacts of compound precipitation and temperature extremes in the coastal region. By exploring the relationships between compound extremes and large-scale atmospheric circulation patterns, the study offers valuable information for enhancing early warning systems and developing adaptation strategies to mitigate the impacts of changing climate conditions, particularly on agriculture. The findings will contribute to a better understanding of climate change in the region and assist in implementing risk management measures.

Results and discussion

Frequency of Compound Extremes

Figure 70 provides insights into the frequency of four compound extremes during different seasons (monsoon and winter) spanning the period from 1971 to 2021. The analysis uncovers the following trends:

During the Monsoon Season (June to September - JJAS), compound dry/hot extremes are found to be highly prevalent across most regions within the study area. This suggests that during the monsoon season, many locations experience simultaneous hot and dry conditions, which can have implications for drought conditions and heat-related impacts on various sectors.

In contrast, the frequency of compound wet/hot extremes is relatively lower during the monsoon season. This indicates that the combination of wet and hot conditions occurs less frequently during this period. Nonetheless, the occurrence of wet and hot conditions can have its own set of impacts, such as heat stress in humid regions or increased risks of waterborne diseases.

Moving on to the Winter Season (December to February - DJF), the western part of the study area (Indian part) stands out as experiencing a high frequency of compound dry/hot extremes. This indicates that during winter, this particular region is more prone to simultaneous hot and dry conditions, which might influence the availability of water resources and impact agriculture and other activities that rely on adequate moisture.

Conversely, the frequency of compound wet/cold extremes is observed to be less common during the winter season. This suggests that the occurrence of wet and cold conditions together is relatively rarer in this region during winter.

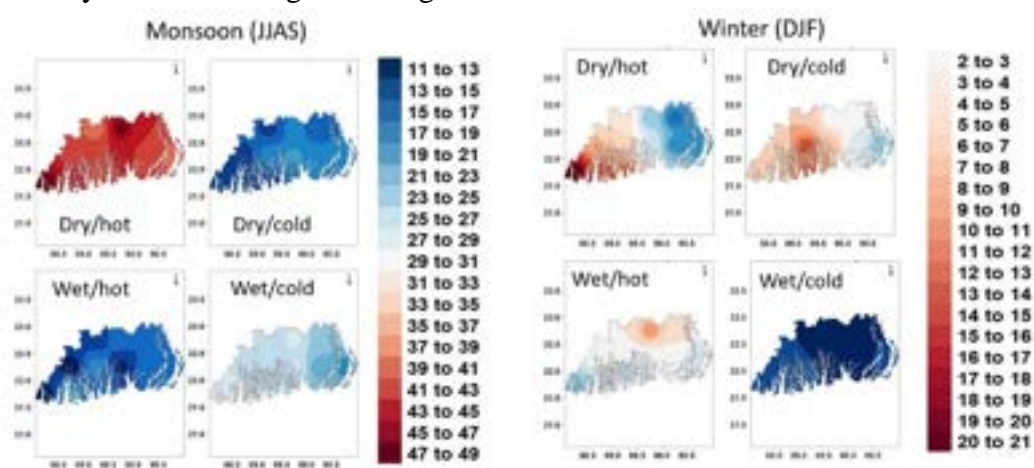


Figure 70. Frequency (months) of compound precipitation and temperature extremes during, monsoon, and winter for the period 1971–2021.

The frequency of compound extremes varies across seasons and regions, with monsoon seasons characterized by a higher frequency of compound dry/hot extremes, and compound dry/cold extremes dominating the winter seasons. These patterns can be partly explained by the correlation between precipitation and temperature, where wet conditions are associated with lower temperatures (dry/cold) and hot conditions are associated with lower precipitation (dry/hot).

Changes in the Frequency

Figure 71 presents the changes in the frequency of compound extremes across different seasons and locations within the study area. The key trends identified are as follows:

During the Monsoon Season (June to September - JJAS), there has been a notable increase in the occurrence of hot extremes from 1996 to 2021 compared to the period from 1971 to 1995. This rise in hot extremes suggests a significant warming trend during the monsoon season over the recent decades. In contrast, there is a decreasing trend in the occurrence of cold extremes during the same period. This decline in cold extremes could indicate a milder monsoon season in terms of cold events.

In the Winter Season (December to February - DJF), there has been a significant overall decrease in compound extremes across the study area during 1996 to 2021. However, it is worth noting that dry/hot extremes have not exhibited a similar decreasing trend during this period. This implies that while other types of compound extremes have reduced in frequency, dry/hot extremes have either remained stable or even increased in occurrence during winter.

These findings indicate changing patterns of extreme weather events in the study area. The increase in hot extremes during the pre-monsoon season and localized increase in wet/hot extremes in the Sundarbans region highlight the need for adaptation strategies to address these specific challenges. The decreasing trends in compound extremes during monsoon and post-monsoon seasons provide valuable insights for planning and preparedness for natural disasters. The persistence of dry/hot extremes during winter calls for targeted mitigation measures to address this specific type of extreme event.

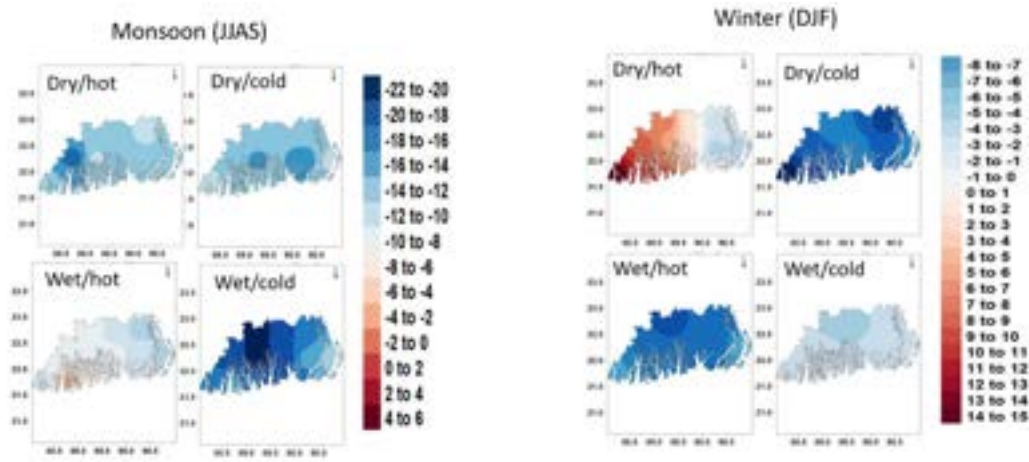


Fig. 71. Changes in the frequency (months) of compound precipitation and temperature extremes during monsoon (JJAS) and winter (DJF) for the period 1996–2021 relative to 1971–1995 in coastal region of Bangladesh and West Bengal, India

Changes in the Spatial Extent

Figure 72 showcases changing trends in the spatial extent of compound extremes during the Monsoon (JJAS) and Winter (DJF) seasons, each having unique implications. The Monsoon season is characterized by a significant increase in the spatial extent of compound hot (dry/hot and wet/hot) and cold (wet/cold and dry/cold) extremes. This indicates an expanding occurrence of combined dry and hot, and wet and hot conditions, which could significantly affect regions experiencing these extremes. On the contrary, the Winter season reveals a minor negative trend in the spatial extent of compound cold conditions (wet/cold and dry/cold), with an insignificant negative trend in wet/hot conditions but a positive trend in dry/hot conditions. This shift suggests a reduction in cold and wet conditions, potentially impacting ecological and hydrological processes in these regions.

The variations in climate conditions during both seasons also have noteworthy impacts on rice cultivation. The increased hot and dry conditions during the Monsoon season may induce water stress in rice paddies, affecting crop growth and yield. During the Winter season, reduced cold and wet conditions may influence winter rice cultivation, altering the crop's development timings and impacting crucial stages like flowering and grain filling. Adapting strategies like adopting climate-resilient rice varieties, improving irrigation and water conservation methods, and integrating climate change considerations into agricultural planning can be instrumental in ensuring sustainable rice cultivation amidst these evolving climate extremes.

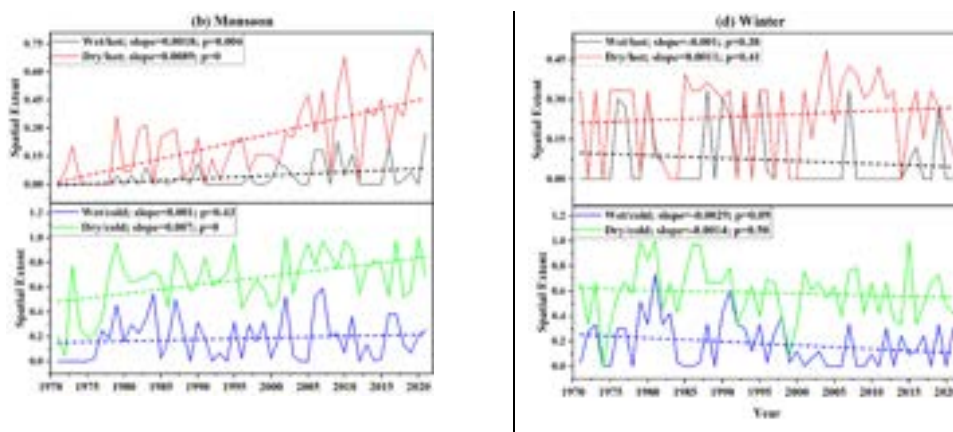


Fig. 72. Changes in the spatial extent of compound precipitation and temperature extremes during monsoon (JJAS), and winter (DJF) for the period 1971–2021 in coastal region of Bangladesh and West Bengal, India (the solid lines are the annual series of spatial extent, and the dashed lines are the linear trends).

Teleconnection between Compound Extreme Indices and Large-Scale Atmospheric Circulation

Table 55 shows the statistical relationships between the compound extremes and atmospheric circulation modes for each season in the study area. The study found significant correlations between compound extremes and atmospheric circulation modes in the coastal region of Bangladesh and West Bengal, India, during different seasons. Notably, during the monsoon season, wet/hot conditions were strongly influenced by the North Atlantic Oscillation (NAO), with a significant negative correlation ($r=-0.50$; $p<0.01$). Dry/hot conditions also showed a moderate negative correlation with NAO ($r=-0.33$; $p<0.05$). However, Wet/cold and Dry/cold conditions did not exhibit significant correlations with NINO3.4, PDO, and SOI. In winter, NINO3.4 had a notable positive correlation with wet/hot ($r=0.33$, $p<0.05$) and wet/cold ($r=0.38$, $p<0.01$) conditions. Additionally, Dry/cold conditions showed a significant positive correlation with PDO ($r=0.32$, $p<0.05$).

These results emphasize the importance of considering specific atmospheric circulation modes, such as NAO and NINO3.4, in understanding extreme weather events in the study area during different seasons. The findings contribute valuable insights to climate dynamics and variability, aiding climate adaptation and disaster preparedness efforts in the coastal region.

Table 55. Correlation coefficients between the spatial extent of compound extremes and atmospheric circulation modes in the coastal region of Bangladesh and West Bengal, India during monsoon (JJAS), post-monsoon (ON), and winter (DJF) for the period 1971–2021.

Compound Extremes		NAO	Nino3.4	PDO	SOI
Monsoon	Wet/hot	-0.50**	-0.01	-0.09	0.11
	Wet/cold	-0.08	0.08	0.15	-0.08
	Dry/hot	-0.33*	0.08	0.01	0.05
	Dry/cold	-0.06	0.01	0.08	0.00
Winter	Wet/hot	0.12	0.33*	0.05	-0.22
	Wet/cold	0.11	0.38**	-0.10	-0.27
	Dry/hot	-0.21	0.09	0.10	-0.03
	Dry/cold	-0.23	0.18	0.32*	-0.18

(* Statistically significant at the $P<0.05$ level; ** Statistically significant at the $P<0.01$ level)

Conclusion and discussion

Changes in the frequency and spatial extent of compound extremes can significantly impact rice cultivation in **of coastal region of Ganges Delta**. Rising temperatures during the monsoon season (JJAS) can induce heat stress in rice plants, while a decrease in cold extremes could influence rice varieties that require specific cold exposures. In the winter season (DJF), reduced occurrences of wet/cold conditions could be beneficial for rice growth, whereas persistent dry/hot extremes could result in water stress.

Changes in the spatial extent of compound extremes could also reshape rice cultivation patterns. Increased dry/hot and wet/hot extremes during the monsoon season may create unfavorable conditions for rice growth, while the decreasing spatial extent of wet/cold conditions in winter could offer more favorable conditions for rice cultivation.

These changes underscore the need for climate-resilient agricultural practices, early warning systems, and targeted adaptation measures. Policymakers, farmers, and stakeholders should develop strategies that consider the impacts of changing weather patterns on rice cultivation, thus ensuring food security and sustainable production.

Significant correlations between atmospheric circulation modes and compound extremes further highlight potential impacts on rice cultivation. During the monsoon season, NAO-influenced wet/hot conditions can affect rice production due to varying rainfall and temperature. In winter, NINO3.4-related variability can influence extreme weather events, impacting rice cultivation in various ways depending on local factors and rice varieties. Moreover, the significant positive correlation between Dry/cold conditions and PDO during winter suggests that PDO could influence cold and dry extremes, potentially leading to frost damage and growth disruption. These findings highlight the need for stakeholders in the agriculture sector to use this information in developing targeted strategies for climate adaptation and disaster preparedness, ultimately enhancing rice production and food security in the study area.

PROJECT 5: INDUSTRIAL AND FARM LEVEL EXTENSION OF AGRICULTURAL MACHINERY

Training on operation, repair, and maintenance of BRRI's newly developed farm machinery

Principal Investigator: Arafat Ullah Khan

Co-Investigator: All Scientists of FMPHT

Objectives

- To introduce BRRI-developed and other agricultural machines at farmer's levels
- To develop skilled operators on agricultural machinery at farm levels
- To build up awareness about the use and benefit of using agricultural machines

Major activities

BRRI developed machinery; technologies and other agricultural machinery were introduced and practically operated to the trainees-

- Demonstration and Operation on BRRI seed sower machine for seedling technique and tray procedure
- Operation and maintenance on BRRI whole feed combine harvester
- Demonstration on seedling raising technique for BRRI manual and Power rice transplanter
- Operation and maintenance on BRRI manual and Power rice transplanter
- Operation and maintenance on BRRI prilled urea applicator
- Operation and maintenance on BRRI manual and power weeder
- Operation and maintenance on self-propelled rice/wheat reaper
- Operation and maintenance on BRRI open drum thresher
- Operation and maintenance on BRRI closed drum thresher
- Operation and maintenance on BRRI winnower
- Hands-on repair and maintenance on diesel engine
- Practical field operation of agricultural machinery in the farm level
- Developed the operators cum entrepreneur of the agricultural machinery for sustainable mechanization

Mechanic training on repair, operation, and maintenance

A training programme is a very useful and easy technique for using agricultural machinery in the optimum way that enhances rice mechanization in the country. Two days training program was conducted at the FMPHT division funded by the SFMRA project for the specific district's DAE personnel's and farmers for land & seedling raising technique, operation, repair, and maintenance of seed sower machine, BRRI manual, and power rice transplanter, BRRI solar light trap, BRRI manual and power weeder & BRRI whole feed combine harvester. SFMRA project provides all types of training materials and all other technical support (Plate 31). A total number of 40 participants are attending in two batches training program.

One training programme was organized for research workshop staff on safety measure, operation, and repair-maintenance of workshop machinery, and 30 workshop personnel's were attended the programme. Ten days long three batches training program was arranged at Alim Industry Ltd., Sylhet financed by the "Strengthening Farm Machinery Research Activity for Mechanized Rice Cultivation project". Two days training program is on-going at the FMPHT division funded by the SFMRA project for the specific district's farmers. Farmers were very happy to participate in the operation, repair and maintenance training programme and enriched their knowledge of BRRI-developed machinery & technologies and others agricultural machinery. During practical session machinery like BRRI seed sower, BRRI rice transplanter, BRRI whole feed combine harvester, power tiller, tractor and reaper were operated by the participants for gathering experience on agricultural machinery operations in no load condition in the drying yard/road. Successful completion of primary agricultural machinery operation, participants were taken to the main field for final operation. At the end of the training, a post-evaluation and trainee's reactions regarding the training were collected. Certificates, training honarium and a set of tools were distributed among the participants (Plate 30).



Plate 30. Inaugural & Closing session of the training programme.



Plate 31. Practical session of the training programme.

Hands-on training under KGF funded project

A total of 08 training programs were conducted during the reporting period. Detailed information about the training program is presented in Table 56. Theoretical sessions along with practical operations were the parts of the training. The sessions were 1. Importance, problems, and prospects of mechanization, 2. Mat type seedling raising techniques, 3. Seed and soil treatments, disease control, and cold combination during Boro season, 4. Rice transplanter cum fertilizer applicator and combine harvester introduction, operation, repair, and maintenance, 5. Problems of rice transplanter operation in the field and troubleshooting and 6. Power weeder, rice transplanter or combine harvester operation, repair, and maintenance.

Table 56. Detail information on the training conducted during the reporting period.

Sl. no.	Crop season	Date	Participants		Total participants	Place	Technology used
			Male	Female			
1	Aman/22	25/01/23	30	-	30	Bandakhin, Sadar, Habiganj	Trasplanter
2	Aman/22	17/02/23	30	-	30	Anandapur Sadar Habiganj	Trasplanter
3	Aman/22	10/02/23	26	4	30	Choknur, Raiganj, Sirjgonj	Trasplanter
4	Aman/22	11/02/23	28	2	30	Gopalpur Raigonj, Sirajgonj	Trasplanter
5	Boro/2022-23	10/07/2023	30	-	30	Anandapur Sadar Habiganj	Trasplanter and weeder
6	Boro/2022-23	13/07/2023	30	-	30	Chaknur, Raiganj, Sirajganj	Trasplanter and weeder
7	Boro/2022-23	21/10/23	30	-	30	Gopalpur Sirajganj	Combine harvester
8	Boro/2022-23	29/10/23	30	-	30	Anandapur Sadar Habiganj	Combine harvester

Field demonstration under KGF funded project

A total of 06 field demonstration cum training programs were conducted during the reporting period. Detailed information about the demonstration program is presented in Table 57. Practical operation and discussion were the parts of the training. Training programs were conducted on rice transplanter cum mixed fertilizer applicator and multi-rows power weeder.

Table 57. Detail information on the demonstration program conducted during the reporting period.

Sl. no.	Crop season	Date	Participants		Total Participants	Place	Technology used
			Male	Female			
1	Aman/22	30/11/22	30	-	30	Sirajgonj	Combine Harvester
2	Aman/22	01/12/22	30	-	30	Sirjgonj	Combine Harvester
3	Boro/22-23	19/12/22	30	-	30	Hobigonj	Mat Tipe Tre
4	Boro/22-23	20/12/22	30	-	30	Hobigonj	Mat Tipe Tre
5	Boro/22-23	21/12/22	30	-	30	Sirjgonj	Mat Tipe Tre
6	Boro/22-23	22/12/22	30	-	30	Sirjgonj	Mat Tipe Tre
7	Aman/23	2/6/2023	30	-	30	Sirjgonj	Trabsplanter & Weeder
8	Aman/23	3/6/2023	30	-	30	Hobigonj	Trabsplanter & Weeder
9	Aman/23	5/6/2023	30	-	30	Sirjgonj	Trabsplanter & Weeder
10	Aman/23	6/6/2023	30	-	30	Hobigonj	Trabsplanter & Weeder
11	Aman/23	21/8/2023	30	-	30	Sirjgonj	Trabsplanter & Weeder
12	Aman/23	6/9/2023	30	-	30	Hobigonj	Trabsplanter & Weeder
13	Aman/23	5/10/2023	30	-	30	Sirjgonj	Trabsplanter & Weeder
14	Aman/23	10/10/2023	30	-	30	Sirjgonj	Trabsplanter & Weeder



Plate 32. Inaugural session of the training programme.



Plate 33. Practical session of the training programme.



Plate 34. Practical session of the training programme.

MAINTENANCE WORK

Appendix I: Support service for different division of BRR I rendered by FMPHT Divisional Research Workshop during 2022-2023.

Division Name	Type of Work	No. of job	Total
Farm Management	Hydraulic repair	1	44
	Hydro tiller repair	7	
	Power tiller wheel repair	9	
	Power thresher repair	16	
	Chain box welding	2	
	Power tiller machine repair	1	
	Air cleaner & rotary chain welding	4	
	Drum cutting and adding handle	3	
	Winnower machine repair	1	
Building Construction	Cutting Drum	10	21
	Cutting oil Drum	2	
	Door welding	3	
	Pipe welding	4	
	Van vehicle axle welding	1	
	3in GI pipe repair	1	
Soil Science	Distill water machine repair	1	7
	Open drum repair	1	
	Paddle thresher repair	5	
Agronomy	Thresher machine repair	1	2
	Close drum repair	1	
Biotechnology	Threshing machine repair	1	5
	Paddle thresher repair	2	
	Hand chopper	2	
ARD	Power thresher repair	3	3
Hybrid	Thresher machine repair	1	1
Agricultural Economics	Thresher machine repair	1	1
GRS	Repairing Thresher machine	2	4
	Trolley repair	1	
	Grading net repair	1	
Plant Pathology	Winnower machine welding	2	2
Entomology	Winnower machine welding & repair	2	53
	Making hole on Mylar's seat	50	
	Hand trolley repair	1	
Irrigation and water management	Irrigation pipe repair	1	21
	Making AWD pipe	10	
	GI pipe cutting	10	
Plant Breeding	Thresher cum Winnower machine repair	2	4
	Winnower machine repair	1	
	Thresher machine repair	1	
Physiology	Making singhboard	1	1
Hostel	Key holder ring repair	1	16
	Making Dish rack	4	
	Making Stove ring	5	
	Gas stove repair	6	
Security	Ring clamp and Fitting	1	2
	Steel tool, file cabinet and gate welding	1	
Total		187	

Appendix II: Repair and maintenance works of transports/vehicles and different farm machinery

PI: MGKB,

CI: MafH, HR, MMA

BRR I has different kinds of transport/vehicles and farm machinery. WMM Division of BRR I does the repair and maintenance works of different kinds of transport/vehicles and farm machinery. There were 40 vehicles (4-wheeler), 112 motor cycles, 05 tractors, 25 power tillers, 15 hydro-tillers, one reaper, threshers and others were repaired and changed of spare parts under major and moderate/minor repair and maintenance work. The repair and maintenance works have been divided into two groups such as:

- Moderate/minor repair and maintenance work and
- Major repair and maintenance work

Moderate/minor repair and maintenance work

Moderate/minor repair and maintenance works have been classified into three groups:

- Moderate/minor spare parts change and repair
- Minor CNG related trouble shooting and electrical works of vehicles
- Transport/vehicles/machinery cleaning and servicing

Moderate/minor spare parts change and repair works of all the vehicles and different farm machinery were done day to day in BRRI except CNG related trouble shootings of these vehicles, because there was no trained manpower in BRRI regarding CNG related trouble shootings. As a result, major/moderate/minor/or any kind of CNG related trouble shootings of these vehicles were totally done outside BRRI. A total of 40 vehicles (4-wheeler) in 461 times, 112 motor cycles in 231 times, 05 tractors in 60 times, 25 power tillers in 259 times, 15 hydro tillers in 53 times and others farm machinery in 30 times were repaired and changed of spare parts under moderate/minor repair and maintenance work.

Major repair and maintenance work

WMM division does seven types of major repair and maintenance works:

- Major spare parts change and repair
- Overhauling
- CNG conversion
- Denting-painting
- Tyre-tube
- Battery
- Major CNG related trouble shooting

Major repair and maintenance works have been done in BRRI workshop and outside BRRI. Some of the major spare parts change, overhauling and repair works have been done in BRRI workshop but major works were done outside BRRI due to fund limitation and some of the major works have been done by direct contracting through Vehicle Solution, AG Automobiles, New S.N. motors, Ranks Motors Workshop and also in local workshops. At present electrical works have been done in BRRI workshop. Purchasing the battery and tyre tube or taking the tyre-tube from BRRI store (if available) through requisition were attached to the vehicles/transport in BRRI workshop. Total cost of maintenance was Tk 92,60,467.00 from July 2022 to June 2023 whereas major repair and maintenance cost was Tk 60,17,166.00 and moderate/minor repair and maintenance cost was Tk 32,43,301.00.

Appendix II. Maintenance cost at 2022-23 financial year.

S.I no	Type of vehicle	vehicle/Machine (no.)	Time of major works	Time of minor works	Cost of major works	Cost of minor works	Total cost (TK)
1	Bus	SAS 65-3831		3		26780	26780
2	-do-	Gazipur- Sa-11-0012		30		297274	297274
3	-do-	Gazipur- Sa-11-0013	1	28	47576	260975	308551
4	Mini-bus	Gazipur- Ja-11-0018		17		89417	89417
5	-do-	Gazipur- Ja-11-0019	1	23	121472	178550	300022
6	Micro-bus	SAS 65-0034	1	15	49700	97300	147000
7	-do-	Gazipur-Cha-02-0076	1	19	91000	127090	218090
8	-do-	SAS 65-3870		13		52070	52070
9	-do-	Gazipur-Ch-02-0052		14		68488	68488
10	-do-	Gazipur- Ch-02-0053		16		73815	73815
11	-do-	Fpha-005	1	24	93700	136070	229770
12	-do-	Gazipur-Cha-11-0009	1	12	861756	66250	928006
13	-do-	Gazipur-Cha-11-0010	1	2	897718	7400	905118
14	jeep	Gazipur-Gha-02-0170	1	20	67500	62879	130379
15	-do-	Gazipur-Gha-11-0077	2	8	343708	8760	352468
16	-do-	Gazipur-Gha-02-0150		14		67210	67210
17	-do-	Dhaka Metro-Gha-18-7014		12		149270	149270
18	-do-	Aza-15-006	2	9	271100	88386	359486
19	-do-	Aza-15-007		8		88380	88380
20	-do-	Gazipur-Gha-02-0194	1	4	668950	17100	686050
21	-do-	Gazipur-Gha-02-0103	2	16	239400	28600	268000
22	-do-	Gazipur-Gha-02-0105		1		1800	1800
23	-do-	Gazipur-Gha-11-0024	3	7	452380	16000	468380
24	-do-	Gazipur-Gha-11-0025	1	16	39996	147337	187333
25	-do-	Gazipur-Gha-11-0026	1	7	689448	21844	711292
26	-do-	Gazipur-Gha-11-0082	1	5	49837	24872	74709
27	-do-	Gazipur-Gha-11-0036	2	16	181225	64716	245941
28	-do-	Gazipur-Gha-11-0055	-	04		47460	47460
29	pickup	Gazipur-Ma-02-0056	1	13	154800	42700	197500
30	-do-	Gazipur-Tha-11-0002	2	2	318800	71676	390476
31	-do-	Gazipur-Ma-02-0087		5		21488	21488
32	-do-	Gazipur-Tha-11-0008		13		85070	85070
33	-do-	Apha-009		7		12450	12450
34	-do-	Gazipur-Ma-02-0088		6		12740	12740
35	-do-	Gazipur-Tha-11-0042	1	16	55200	103100	158300
36	-do-	Dhaka Metro-Tha-13-1641	1	9	98100	56100	154200
37	-do-	Gazipur-Tha-11-0040	2	21	96800	132636	229436
38	Truck	Gazipur-Ma-07-0020		15		103300	103300
39	-do-	Gazipur-A-11-0001		8		16948	16948
40	-do-	Gazipur-A-11-0011		10		43470	43470
Sub total			29	461	5890166	3017771	8907937
41	Motor cycle	(112 nos.)		231		31000	31000
42	Tractor	(5 nos.)		60		98300	98300
43	power tiller	(25 nos.)		259		65030	65030
44	Hydro tiller	(15 nos.)	1	53	127000	20200	147200
45	Tyres & tubes			0	0	0	0
46	others/Threshers	(15 nos.)		30		11000	11000
Sub total			1	633	127000	225530	352530
Grand total			30	1094	6017166	3243301	9260467